13

Molecular spectroscopy 1: rotational and vibrational spectra

The general strategy we adopt in the chapter is to set up expressions for the energy levels of molecules and then apply selection rules and considerations of populations to infer the form of spectra. Rotational energy levels are considered first, and we see how to derive expressions for their values and how to interpret rotational spectra in terms of molecular dimensions. Not all molecules can occupy all rotational states: we see the experimental evidence for this restriction and its explanation in terms of nuclear spin and the Pauli principle. Next, we consider the vibrational energy levels of diatomic molecules, and see that we can use the properties of harmonic oscillators developed in Chapter 9. Then we consider polyatomic molecules and find that their vibrations may be discussed as though they consisted of a set of independent harmonic oscillators, so the same approach as employed for diatomic molecules may be used. We also see that the symmetry properties of the vibrations of polyatomic molecules are helpful for deciding which modes of vibration can be studied spectroscopically.

The origin of spectral lines in molecular spectroscopy is the absorption, emission, or scattering of a photon when the energy of a molecule changes. The difference from atomic spectroscopy is that the energy of a molecule can change not only as a result of electronic transitions but also because it can undergo changes of rotational and vibrational state. Molecular spectra are therefore more complex than atomic spectra. However, they also contain information relating to more properties, and their analysis leads to values of bond strengths, lengths, and angles. They also provide a way of determining a variety of molecular properties, particularly molecular dimensions, shapes, and dipole moments. Molecular spectroscopy is also useful to astrophysicists and environmental scientists, for the chemical composition of interstellar space and of planetary atmospheres can be inferred from their rotational, vibrational, and electronic spectra.

Pure rotational spectra, in which only the rotational state of a molecule changes, can be observed in the gas phase. Vibrational spectra of gaseous samples show features that arise from rotational transitions that accompany the excitation of vibration. Electronic spectra, which are described in Chapter 14, show features arising from simultaneous vibrational and rotational transitions. The simplest way of dealing with these complexities is to tackle each type of transition in turn, and then to see how simultaneous changes affect the appearance of spectra.

General features of spectroscopy

All types of spectra have some features in common, and we examine these first. In **emission spectroscopy**, a molecule undergoes a transition from a state of high energy E_1 to a state of lower energy E_2 and emits the excess energy as a photon. In **absorption spectroscopy**, the net absorption of nearly monochromatic (single frequency) incident radiation is monitored as the radiation is swept over a range of frequencies. We say *net* absorption, because it will become clear that, when a sample is irradiated, both absorption and emission at a given frequency are stimulated, and the detector measures the difference, the net absorption.

The energy, $h\nu$, of the photon emitted or absorbed, and therefore the frequency ν of the radiation emitted or absorbed, is given by the Bohr frequency condition, $h\nu = |E_1 - E_2|$ (eqn 8.10). Emission and absorption spectroscopy give the same information about energy level separations, but practical considerations generally determine which technique is employed. We shall discuss emission spectroscopy in Chapter 14; here we focus on absorption spectroscopy, which is widely employed in studies of electronic transitions, molecular rotations, and molecular vibrations.

In Chapter 9 we saw that transitions between electronic energy levels are stimulated by or emit ultraviolet, visible, or near-infrared radiation. Vibrational and rotational transitions, the focus of the discussion in this chapter, can be induced in two ways. First, the direct absorption or emission of infrared radiation can cause changes in vibrational energy levels, whereas absorption or emission of microwave radiation gives information about rotational energy levels. Second, vibrational and rotational energy levels can be explored by examining the frequencies present in the radiation scattered by molecules in **Raman spectroscopy**. About 1 in 10^7 of the incident photons collide with the molecules, give up some of their energy, and emerge with a lower energy. These scattered photons constitute the lower-frequency **Stokes radiation** from the sample (Fig. 13.1). Other incident photons may collect energy from the molecules (if they are already excited), and emerge as higher-frequency **anti-Stokes radiation**. The component of radiation scattered without change of frequency is called **Rayleigh radiation**.

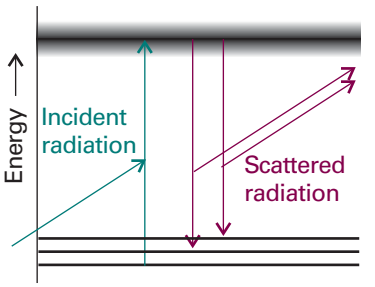

Fig. 13.1 In Raman spectroscopy, an incident photon is scattered from a molecule with either an increase in frequency (if the radiation collects energy from the molecule) or—as shown here for the case of scattered Stokes radiation—with a lower frequency if it loses energy to the molecule. The process can be regarded as taking place by an excitation of the molecule to a wide range of states (represented by the shaded band), and the subsequent return of the molecule to a lower state; the net energy change is then carried away by the photon.

13.1 Experimental techniques

A **spectrometer** is an instrument that detects the characteristics of light scattered, emitted, or absorbed by atoms and molecules. Figure 13.2 shows the general layouts of absorption and emission spectrometers operating in the ultraviolet and visible ranges. Radiation from an appropriate source is directed toward a sample. In most

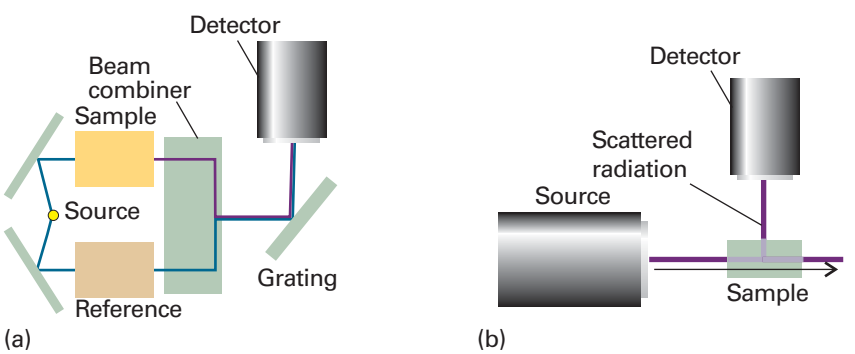

Fig. 13.2 Two examples of spectrometers: (a) the layout of an absorption spectrometer, used primarily for studies in the ultraviolet and visible ranges, in which the exciting beams of radiation pass alternately through a sample and a reference cell, and the detector is synchronized with them so that the relative absorption can be determined, and (b) a simple emission spectrometer, where light emitted or scattered by the sample is detected at right angles to the direction of propagation of an incident beam of radiation.

Comment 13.1

The principles of operation of radiation sources, dispersing elements, Fourier transform spectrometers, and detectors are described in *Further information 13.1*.

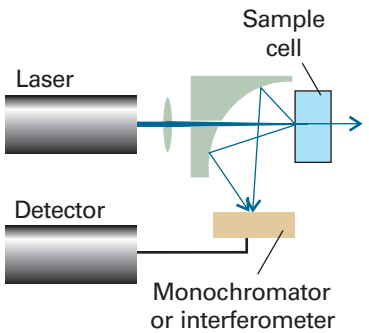

Fig. 13.3 A common arrangement adopted in Raman spectroscopy. A laser beam first passes through a lens and then through a small hole in a mirror with a curved reflecting surface. The focused beam strikes the sample and scattered light is both deflected and focused by the mirror. The spectrum is analysed by a monochromator or an interferometer.

spectrometers, light transmitted, emitted, or scattered by the sample is collected by mirrors or lenses and strikes a **dispersing element** that separates radiation into different frequencies. The intensity of light at each frequency is then analysed by a suitable detector. In a typical Raman spectroscopy experiment, a monochromatic incident laser beam is passed through the sample and the radiation scattered from the front face of the sample is monitored (Fig. 13.3). This detection geometry allows for the study of gases, pure liquids, solutions, suspensions, and solids.

Modern spectrometers, particularly those operating in the infrared and near-infrared, now almost always use **Fourier transform techniques** of spectral detection and analysis. The heart of a Fourier transform spectrometer is a *Michelson interferometer*, a device for analysing the frequencies present in a composite signal. The total signal from a sample is like a chord played on a piano, and the Fourier transform of the signal is equivalent to the separation of the chord into its individual notes, its spectrum.

13.2 The intensities of spectral lines

The ratio of the transmitted intensity, I, to the incident intensity, I_0, at a given frequency is called the **transmittance**, T, of the sample at that frequency:

$$T = \frac{I}{I_0} \qquad [13.1]$$

It is found empirically that the transmitted intensity varies with the length, l, of the sample and the molar concentration, [J], of the absorbing species J in accord with the **Beer–Lambert law**:

$$I = I_0 10^{-\varepsilon[\mathrm{J}]l} \qquad (13.2)$$

The quantity ε is called the **molar absorption coefficient** (formerly, and still widely, the 'extinction coefficient'). The molar absorption coefficient depends on the frequency of the incident radiation and is greatest where the absorption is most intense. Its dimensions are 1/(concentration × length), and it is normally convenient to express it in cubic decimetres per mole per centimetre ($\mathrm{dm^3\ mol^{-1}\ cm^{-1}}$). Alternative units are square centimetres per mole ($\mathrm{cm^2\ mol^{-1}}$). This change of units demonstrates that ε may be regarded as a molar cross-section for absorption and, the greater the cross-sectional area of the molecule for absorption, the greater its ability to block the passage of the incident radiation.

To simplify eqn 13.2, we introduce the **absorbance**, A, of the sample at a given wavenumber as

$$A = \log\frac{I_0}{I} \qquad \text{or} \qquad A = -\log T \qquad [13.3]$$

Then the Beer–Lambert law becomes

$$A = \varepsilon[\mathrm{J}]l \qquad (13.4)$$

The product $\varepsilon[\mathrm{J}]l$ was known formerly as the *optical density* of the sample. Equation 13.4 suggests that, to achieve sufficient absorption, path lengths through gaseous samples must be very long, of the order of metres, because concentrations are low. Long path lengths are achieved by multiple passage of the beam between parallel mirrors at each end of the sample cavity. Conversely, path lengths through liquid samples can be significantly shorter, of the order of millimetres or centimetres.

Justification 13.1 *The Beer–Lambert law*

The Beer–Lambert law is an empirical result. However, it is simple to account for its form. The reduction in intensity, $\mathrm{d}I$, that occurs when light passes through a layer of thickness $\mathrm{d}l$ containing an absorbing species J at a molar concentration [J] is proportional to the thickness of the layer, the concentration of J, and the intensity, I, incident on the layer (because the rate of absorption is proportional to the intensity, see below). We can therefore write

$$\mathrm{d}I = -\kappa[\mathrm{J}]I\mathrm{d}l$$

where κ (kappa) is the proportionality coefficient, or equivalently

$$\frac{\mathrm{d}I}{I} = -\kappa[\mathrm{J}]\mathrm{d}l$$

This expression applies to each successive layer into which the sample can be regarded as being divided. Therefore, to obtain the intensity that emerges from a sample of thickness l when the intensity incident on one face of the sample is I_0, we sum all the successive changes:

$$\int_{I_0}^{I} \frac{\mathrm{d}I}{I} = -\kappa \int_0^l [\mathrm{J}]\mathrm{d}l$$

If the concentration is uniform, [J] is independent of location, and the expression integrates to

$$\ln \frac{I}{I_0} = -\kappa[\mathrm{J}]l$$

This expression gives the Beer–Lambert law when the logarithm is converted to base 10 by using $\ln x = (\ln 10)\log x$ and replacing κ by $\varepsilon \ln 10$.

Illustration 13.1 *Using the Beer–Lambert law*

The Beer–Lambert law implies that the intensity of electromagnetic radiation transmitted through a sample at a given wavenumber decreases exponentially with the sample thickness and the molar concentration. If the transmittance is 0.1 for a path length of 1 cm (corresponding to a 90 per cent reduction in intensity), then it would be $(0.1)^2 = 0.01$ for a path of double the length (corresponding to a 99 per cent reduction in intensity overall).

The maximum value of the molar absorption coefficient, $\varepsilon_{\max}$, is an indication of the intensity of a transition. However, as absorption bands generally spread over a range of wavenumbers, quoting the absorption coefficient at a single wavenumber might not give a true indication of the intensity of a transition. The **integrated absorption coefficient**, $\mathcal{A}$, is the sum of the absorption coefficients over the entire band (Fig. 13.4), and corresponds to the area under the plot of the molar absorption coefficient against wavenumber:

$$\mathcal{A} = \int_{\text{band}} \varepsilon(\tilde{\nu})\, \mathrm{d}\tilde{\nu} \qquad [13.5]$$

For lines of similar widths, the integrated absorption coefficients are proportional to the heights of the lines.

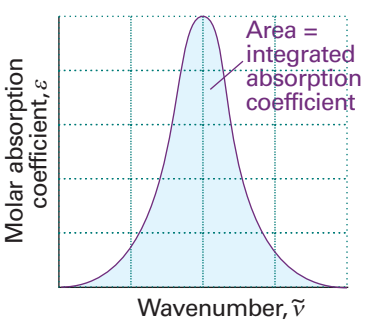

Fig. 13.4 The integrated absorption coefficient of a transition is the area under a plot of the molar absorption coefficient against the wavenumber of the incident radiation.

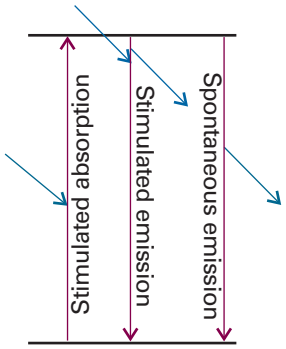

Fig. 13.5 The processes that account for absorption and emission of radiation and the attainment of thermal equilibrium. The excited state can return to the lower state spontaneously as well as by a process stimulated by radiation already present at the transition frequency.

Comment 13.2

The slight difference between the forms of the Planck distribution shown in eqns 8.5 and 13.7 stems from the fact that it is written here as $\rho \mathrm{d}\nu$, and $\mathrm{d}\lambda = (c/\nu^2)\mathrm{d}\nu$.

(a) Absorption intensities

Einstein identified three contributions to the transitions between states. **Stimulated absorption** is the transition from a low energy state to one of higher energy that is driven by the electromagnetic field oscillating at the transition frequency. We saw in Section 9.10 that the transition rate, w, is the rate of change of probability of the molecule being found in the upper state. We also saw that the more intense the electromagnetic field (the more intense the incident radiation), the greater the rate at which transitions are induced and hence the stronger the absorption by the sample (Fig. 13.5). Einstein wrote the transition rate as

$$w = B\rho \tag{13.6}$$

The constant B is the **Einstein coefficient of stimulated absorption** and $\rho \mathrm{d}\nu$ is the energy density of radiation in the frequency range ν to $\nu + \mathrm{d}\nu$, where ν is the frequency of the transition. When the molecule is exposed to black-body radiation from a source of temperature T, ρ is given by the Planck distribution (eqn 8.5):

$$\rho = \frac{8\pi h\nu^3/c^3}{\mathrm{e}^{h\nu/kT} - 1} \tag{13.7}$$

For the time being, we can treat B as an empirical parameter that characterizes the transition: if B is large, then a given intensity of incident radiation will induce transitions strongly and the sample will be strongly absorbing. The **total rate of absorption**, W, the number of molecules excited during an interval divided by the duration of the interval, is the transition rate of a single molecule multiplied by the number of molecules N in the lower state: $W = Nw$.

Einstein considered that the radiation was also able to induce the molecule in the upper state to undergo a transition to the lower state, and hence to generate a photon of frequency ν. Thus, he wrote the rate of this stimulated emission as

$$w' = B'\rho \tag{13.8}$$

where B' is the **Einstein coefficient of stimulated emission**. Note that only radiation of the same frequency as the transition can stimulate an excited state to fall to a lower state. However, he realized that stimulated emission was not the only means by which the excited state could generate radiation and return to the lower state, and suggested that an excited state could undergo **spontaneous emission** at a rate that was independent of the intensity of the radiation (of any frequency) that is already present. Einstein therefore wrote the total rate of transition from the upper to the lower state as

$$w' = A + B'\rho \tag{13.9}$$

The constant A is the **Einstein coefficient of spontaneous emission**. The overall rate of emission is

$$W' = N'(A + B'\rho) \tag{13.10}$$

where N' is the population of the upper state.

As demonstrated in the *Justification* below, Einstein was able to show that the two coefficients of stimulated absorption and emission are equal, and that the coefficient of spontaneous emission is related to them by

$$A = \left(\frac{8\pi h\nu^3}{c^3}\right)B \tag{13.11}$$

Justification 13.2 *The relation between the Einstein coefficients*

At thermal equilibrium, the total rates of emission and absorption are equal, so

$$NB\rho = N'(A + B'\rho)$$

This expression rearranges into

$$\rho = \frac{N'A}{NB - N'B'} = \frac{A/B}{N/N' - B'/B} = \frac{A/B}{e^{h\nu/kT} - B'/B}$$

We have used the Boltzmann expression (*Molecular interpretation* 3.1) for the ratio of populations of states of energies E and E' in the last step:

$$\frac{N'}{N} = e^{-h\nu/kT} \qquad h\nu = E' - E$$

This result has the same form as the Planck distribution (eqn 13.7), which describes the radiation density at thermal equilibrium. Indeed, when we compare the two expressions for ρ, we can conclude that $B' = B$ and that A is related to B by eqn 13.11.

The growth of the importance of spontaneous emission with increasing frequency is a very important conclusion, as we shall see when we consider the operation of lasers (Section 14.5). The equality of the coefficients of stimulated emission and absorption implies that, if two states happen to have equal populations, then the rate of stimulated emission is equal to the rate of stimulated absorption, and there is then no net absorption.

Spontaneous emission can be largely ignored at the relatively low frequencies of rotational and vibrational transitions, and the intensities of these transitions can be discussed in terms of stimulated emission and absorption. Then the net rate of absorption is given by

$$W_{\text{net}} = NB\rho - N'B'\rho = (N - N')B\rho \tag{13.12}$$

and is proportional to the population difference of the two states involved in the transition.

(b) Selection rules and transition moments

We met the concept of a 'selection rule' in Sections 10.3 and 12.6 as a statement about whether a transition is forbidden or allowed. Selection rules also apply to molecular spectra, and the form they take depends on the type of transition. The underlying classical idea is that, for the molecule to be able to interact with the electromagnetic field and absorb or create a photon of frequency ν, it must possess, at least transiently, a dipole oscillating at that frequency. We saw in Section 9.10 that this transient dipole is expressed quantum mechanically in terms of the transition dipole moment, $\boldsymbol{\mu}_{\text{fi}}$, between states ψ_{i} and ψ_{f}:

$$\boldsymbol{\mu}_{\text{fi}} = \int \psi_{\text{f}}^{*} \hat{\boldsymbol{\mu}} \psi_{\text{i}} \, d\tau \tag{13.13}$$

where $\hat{\boldsymbol{\mu}}$ is the electric dipole moment operator. The size of the transition dipole can be regarded as a measure of the charge redistribution that accompanies a transition: a transition will be active (and generate or absorb photons) only if the accompanying charge redistribution is dipolar (Fig. 13.6).

We know from time-dependent perturbation theory (Section 9.10) that the transition rate is proportional to $|\mu_{\text{fi}}|^2$. It follows that the coefficient of stimulated absorption

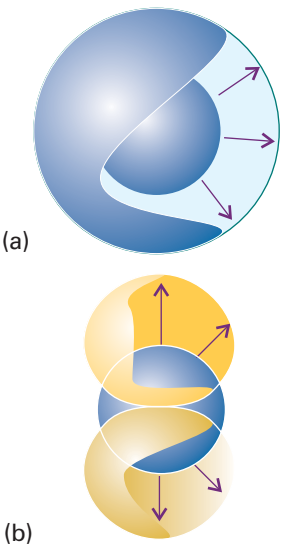

Fig. 13.6 (a) When a 1*s* electron becomes a 2*s* electron, there is a spherical migration of charge; there is no dipole moment associated with this migration of charge; this transition is electric-dipole forbidden. (b) In contrast, when a 1*s* electron becomes a 2*p* electron, there is a dipole associated with the charge migration; this transition is allowed. (There are subtle effects arising from the sign of the wavefunction that give the charge migration a dipolar character, which this diagram does not attempt to convey.)

(and emission), and therefore the intensity of the transition, is also proportional to $|\mu_{fi}|^2$. A detailed analysis gives

$$B = \frac{|\mu_{fi}|^2}{6\varepsilon_0\hbar^2} \tag{13.14}$$

Only if the transition moment is nonzero does the transition contribute to the spectrum. It follows that, to identify the selection rules, we must establish the conditions for which $\boldsymbol{\mu}_{fi} \neq 0$.

A **gross selection rule** specifies the general features a molecule must have if it is to have a spectrum of a given kind. For instance, we shall see that a molecule gives a rotational spectrum only if it has a permanent electric dipole moment. This rule, and others like it for other types of transition, will be explained in the relevant sections of the chapter. A detailed study of the transition moment leads to the **specific selection rules** that express the allowed transitions in terms of the changes in quantum numbers. We have already encountered examples of specific selection rules when discussing atomic spectra (Section 10.3), such as the rule $\Delta l = \pm 1$ for the angular momentum quantum number.

13.3 Linewidths

A number of effects contribute to the widths of spectroscopic lines. Some contributions to linewidths can be modified by changing the conditions, and to achieve high resolutions we need to know how to minimize these contributions. Other contributions cannot be changed, and represent an inherent limitation on resolution.

(a) Doppler broadening

The study of gaseous samples is very important, as it can inform our understanding of atmospheric chemistry. In some cases, meaningful spectroscopic data can be obtained only from gaseous samples. For example, they are essential for rotational spectroscopy, for only in gases can molecules rotate freely.

One important broadening process in gaseous samples is the **Doppler effect**, in which radiation is shifted in frequency when the source is moving towards or away from the observer. When a source emitting electromagnetic radiation of frequency ν moves with a speed s relative to an observer, the observer detects radiation of frequency

$$\nu_{\text{receding}} = \nu\left(\frac{1 - s/c}{1 + s/c}\right)^{1/2} \qquad \nu_{\text{approaching}} = \nu\left(\frac{1 + s/c}{1 - s/c}\right)^{1/2} \tag{13.15}$$

where c is the speed of light (see *Further reading* for derivations). For nonrelativistic speeds ($s \ll c$), these expressions simplify to

$$\nu_{\text{receding}} \approx \frac{\nu}{1 + s/c} \qquad \nu_{\text{approaching}} \approx \frac{\nu}{1 - s/c} \tag{13.16}$$

Molecules reach high speeds in all directions in a gas, and a stationary observer detects the corresponding Doppler-shifted range of frequencies. Some molecules approach the observer, some move away; some move quickly, others slowly. The detected spectral 'line' is the absorption or emission profile arising from all the resulting Doppler shifts. As shown in the following *Justification*, the profile reflects the distribution of molecular velocities parallel to the line of sight, which is a bell-shaped Gaussian curve. The Doppler line shape is therefore also a Gaussian (Fig. 13.7), and we show in the

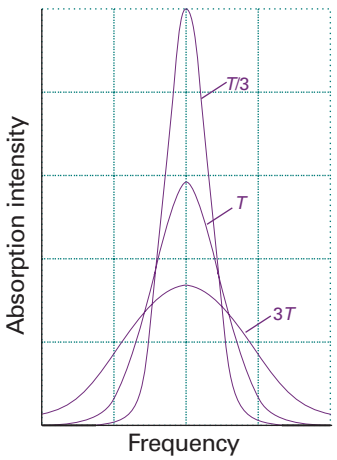

Fig. 13.7 The Gaussian shape of a Doppler-broadened spectral line reflects the Maxwell distribution of speeds in the sample at the temperature of the experiment. Notice that the line broadens as the temperature is increased.

Exploration In a spectrometer that makes use of *phase-sensitive detection* the output signal is proportional to the first derivative of the signal intensity, $dI/d\nu$. Plot the resulting line shape for various temperatures. How is the separation of the peaks related to the temperature?

Justification that, when the temperature is T and the mass of the molecule is m, then the observed width of the line at half-height (in terms of frequency or wavelength) is

$$\delta\nu_{\text{obs}} = \frac{2\nu}{c}\left(\frac{2kT\ln 2}{m}\right)^{1/2} \qquad \delta\lambda_{\text{obs}} = \frac{2\lambda}{c}\left(\frac{2kT\ln 2}{m}\right)^{1/2} \tag{13.17}$$

For a molecule like N_2 at room temperature ($T \approx 300$ K), $\delta\nu/\nu \approx 2.3 \times 10^{-6}$. For a typical rotational transition wavenumber of 1 cm^{-1} (corresponding to a frequency of 30 GHz), the linewidth is about 70 kHz. Doppler broadening increases with temperature because the molecules acquire a wider range of speeds. Therefore, to obtain spectra of maximum sharpness, it is best to work with cold samples.

A note on good practice You will often hear people speak of 'a frequency as so many wavenumbers'. This usage is doubly wrong. First, *frequency* and *wavenumber* are two distinct physical observables with different units, and should be distinguished. Second, 'wavenumber' is not a unit, it is an observable with the dimensions of 1/length and commonly reported in reciprocal centimetres (cm^{-1}).

Comment 13.3
A Gaussian function of the general form $y(x) = ae^{-(x-b)^2/2\sigma^2}$, where a, b, and σ are constants, has a maximum $y(b) = a$ and a width at half-height $\delta x = 2\sigma(2\ln 2)^{1/2}$.

Justification 13.3 *Doppler broadening*

We know from the Boltzmann distribution (*Molecular interpretation 3.1*) that the probability that a gas molecule of mass m and speed s in a sample with temperature T has kinetic energy $E_K = \frac{1}{2}ms^2$ is proportional to $e^{-ms^2/2kT}$. The observed frequencies, ν_{obs}, emitted or absorbed by the molecule are related to its speed by eqn 13.16:

$$\nu_{\text{obs}} = \nu\left(\frac{1}{1 \pm s/c}\right)$$

where ν is the unshifted frequency. When $s \ll c$, the Doppler shift in the frequency is

$$\nu_{\text{obs}} - \nu \approx \pm\nu s/c$$

which implies a symmetrical distribution of observed frequencies with respect to molecular speeds. More specifically, the intensity I of a transition at ν_{obs} is proportional to the probability of finding the molecule that emits or absorbs at ν_{obs}, so it follows from the Boltzmannm distribution and the expression for the Doppler shift that

$$I(\nu_{\text{obs}}) \propto e^{-mc^2(\nu_{\text{obs}}-\nu)^2/2\nu^2kT}$$

which has the form of a Gaussian function. The width at half-height can be calculated directly from the exponent (see *Comment 13.3*) to give eqn 13.17.

(b) Lifetime broadening

It is found that spectroscopic lines from gas-phase samples are not infinitely sharp even when Doppler broadening has been largely eliminated by working at low temperatures. The same is true of the spectra of samples in condensed phases and solution. This residual broadening is due to quantum mechanical effects. Specifically, when the Schrödinger equation is solved for a system that is changing with time, it is found that it is impossible to specify the energy levels exactly. If on average a system survives in a state for a time τ (tau), the **lifetime** of the state, then its energy levels are blurred to an extent of order δE, where

$$\delta E \approx \frac{\hbar}{\tau} \tag{13.18}$$

This expression is reminiscent of the Heisenberg uncertainty principle (eqn 8.40), and consequently this **lifetime broadening** is often called 'uncertainty broadening'. When the energy spread is expressed as a wavenumber through $\delta E = hc\delta\tilde{\nu}$, and the values of the fundamental constants introduced, this relation becomes

$$\delta\tilde{\nu} \approx \frac{5.3\ \text{cm}^{-1}}{\tau/\text{ps}} \tag{13.19}$$

No excited state has an infinite lifetime; therefore, all states are subject to some lifetime broadening and, the shorter the lifetimes of the states involved in a transition, the broader the corresponding spectral lines.

Two processes are responsible for the finite lifetimes of excited states. The dominant one for low frequency transitions is **collisional deactivation**, which arises from collisions between molecules or with the walls of the container. If the **collisional lifetime**, the mean time between collisions, is τ_{col}, the resulting collisional linewidth is $\delta E_{\text{col}} \approx \hbar/\tau_{\text{col}}$. Because $\tau_{\text{col}} = 1/z$, where z is the collision frequency, and from the kinetic model of gases (Section 1.3) we know that z is proportional to the pressure, we see that the collisional linewidth is proportional to the pressure. The collisional linewidth can therefore be minimized by working at low pressures.

The rate of spontaneous emission cannot be changed. Hence it is a natural limit to the lifetime of an excited state, and the resulting lifetime broadening is the **natural linewidth** of the transition. The natural linewidth is an intrinsic property of the transition, and cannot be changed by modifying the conditions. Natural linewidths depend strongly on the transition frequency (they increase with the coefficient of spontaneous emission A and therefore as ν^3), so low frequency transitions (such as the microwave transitions of rotational spectroscopy) have very small natural linewidths, and collisional and Doppler line-broadening processes are dominant. The natural lifetimes of electronic transitions are very much shorter than for vibrational and rotational transitions, so the natural linewidths of electronic transitions are much greater than those of vibrational and rotational transitions. For example, a typical electronic excited state natural lifetime is about 10^{-8} s (10 ns), corresponding to a natural width of about 5×10^{-4} cm^{-1} (15 MHz). A typical rotational state natural lifetime is about 10^3 s, corresponding to a natural linewidth of only 5×10^{-15} cm^{-1} (of the order of 10^{-4} Hz).

IMPACT ON ASTROPHYSICS

I13.1 Rotational and vibrational spectroscopy of interstellar space

Observations by the Cosmic Background Explorer (COBE) satellite support the long-held hypothesis that the distribution of energy in the current Universe can be modelled by a Planck distribution (eqn. 8.5) with $T = 2.726 \pm 0.001$ K, the bulk of the radiation spanning the microwave region of the spectrum. This *cosmic microwave background radiation* is the residue of energy released during the Big Bang, the event that brought the Universe into existence. Very small fluctuations in the background temperature are believed to account for the large-scale structure of the Universe.

The interstellar space in our galaxy is a little warmer than the cosmic background and consists largely of dust grains and gas clouds. The dust grains are carbon-based compounds and silicates of aluminium, magnesium, and iron, in which are embedded trace amounts of methane, water, and ammonia. Interstellar clouds are significant because it is from them that new stars, and consequently new planets, are formed. The hottest clouds are plasmas with temperatures of up to 10^6 K and densities of only about 3×10^3 particles m^{-3}. Colder clouds range from 0.1 to 1000 solar masses (1 solar

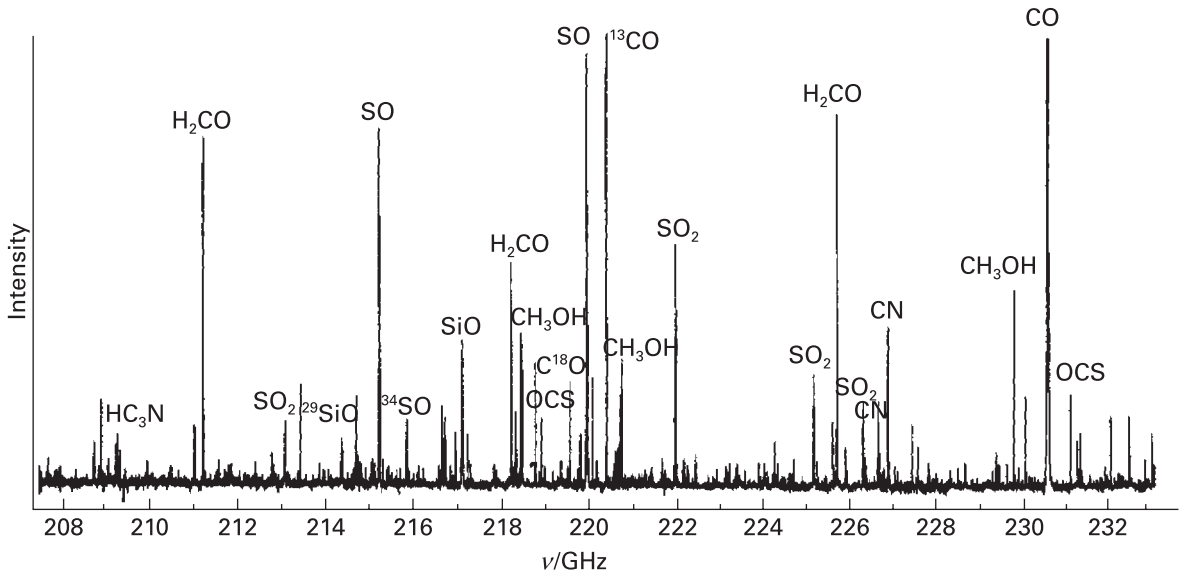

Fig. 13.8 Rotational spectrum of the Orion nebula, showing spectral fingerprints of diatomic and polyatomic molecules present in the interstellar cloud. Adapted from G.A. Blake *et al.*, *Astrophys. J.* **315**, 621 (1987).

mass = 2×10^{30} kg), have a density of about 5×10^5 particles m^{-3}, consist largely of hydrogen atoms, and have a temperature of about 80 K. There are also colder and denser clouds, some with masses greater than 500 000 solar masses, densities greater than 10^9 particles m^{-3}, and temperatures that can be lower than 10 K. They are also called *molecular clouds*, because they are composed primarily of H_2 and CO gas in a proportion of about 10^5 to 1. There are also trace amounts of larger molecules. To place the densities in context, the density of liquid water at 298 K and 1 bar is about 3×10^{28} particles m^{-3}.

It follows from the the Boltzmann distribution and the low temperature of a molecular cloud that the vast majority of a cloud's molecules are in their vibrational and electronic ground states. However, rotational excited states are populated at 10–100 K and decay by spontaneous emission. As a result, the spectrum of the cloud in the radiofrequency and microwave regions consists of sharp lines corresponding to rotational transitions (Fig. 13.8). The emitted light is collected by Earth-bound or spaceborne radiotelescopes, telescopes with antennas and detectors optimized for the collection and analysis of radiation in the microwave–radiowave range of the spectrum. Earth-bound radiotelescopes are often located at the tops of high mountains, as atmospheric water vapour can reabsorb microwave radiation from space and hence interfere with the measurement.

Over 100 interstellar molecules have been identified by their rotational spectra, often by comparing radiotelescope data with spectra obtained in the laboratory or calculated by computational methods. The experiments have revealed the presence of trace amounts (with abundances of less than 10^{-8} relative to hydrogen) of neutral molecules, ions, and radicals. Examples of neutral molecules include hydrides, oxides (including water), sulfides, halogenated compounds, nitriles, hydrocarbons, aldehydes, alcohols, ethers, ketones, and amides. The largest molecule detected by rotational spectroscopy is the nitrile $HC_{11}N$.

Interstellar space can also be investigated with vibrational spectroscopy by using a combination of telescopes and infrared detectors. The experiments are conducted

Table 13.1 Moments of inertia*

1. *Diatomic molecules*

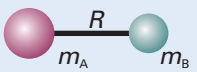

$$I = \mu R^2 \qquad \mu = \frac{m_A m_B}{m}$$

2. *Triatomic linear rotors*

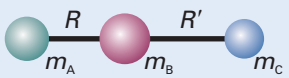

$$I = m_A R^2 + m_C R'^2 - \frac{(m_A R - m_C R')^2}{m}$$

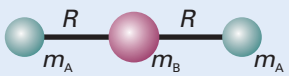

$$I = 2m_A R^2$$

3. *Symmetric rotors*

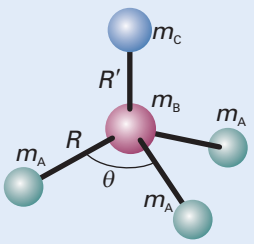

$$I_\parallel = 2m_A(1-\cos\theta)R^2$$

$$I_\perp = m_A(1-\cos\theta)R^2 + \frac{m_A}{m}(m_B+m_C)(1+2\cos\theta)R^2 + \frac{m_C}{m}\{(3m_A+m_B)R' + 6m_A R[\tfrac{1}{3}(1+2\cos\theta)]^{1/2}\}R'$$

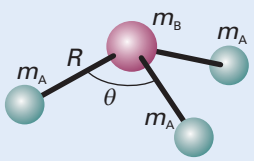

$$I_\parallel = 2m_A(1-\cos\theta)R^2$$

$$I_\perp = m_A(1-\cos\theta)R^2 + \frac{m_A m_B}{m}(1+2\cos\theta)R^2$$

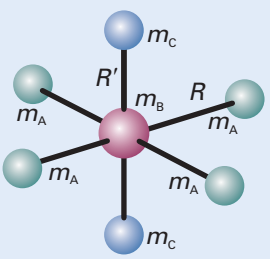

$$I_\parallel = 4m_A R^2$$

$$I_\perp = 2m_A R^2 + 2m_C R'^2$$

4. *Spherical rotors*

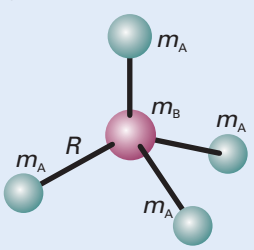

$$I = \tfrac{8}{3}m_A R^2$$

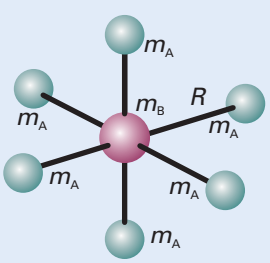

$$I = 4m_A R^2$$

* In each case, m is the total mass of the molecule.

primarily in space-borne telescopes because the Earth's atmosphere absorbs a great deal of infrared radiation (see *Impact I13.2*). In most cases, absorption by an interstellar species is detected against the background of infrared radiation emitted by a nearby star. The data can detect the presence of gas and solid water, CO, and CO_2 in molecular clouds. In certain cases, infrared emission can be detected, but these events are rare because interstellar space is too cold and does not provide enough energy to promote a significant number of molecules to vibrational excited states. However, infrared emissions can be observed if molecules are occasionally excited by high-energy photons emitted by hot stars in the vicinity of the cloud. For example, the polycyclic aromatic hydrocarbons hexabenzocoronene ($C_{48}H_{24}$) and circumcoronene ($C_{54}H_{18}$) have been identified from characteristic infrared emissions.

Pure rotation spectra

The general strategy we adopt for discussing molecular spectra and the information they contain is to find expressions for the energy levels of molecules and then to calculate the transition frequencies by applying the selection rules. We then predict the appearance of the spectrum by taking into account the transition moments and the populations of the states. In this section we illustrate the strategy by considering the rotational states of molecules.

13.4 Moments of inertia

The key molecular parameter we shall need is the **moment of inertia**, I, of the molecule (Section 9.6). The moment of inertia of a molecule is defined as the mass of each atom multiplied by the square of its distance from the rotational axis through the centre of mass of the molecule (Fig. 13.9):

$$I = \sum_i m_i r_i^2 \qquad [13.20]$$

where r_i is the perpendicular distance of the atom i from the axis of rotation. The moment of inertia depends on the masses of the atoms present and the molecular geometry, so we can suspect (and later shall see explicitly) that rotational spectroscopy will give information about bond lengths and bond angles.

In general, the rotational properties of any molecule can be expressed in terms of the moments of inertia about three perpendicular axes set in the molecule (Fig. 13.10). The convention is to label the moments of inertia I_a, I_b, and I_c, with the axes chosen so that $I_c \geq I_b \geq I_a$. For linear molecules, the moment of inertia around the internuclear axis is zero. The explicit expressions for the moments of inertia of some symmetrical molecules are given in Table 13.1.

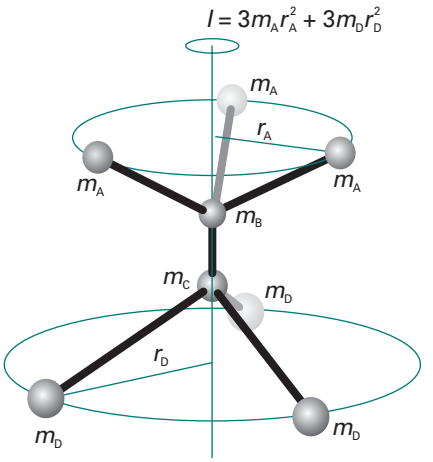

Fig. 13.9 The definition of moment of inertia. In this molecule there are three identical atoms attached to the B atom and three different but mutually identical atoms attached to the C atom. In this example, the centre of mass lies on an axis passing through the B and C atom, and the perpendicular distances are measured from this axis.

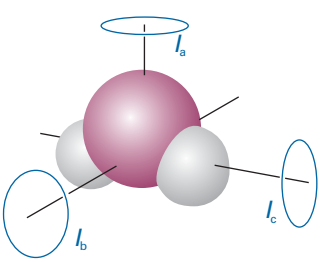

Fig. 13.10 An asymmetric rotor has three different moments of inertia; all three rotation axes coincide at the centre of mass of the molecule.

Example 13.1 *Calculating the moment of inertia of a molecule*

Calculate the moment of inertia of an H_2O molecule around the axis defined by the bisector of the HOH angle (**1**). The HOH bond angle is 104.5° and the bond length is 95.7 pm.

Method According to eqn 13.20, the moment of inertia is the sum of the masses multiplied by the squares of their distances from the axis of rotation. The latter can be expressed by using trigonometry and the bond angle and bond length.

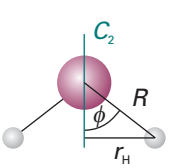

1

Answer From eqn 13.20,

$$I = \sum_i m_i r_i^2 = m_H r_H^2 + 0 + m_H r_H^2 = 2m_H r_H^2$$

If the bond angle of the molecule is denoted 2ϕ and the bond length is R, trigonometry gives $r_H = R \sin \phi$. It follows that

$$I = 2m_H R^2 \sin^2 \phi$$

Substitution of the data gives

$$I = 2 \times (1.67 \times 10^{-27}\ \text{kg}) \times (9.57 \times 10^{-11}\ \text{m})^2 \times \sin^2 52.3° = 1.91 \times 10^{-47}\ \text{kg m}^2$$

Note that the mass of the O atom makes no contribution to the moment of inertia for this mode of rotation as the atom is immobile while the H atoms circulate around it.

A note on good practice The mass to use in the calculation of the moment of inertia is the actual atomic mass, not the element's molar mass; don't forget to convert from atomic mass units (u, formerly amu) to kilograms.

Self-test 13.1 Calculate the moment of inertia of a $CH^{35}Cl_3$ molecule around a rotational axis that contains the C—H bond. The C—Cl bond length is 177 pm and the HCCl angle is 107°; $m(^{35}Cl) = 34.97$ u. $[4.99 \times 10^{-45}\ \text{kg m}^2]$

We shall suppose initially that molecules are **rigid rotors**, bodies that do not distort under the stress of rotation. Rigid rotors can be classified into four types (Fig. 13.11):

Spherical rotors have three equal moments of inertia (examples: CH_4, SiH_4, and SF_6).

Symmetric rotors have two equal moments of inertia (examples: NH_3, CH_3Cl, and CH_3CN).

Linear rotors have one moment of inertia (the one about the molecular axis) equal to zero (examples: CO_2, HCl, OCS, and HC≡CH).

Asymmetric rotors have three different moments of inertia (examples: H_2O, H_2CO, and CH_3OH).

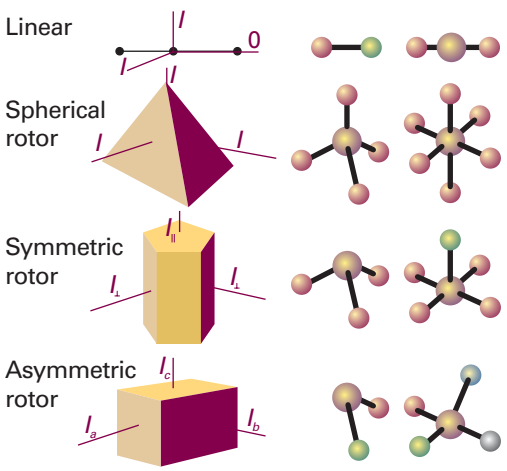

Fig. 13.11 A schematic illustration of the classification of rigid rotors.

13.5 The rotational energy levels

The rotational energy levels of a rigid rotor may be obtained by solving the appropriate Schrödinger equation. Fortunately, however, there is a much less onerous short cut to the exact expressions that depends on noting the classical expression for the energy of a rotating body, expressing it in terms of the angular momentum, and then importing the quantum mechanical properties of angular momentum into the equations.

The classical expression for the energy of a body rotating about an axis a is

$$E_a = \tfrac{1}{2} I_a \omega_a^2 \tag{13.21}$$

where ω_a is the angular velocity (in radians per second, rad s^{-1}) about that axis and I_a is the corresponding moment of inertia. A body free to rotate about three axes has an energy

$$E = \tfrac{1}{2} I_a \omega_a^2 + \tfrac{1}{2} I_b \omega_b^2 + \tfrac{1}{2} I_c \omega_c^2$$

Because the classical angular momentum about the axis a is $J_a = I_a \omega_a$, with similar expressions for the other axes, it follows that

$$E = \frac{J_a^2}{2I_a} + \frac{J_b^2}{2I_b} + \frac{J_c^2}{2I_c} \tag{13.22}$$

This is the key equation. We described the quantum mechanical properties of angular momentum in Section 9.7b, and can now make use of them in conjunction with this equation to obtain the rotational energy levels.

(a) Spherical rotors

When all three moments of inertia are equal to some value I, as in CH_4 and SF_6, the classical expression for the energy is

$$E = \frac{J_a^2 + J_b^2 + J_c^2}{2I} = \frac{\mathcal{J}^2}{2I}$$

where $\mathcal{J}^2 = J_a^2 + J_b^2 + J_c^2$ is the square of the magnitude of the angular momentum. We can immediately find the quantum expression by making the replacement

$$\mathcal{J}^2 \to J(J+1)\hbar^2 \qquad J = 0, 1, 2, \ldots$$

Therefore, the energy of a spherical rotor is confined to the values

$$E_J = J(J+1)\frac{\hbar^2}{2I} \qquad J = 0, 1, 2, \ldots \tag{13.23}$$

The resulting ladder of energy levels is illustrated in Fig. 13.12. The energy is normally expressed in terms of the **rotational constant**, B, of the molecule, where

$$hcB = \frac{\hbar^2}{2I} \qquad \text{so} \qquad B = \frac{\hbar}{4\pi cI} \tag{13.24}$$

The expression for the energy is then

$$E_J = hcBJ(J+1) \qquad J = 0, 1, 2, \ldots \tag{13.25}$$

The rotational constant as defined by eqn 13.25 is a wavenumber. The energy of a rotational state is normally reported as the **rotational term**, $F(J)$, a wavenumber, by division by hc:

$$F(J) = BJ(J+1) \tag{13.26}$$

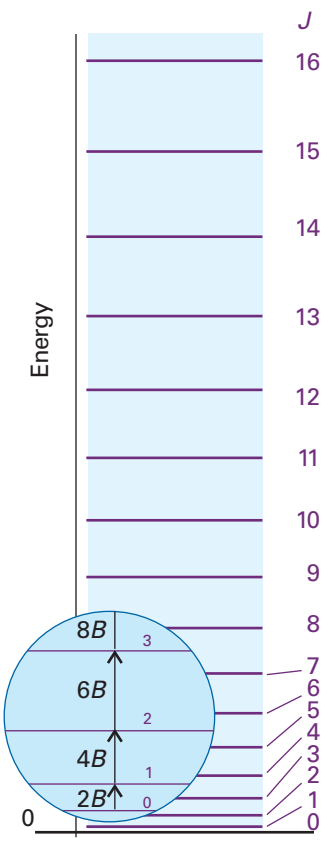

Fig. 13.12 The rotational energy levels of a linear or spherical rotor. Note that the energy separation between neighbouring levels increases as J increases.

Comment 13.4

The definition of B as a wavenumber is convenient when we come to vibration–rotation spectra. However, for pure rotational spectroscopy it is more common to define B as a frequency. Then $B = \hbar/4\pi cI$ and the energy is $E = hBJ(J+1)$.

The separation of adjacent levels is

$$F(J) - F(J-1) = 2BJ \tag{13.27}$$

Because the rotational constant decreases as I increases, we see that large molecules have closely spaced rotational energy levels. We can estimate the magnitude of the separation by considering CCl_4: from the bond lengths and masses of the atoms we find $I = 4.85 \times 10^{-45}$ kg m^2, and hence $B = 0.0577$ cm^{-1}.

(b) Symmetric rotors

In symmetric rotors, two moments of inertia are equal but different from the third (as in CH_3Cl, NH_3, and C_6H_6); the unique axis of the molecule is its **principal axis** (or *figure axis*). We shall write the unique moment of inertia (that about the principal axis) as $I_\parallel$ and the other two as $I_\perp$. If $I_\parallel > I_\perp$, the rotor is classified as **oblate** (like a pancake, and C_6H_6); if $I_\parallel < I_\perp$ it is classified as **prolate** (like a cigar, and CH_3Cl). The classical expression for the energy, eqn 13.22, becomes

$$E = \frac{J_b^2 + J_c^2}{2I_\perp} + \frac{J_a^2}{2I_\parallel}$$

Again, this expression can be written in terms of $\mathcal{J}^2 = J_a^2 + J_b^2 + J_c^2$:

$$E = \frac{\mathcal{J}^2 - J_a^2}{2I_\perp} + \frac{J_a^2}{2I_\parallel} = \frac{\mathcal{J}^2}{2I} + \left(\frac{1}{2I_\parallel} - \frac{1}{2I_\perp}\right)J_a^2 \tag{13.28}$$

Now we generate the quantum expression by replacing $\mathcal{J}^2$ by $J(J+1)\hbar^2$, where J is the angular momentum quantum number. We also know from the quantum theory of angular momentum (Section 9.7b) that the component of angular momentum about any axis is restricted to the values $K\hbar$, with $K = 0, \pm 1, \ldots, \pm J$. ($K$ is the quantum number used to signify a component on the principal axis; M_J is reserved for a component on an externally defined axis.) Therefore, we also replace J_a^2 by $K^2\hbar^2$. It follows that the rotational terms are

$$F(J,K) = BJ(J+1) + (A-B)K^2 \qquad J = 0, 1, 2, \ldots \qquad K = 0, \pm 1, \ldots, \pm J \tag{13.29}$$

with

$$A = \frac{\hbar}{4\pi c I_\parallel} \qquad B = \frac{\hbar}{4\pi c I_\perp} \tag{13.30}$$

Equation 13.29 matches what we should expect for the dependence of the energy levels on the two distinct moments of inertia of the molecule. When $K = 0$, there is no component of angular momentum about the principal axis, and the energy levels depend only on $I_\perp$ (Fig. 13.13). When $K = \pm J$, almost all the angular momentum arises from rotation around the principal axis, and the energy levels are determined largely by $I_\parallel$. The sign of K does not affect the energy because opposite values of K correspond to opposite senses of rotation, and the energy does not depend on the sense of rotation.

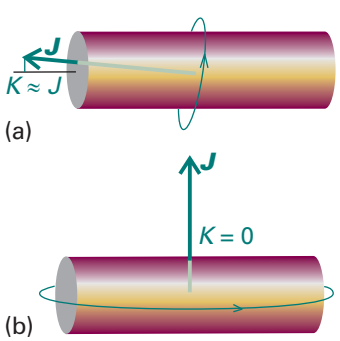

Fig. 13.13 The significance of the quantum number K. (a) When $|K|$ is close to its maximum value, J, most of the molecular rotation is around the figure axis. (b) When $K = 0$ the molecule has no angular momentum about its principal axis: it is undergoing end-over-end rotation.

Example 13.2 *Calculating the rotational energy levels of a molecule*

A $^{14}NH_3$ molecule is a symmetric rotor with bond length 101.2 pm and HNH bond angle 106.7°. Calculate its rotational terms.

A note on good practice To calculate moments of inertia precisely, we need to specify the nuclide.

Method Begin by calculating the rotational constants A and B by using the expressions for moments of inertia given in Table 13.1. Then use eqn 13.29 to find the rotational terms.

Answer Substitution of $m_A = 1.0078$ u, $m_B = 14.0031$ u, $R = 101.2$ pm, and $\theta = 106.7°$ into the second of the symmetric rotor expressions in Table 13.1 gives $I_{\parallel} = 4.4128 \times 10^{-47}$ kg m^2 and $I_{\perp} = 2.8059 \times 10^{-47}$ kg m^2. Hence, $A = 6.344$ cm^{-1} and $B = 9.977$ cm^{-1}. It follows from eqn 13.29 that

$$F(J,K)/\text{cm}^{-1} = 9.977J(J+1) - 3.633K^2$$

Upon multiplication by c, $F(J,K)$ acquires units of frequency:

$$F(J,K)/\text{GHz} = 299.1J(J+1) - 108.9K^2$$

For $J = 1$, the energy needed for the molecule to rotate mainly about its figure axis ($K = \pm J$) is equivalent to 16.32 cm^{-1} (489.3 GHz), but end-over-end rotation ($K = 0$) corresponds to 19.95 cm^{-1} (598.1 GHz).

Self-test 13.2 A $CH_3{}^{35}Cl$ molecule has a C—Cl bond length of 178 pm, a C—H bond length of 111 pm, and an HCH angle of 110.5°. Calculate its rotational energy terms.

[$F(J,K)/\text{cm}^{-1} = 0.444J(J+1) + 4.58K^2$; also $F(J,K)/\text{GHz} = 13.3J(J+1) + 137K^2$]

(c) Linear rotors

For a linear rotor (such as CO_2, HCl, and C_2H_2), in which the nuclei are regarded as mass points, the rotation occurs only about an axis perpendicular to the line of atoms and there is zero angular momentum around the line. Therefore, the component of angular momentum around the figure axis of a linear rotor is identically zero, and $K \equiv 0$ in eqn 13.29. The rotational terms of a linear molecule are therefore

$$F(J) = BJ(J+1) \qquad J = 0, 1, 2, \ldots \tag{13.31}$$

This expression is the same as eqn 13.26 but we have arrived at it in a significantly different way: here $K \equiv 0$ but for a spherical rotor $A = B$.

(d) Degeneracies and the Stark effect

The energy of a symmetric rotor depends on J and K, and each level except those with $K = 0$ is doubly degenerate: the states with K and $-K$ have the same energy. However, we must not forget that the angular momentum of the molecule has a component on an external, laboratory-fixed axis. This component is quantized, and its permitted values are $M_J\hbar$, with $M_J = 0, \pm 1, \ldots, \pm J$, giving $2J + 1$ values in all (Fig. 13.14). The quantum number M_J does not appear in the expression for the energy, but it is necessary for a complete specification of the state of the rotor. Consequently, all $2J + 1$ orientations of the rotating molecule have the same energy. It follows that a symmetric rotor level is $2(2J + 1)$-fold degenerate for $K \neq 0$ and $(2J + 1)$-fold degenerate for $K = 0$. A linear rotor has K fixed at 0, but the angular momentum may still have $2J + 1$ components on the laboratory axis, so its degeneracy is $2J + 1$.

A spherical rotor can be regarded as a version of a symmetric rotor in which A is equal to B: The quantum number K may still take any one of $2J + 1$ values, but the energy is independent of which value it takes. Therefore, as well as having a $(2J + 1)$-fold degeneracy arising from its orientation in space, the rotor also has a $(2J + 1)$-fold degeneracy arising from its orientation with respect to an arbitrary axis in the

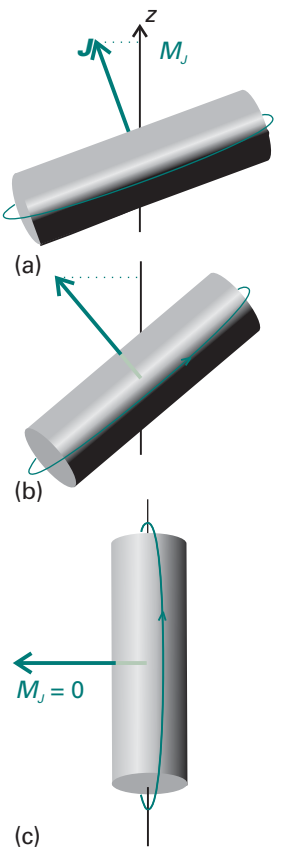

Fig. 13.14 The significance of the quantum number M_J. (a) When M_J is close to its maximum value, J, most of the molecular rotation is around the laboratory z-axis. (b) An intermediate value of M_J. (c) When $M_J = 0$ the molecule has no angular momentum about the z-axis All three diagrams correspond to a state with $K = 0$; there are corresponding diagrams for different values of K, in which the angular momentum makes a different angle to the molecule's principal axis.

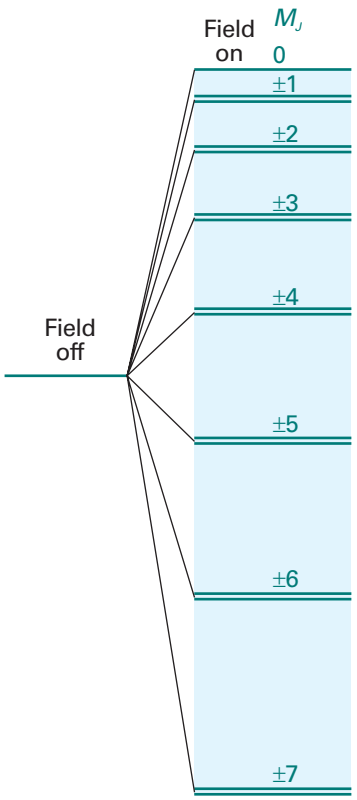

Fig. 13.15 The effect of an electric field on the energy levels of a polar linear rotor. All levels are doubly degenerate except that with $M_J = 0$.

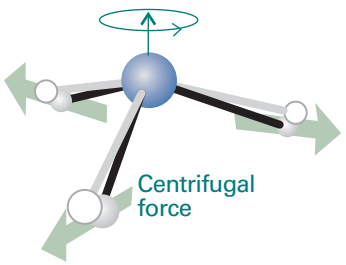

Fig. 13.16 The effect of rotation on a molecule. The centrifugal force arising from rotation distorts the molecule, opening out bond angles and stretching bonds slightly. The effect is to increase the moment of inertia of the molecule and hence to decrease its rotational constant.

molecule. The overall degeneracy of a symmetric rotor with quantum number J is therefore $(2J + 1)^2$. This degeneracy increases very rapidly: when $J = 10$, for instance, there are 441 states of the same energy.

The degeneracy associated with the quantum number M_J (the orientation of the rotation in space) is partly removed when an electric field is applied to a polar molecule (e.g. HCl or NH_3), as illustrated in Fig. 13.15. The splitting of states by an electric field is called the **Stark effect**. For a linear rotor in an electric field $\mathcal{E}$, the energy of the state with quantum numbers J and *M-J* is given by

$$E(J,M_J) = hcBJ(J+1) + a(J,M_J)\mu^2\mathcal{E}^2 \tag{13.32a}$$

where (see *Further reading* for a derivation)

$$a(J,M_J) = \frac{J(J+1) - 3M_J^2}{2hcBJ(J+1)(2J-1)(2J+3)} \tag{13.32b}$$

Note that the energy of a state with quantum number M_J depends on the square of the permanent electric dipole moment, μ. The observation of the Stark effect can therefore be used to measure this property, but the technique is limited to molecules that are sufficiently volatile to be studied by rotational spectroscopy. However, as spectra can be recorded for samples at pressures of only about 1 Pa and special techniques (such as using an intense laser beam or an electrical discharge) can be used to vaporize even some quite nonvolatile substances, a wide variety of samples may be studied. Sodium chloride, for example, can be studied as diatomic NaCl molecules at high temperatures.

(e) Centrifugal distortion

We have treated molecules as rigid rotors. However, the atoms of rotating molecules are subject to centrifugal forces that tend to distort the molecular geometry and change the moments of inertia (Fig. 13.16). The effect of centrifugal distortion on a diatomic molecule is to stretch the bond and hence to increase the moment of inertia. As a result, centrifugal distortion reduces the rotational constant and consequently the energy levels are slightly closer than the rigid-rotor expressions predict. The effect is usually taken into account largely empirically by subtracting a term from the energy and writing

$$F(J) = BJ(J+1) - D_J J^2(J+1)^2 \tag{13.33}$$

The parameter D_J is the **centrifugal distortion constant**. It is large when the bond is easily stretched. The centrifugal distortion constant of a diatomic molecule is related to the vibrational wavenumber of the bond, $\tilde{\nu}$ (which, as we shall see later, is a measure of its stiffness), through the approximate relation (see Problem 13.22)

$$D_J = \frac{4B^3}{\tilde{\nu}^2} \tag{13.34}$$

Hence the observation of the convergence of the rotational levels as J increases can be interpreted in terms of the rigidity of the bond.

13.6 Rotational transitions

Typical values of B for small molecules are in the region of 0.1 to10 cm^{-1} (for example, 0.356 cm^{-1} for NF_3 and 10.59 cm^{-1} for HCl), so rotational transitions lie in the microwave region of the spectrum. The transitions are detected by monitoring the net absorption of microwave radiation. Modulation of the transmitted intensity can be achieved by varying the energy levels with an oscillating electric field. In this **Stark**

modulation, an electric field of about 10^5 V m^{-1} and a frequency of between 10 and 100 kHz is applied to the sample.

(a) Rotational selection rules

We have already remarked (Section 13.2) that the gross selection rule for the observation of a pure rotational spectrum is that a molecule must have a permanent electric dipole moment. That is, *for a molecule to give a pure rotational spectrum, it must be polar*. The classical basis of this rule is that a polar molecule appears to possess a fluctuating dipole when rotating, but a nonpolar molecule does not (Fig.13.17). The permanent dipole can be regarded as a handle with which the molecule stirs the electromagnetic field into oscillation (and vice versa for absorption). Homonuclear diatomic molecules and symmetrical linear molecules such as CO_2 are rotationally inactive. Spherical rotors cannot have electric dipole moments unless they become distorted by rotation, so they are also inactive except in special cases. An example of a spherical rotor that does become sufficiently distorted for it to acquire a dipole moment is SiH_4, which has a dipole moment of about 8.3 μD by virtue of its rotation when $J \approx 10$ (for comparison, HCl has a permanent dipole moment of 1.1 D; molecular dipole moments and their units are discussed in Section 18.1). The pure rotational spectrum of SiH_4 has been detected by using long path lengths (10 m) through high-pressure (4 atm) samples.

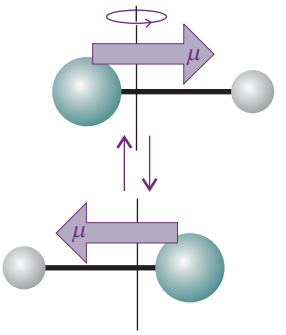

Fig. 13.17 To a stationary observer, a rotating polar molecule looks like an oscillating dipole that can stir the electromagnetic field into oscillation (and vice versa for absorption). This picture is the classical origin of the gross selection rule for rotational transitions.

Illustration 13.2 *Identifying rotationally active molecules*

Of the molecules N_2, CO_2, OCS, H_2O, $CH_2{=}CH_2$, C_6H_6, only OCS and H_2O are polar, so only these two molecules have microwave spectra.

Self-test 13.3 Which of the molecules H_2, NO, N_2O, CH_4 can have a pure rotational spectrum? [NO, N_2O]

The specific rotational selection rules are found by evaluating the transition dipole moment between rotational states. We show in *Further information 13.2* that, for a linear molecule, the transition moment vanishes unless the following conditions are fulfilled:

$$\Delta J = \pm 1 \qquad \Delta M_J = 0, \pm 1 \tag{13.35}$$

The transition $\Delta J = +1$ corresponds to absorption and the transition $\Delta J = -1$ corresponds to emission. The allowed change in J in each case arises from the conservation of angular momentum when a photon, a spin-1 particle, is emitted or absorbed (Fig. 13.18).

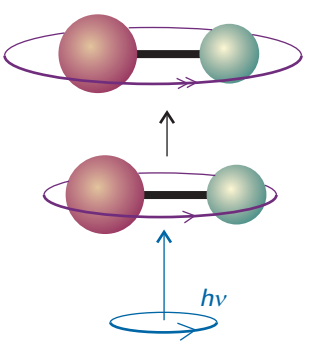

Fig. 13.18 When a photon is absorbed by a molecule, the angular momentum of the combined system is conserved. If the molecule is rotating in the same sense as the spin of the incoming photon, then J increases by 1.

When the transition moment is evaluated for all possible relative orientations of the molecule to the line of flight of the photon, it is found that the total $J + 1 \leftrightarrow J$ transition intensity is proportional to

$$|\mu_{J+1,J}|^2 = \left(\frac{J+1}{2J+1}\right)\mu_0^2 \rightarrow \tfrac{1}{2}\mu_0^2 \qquad \text{for } J \gg 1 \tag{13.36}$$

where μ_0 is the permanent electric dipole moment of the molecule. The intensity is proportional to the square of the permanent electric dipole moment, so strongly polar molecules give rise to much more intense rotational lines than less polar molecules.

For symmetric rotors, an additional selection rule states that $\Delta K = 0$. To understand this rule, consider the symmetric rotor NH_3, where the electric dipole moment lies

parallel to the figure axis. Such a molecule cannot be accelerated into different states of rotation around the figure axis by the absorption of radiation, so $\Delta K = 0$.

(b) The appearance of rotational spectra

When these selection rules are applied to the expressions for the energy levels of a rigid symmetric or linear rotor, it follows that the wavenumbers of the allowed $J + 1 \leftarrow J$ absorptions are

$$\tilde{\nu}(J+1 \leftarrow J) = 2B(J+1) \qquad J = 0, 1, 2, \ldots \tag{13.37}$$

When centrifugal distortion is taken into account, the corresponding expression is

$$\tilde{\nu}(J+1 \leftarrow J) = 2B(J+1) - 4D_J(J+1)^3 \tag{13.38}$$

However, because the second term is typically very small compared with the first, the appearance of the spectrum closely resembles that predicted from eqn 13.37.

Example 13.3 *Predicting the appearance of a rotational spectrum*

Predict the form of the rotational spectrum of $^{14}NH_3$.

Method We calculated the energy levels in Example 13.2. The $^{14}NH_3$ molecule is a polar symmetric rotor, so the selection rules $\Delta J = \pm 1$ and $\Delta K = 0$ apply. For absorption, $\Delta J = +1$ and we can use eqn 13.37. Because $B = 9.977\ \text{cm}^{-1}$, we can draw up the following table for the $J + 1 \leftarrow J$ transitions.

J	0	1	2	3	...
$\tilde{\nu}/\text{cm}^{-1}$	19.95	39.91	59.86	79.82	...
ν/GHz	598.1	1197	1795	2393	...

The line spacing is 19.95 cm^{-1} (598.1 GHz).

Self-test 13.4 Repeat the problem for $C^{35}ClH_3$ (see Self-test 13.2 for details).
[Lines of separation 0.888 cm^{-1} (26.6 GHz)]

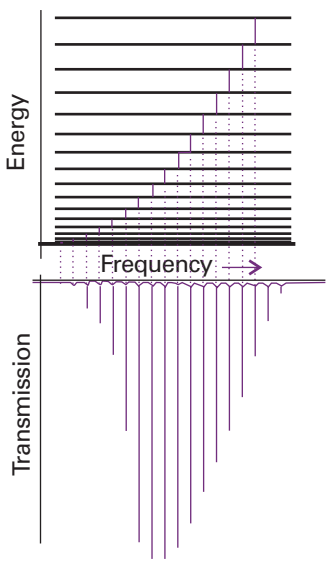

Fig. 13.19 The rotational energy levels of a linear rotor, the transitions allowed by the selection rule $\Delta J = \pm 1$, and a typical pure rotational absorption spectrum (displayed here in terms of the radiation transmitted through the sample). The intensities reflect the populations of the initial level in each case and the strengths of the transition dipole moments.

The form of the spectrum predicted by eqn 13.37 is shown in Fig. 13.19. The most significant feature is that it consists of a series of lines with wavenumbers $2B$, $4B$, $6B$, ... and of separation $2B$. The measurement of the line spacing gives B, and hence the moment of inertia perpendicular to the principal axis of the molecule. Because the masses of the atoms are known, it is a simple matter to deduce the bond length of a diatomic molecule. However, in the case of a polyatomic molecule such as OCS or NH_3, the analysis gives only a single quantity, $I_\perp$, and it is not possible to infer both bond lengths (in OCS) or the bond length and bond angle (in NH_3). This difficulty can be overcome by using isotopically substituted molecules, such as ABC and A′BC; then, by assuming that R(A—B) = R(A′—B), both A—B and B—C bond lengths can be extracted from the two moments of inertia. A famous example of this procedure is the study of OCS; the actual calculation is worked through in Problem 13.10. The assumption that bond lengths are unchanged by isotopic substitution is only an approximation, but it is a good approximation in most cases.

The intensities of spectral lines increase with increasing J and pass through a maximum before tailing off as J becomes large. The most important reason for the maximum in intensity is the existence of a maximum in the population of rotational levels. The Boltzmann distribution (*Molecular interpretation 3.1*) implies that the population of each state decays exponentially with increasing J, but the degeneracy of the levels

increases. Specifically, the population of a rotational energy level J is given by the Boltzmann expression

$$N_J \propto N g_J e^{-E_J/kT}$$

where N is the total number of molecules and g_J is the degeneracy of the level J. The value of J corresponding to a maximum of this expression is found by treating J as a continuous variable, differentiating with respect to J, and then setting the result equal to zero. The result is (see Problem 13.24)

$$J_{\max} \approx \left(\frac{kT}{2hcB}\right)^{1/2} - \tfrac{1}{2} \qquad (13.39)$$

For a typical molecule (for example, OCS, with $B = 0.2\ \text{cm}^{-1}$) at room temperature, $kT \approx 1000hcB$, so $J_{\max} \approx 30$. However, it must be recalled that the intensity of each transition also depends on the value of J (eqn 13.36) and on the population difference between the two states involved in the transition (see Section 13.2). Hence the value of J corresponding to the most intense line is not quite the same as the value of J for the most highly populated level.

13.7 Rotational Raman spectra

The gross selection rule for rotational Raman transitions is *that the molecule must be anisotropically polarizable*. We begin by explaining what this means. A formal derivation of this rule is given in *Further information 13.2*.

The distortion of a molecule in an electric field is determined by its polarizability, α (Section 18.2). More precisely, if the strength of the field is $\mathcal{E}$, then the molecule acquires an induced dipole moment of magnitude

$$\mu = \alpha\mathcal{E} \qquad (13.40)$$

in addition to any permanent dipole moment it may have. An atom is isotropically polarizable. That is, the same distortion is induced whatever the direction of the applied field. The polarizability of a spherical rotor is also isotropic. However, nonspherical rotors have polarizabilities that do depend on the direction of the field relative to the molecule, so these molecules are anisotropically polarizable (Fig. 13.20). The electron distribution in H_2, for example, is more distorted when the field is applied parallel to the bond than when it is applied perpendicular to it, and we write $\alpha_\parallel > \alpha_\perp$.

All linear molecules and diatomics (whether homonuclear or heteronuclear) have anisotropic polarizabilities, and so are rotationally Raman active. This activity is one reason for the importance of rotational Raman spectroscopy, for the technique can be used to study many of the molecules that are inaccessible to microwave spectroscopy. Spherical rotors such as CH_4 and SF_6, however, are rotationally Raman inactive as well as microwave inactive. This inactivity does not mean that such molecules are never found in rotationally excited states. Molecular collisions do not have to obey such restrictive selection rules, and hence collisions between molecules can result in the population of any rotational state.

We show in *Further information 13.2* that the specific rotational Raman selection rules are

$$\text{Linear rotors:} \quad \Delta J = 0, \pm 2 \qquad (13.41)$$

$$\text{Symmetric rotors:} \quad \Delta J = 0, \pm 1, \pm 2; \quad \Delta K = 0$$

The $\Delta J = 0$ transitions do not lead to a shift of the scattered photon's frequency in pure rotational Raman spectroscopy, and contribute to the unshifted Rayleigh radiation.

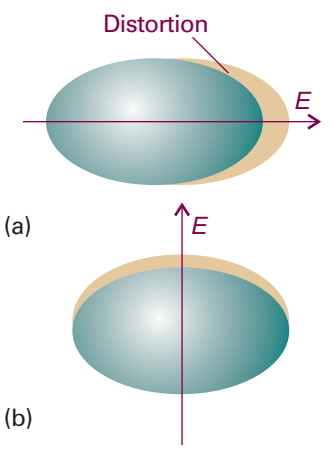

Fig. 13.20 An electric field applied to a molecule results in its distortion, and the distorted molecule acquires a contribution to its dipole moment (even if it is nonpolar initially). The polarizability may be different when the field is applied (a) parallel or (b) perpendicular to the molecular axis (or, in general, in different directions relative to the molecule); if that is so, then the molecule has an anisotropic polarizability.

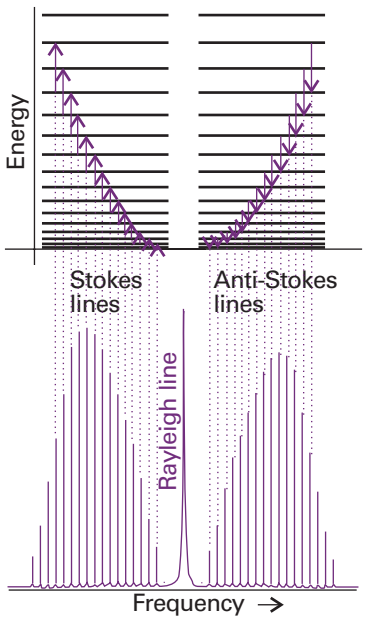

Fig. 13.21 The rotational energy levels of a linear rotor and the transitions allowed by the $\Delta J = \pm 2$ Raman selection rules. The form of a typical rotational Raman spectrum is also shown. The Rayleigh line is much stronger than depicted in the figure; it is shown as a weaker line to improve visualization of the Raman lines.

We can predict the form of the Raman spectrum of a linear rotor by applying the selection rule $\Delta J = \pm 2$ to the rotational energy levels (Fig. 13.21). When the molecule makes a transition with $\Delta J = +2$, the scattered radiation leaves the molecule in a higher rotational state, so the wavenumber of the incident radiation, initially $\tilde{\nu}_i$, is decreased. These transitions account for the Stokes lines in the spectrum:

$$\tilde{\nu}(J+2 \leftarrow J) = \tilde{\nu}_i - \{F(J+2) - F(J)\} = \tilde{\nu}_i - 2B(2J+3) \qquad (13.42a)$$

The Stokes lines appear to low frequency of the incident radiation and at displacements $6B$, $10B$, $14B$, ... from $\tilde{\nu}_i$ for $J = 0, 1, 2, \ldots$. When the molecule makes a transition with $\Delta J = -2$, the scattered photon emerges with increased energy. These transitions account for the anti-Stokes lines of the spectrum:

$$\tilde{\nu}(J-2 \leftarrow J) = \tilde{\nu}_i + \{F(J) - F(J-2)\} = \tilde{\nu}_i + 2B(2J-1) \qquad (13.42b)$$

The anti-Stokes lines occur at displacements of $6B$, $10B$, $14B$, ... (for $J = 2, 3, 4, \ldots$; $J = 2$ is the lowest state that can contribute under the selection rule $\Delta J = -2$) to high frequency of the incident radiation. The separation of adjacent lines in both the Stokes and the anti-Stokes regions is $4B$, so from its measurement $I_\perp$ can be determined and then used to find the bond lengths exactly as in the case of microwave spectroscopy.

Example 13.4 *Predicting the form of a Raman spectrum*

Predict the form of the rotational Raman spectrum of $^{14}N_2$, for which $B = 1.99\ \text{cm}^{-1}$, when it is exposed to monochromatic 336.732 nm laser radiation.

Method The molecule is rotationally Raman active because end-over-end rotation modulates its polarizability as viewed by a stationary observer. The Stokes and anti-Stokes lines are given by eqn 13.42.

Answer Because $\lambda_i = 336.732$ nm corresponds to $\tilde{\nu}_i = 29\,697.2\ \text{cm}^{-1}$, eqns 13.42a and 13.42b give the following line positions:

J	0	1	2	3
Stokes lines				
$\tilde{\nu}/\text{cm}^{-1}$	29 685.3	29 677.3	29 669.3	29 661.4
λ/nm	336.868	336.958	337.048	337.139
Anti-Stokes lines				
$\tilde{\nu}/\text{cm}^{-1}$			29 709.1	29 717.1
λ/nm			336.597	336.507

There will be a strong central line at 336.732 nm accompanied on either side by lines of increasing and then decreasing intensity (as a result of transition moment and population effects). The spread of the entire spectrum is very small, so the incident light must be highly monochromatic.

Self-test 13.5 Repeat the calculation for the rotational Raman spectrum of NH_3 ($B = 9.977\ \text{cm}^{-1}$).

[Stokes lines at 29 637.3, 29 597.4, 29 557.5, 29 517.6 cm^{-1}, anti-Stokes lines at 29 757.1, 29 797.0 cm^{-1}.]

13.8 Nuclear statistics and rotational states

If eqn 13.42 is used in conjunction with the rotational Raman spectrum of CO_2, the rotational constant is inconsistent with other measurements of C—O bond lengths.

The results are consistent only if it is supposed that the molecule can exist in states with even values of J, so the Stokes lines are $2 \leftarrow 0, 4 \leftarrow 2, \ldots$ and not $2 \leftarrow 0, 3 \leftarrow 1, \ldots$.

The explanation of the missing lines is the Pauli principle and the fact that O nuclei are spin-0 bosons: just as the Pauli principle excludes certain electronic states, so too does it exclude certain molecular rotational states. The form of the Pauli principle given in *Justification Section 10.4* states that, when two identical bosons are exchanged, the overall wavefunction must remain unchanged in every respect, including sign. In particular, when a CO_2 molecule rotates through 180°, two identical O nuclei are interchanged, so the overall wavefunction of the molecule must remain unchanged. However, inspection of the form of the rotational wavefunctions (which have the same form as the s, p, etc. orbitals of atoms) shows that they change sign by $(-1)^J$ under such a rotation (Fig. 13.22). Therefore, only even values of J are permissible for CO_2, and hence the Raman spectrum shows only alternate lines.

The selective occupation of rotational states that stems from the Pauli principle is termed **nuclear statistics**. Nuclear statistics must be taken into account whenever a rotation interchanges equivalent nuclei. However, the consequences are not always as simple as for CO_2 because there are complicating features when the nuclei have nonzero spin: there may be several different relative nuclear spin orientations consistent with even values of J and a different number of spin orientations consistent with odd values of J. For molecular hydrogen and fluorine, for instance, with their two identical spin-$\frac{1}{2}$ nuclei, we show in the *Justification* below that there are three times as many ways of achieving a state with odd J than with even J, and there is a corresponding 3:1 alternation in intensity in their rotational Raman spectra (Fig. 13.23). In general, for a homonuclear diatomic molecule with nuclei of spin I, the numbers of ways of achieving states of odd and even J are in the ratio

$$\frac{\text{Number of ways of achieving odd } J}{\text{Number of ways of achieving even } J} = \begin{cases} (I+1)/I \text{ for half-integral spin nuclei} \\ I/(I+1) \text{ for integral spin nuclei} \end{cases} \tag{13.43}$$

For hydrogen, $I = \frac{1}{2}$, and the ratio is 3:1. For N_2, with $I = 1$, the ratio is 1:2.

Justification 13.4 *The effect of nuclear statistics on rotational spectra*

Hydrogen nuclei are fermions, so the Pauli principle requires the overall wavefunction to change sign under particle interchange. However, the rotation of an H_2 molecule through 180° has a more complicated effect than merely relabelling the nuclei, because it interchanges their spin states too if the nuclear spins are paired ($\uparrow\downarrow$) but not if they are parallel ($\uparrow\uparrow$).

For the overall wavefunction of the molecule to change sign when the spins are parallel, the rotational wavefunction must change sign. Hence, only odd values of J are allowed. In contrast, if the nuclear spins are paired, their wavefunction is $\alpha(\mathrm{A})\beta(\mathrm{B}) - \alpha(\mathrm{B})\beta(\mathrm{A})$, which changes sign when α and β are exchanged in order to bring about a simple $\mathrm{A} \leftrightarrow \mathrm{B}$ interchange overall (Fig. 13.24). Therefore, for the overall wavefunction to change sign in this case requires the rotational wavefunction *not* to change sign. Hence, only even values of J are allowed if the nuclear spins are paired.

As there are three nuclear spin states with parallel spins (just like the triplet state of two parallel electrons, as in Fig. 10.24), but only one state with paired spins (the analogue of the singlet state of two electrons, see Fig. 10.18), it follows that the populations of the odd J and even J states should be in the ratio of 3:1, and hence the intensities of transitions originating in these levels will be in the same ratio.

Different relative nuclear spin orientations change into one another only very slowly, so an H_2 molecule with parallel nuclear spins remains distinct from one with

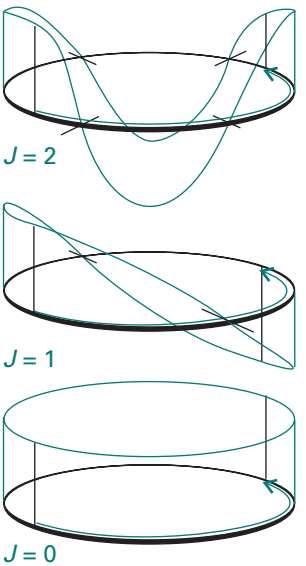

Fig. 13.22 The symmetries of rotational wavefunctions (shown here, for simplicity as a two-dimensional rotor) under a rotation through 180°. Wavefunctions with J even do not change sign; those with J odd do change sign.

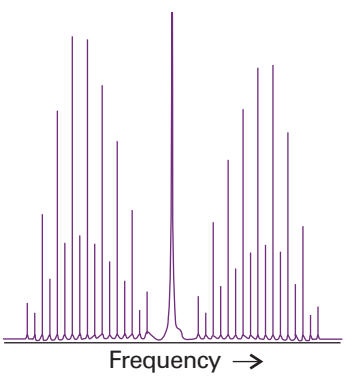

Fig. 13.23 The rotational Raman spectrum of a diatomic molecule with two identical spin-$\frac{1}{2}$ nuclei shows an alternation in intensity as a result of nuclear statistics. The Rayleigh line is much stronger than depicted in the figure; it is shown as a weaker line to improve visualization of the Raman lines.

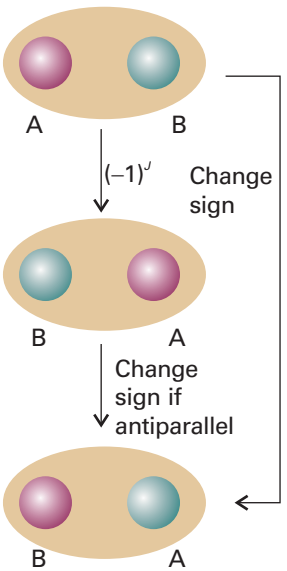

Fig. 13.24 The interchange of two identical fermion nuclei results in the change in sign of the overall wavefunction. The relabelling can be thought of as occurring in two steps: the first is a rotation of the molecule; the second is the interchange of unlike spins (represented by the different colours of the nuclei). The wavefunction changes sign in the second step if the nuclei have antiparallel spins.

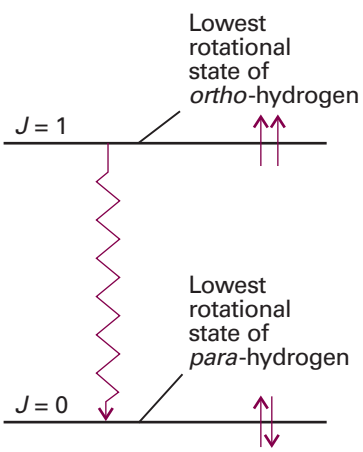

Fig. 13.25 When hydrogen is cooled, the molecules with parallel nuclear spins accumulate in their lowest available rotational state, the one with $J = 0$. They can enter the lowest rotational state ($J = 0$) only if the spins change their relative orientation and become antiparallel. This is a slow process under normal circumstances, so energy is slowly released.

paired nuclear spins for long periods. The two forms of hydrogen can be separated by physical techniques, and stored. The form with parallel nuclear spins is called ***ortho*-hydrogen** and the form with paired nuclear spins is called ***para*-hydrogen**. Because *ortho*-hydrogen cannot exist in a state with $J = 0$, it continues to rotate at very low temperatures and has an effective rotational zero-point energy (Fig. 13.25). This energy is of some concern to manufacturers of liquid hydrogen, for the slow conversion of *ortho*-hydrogen into *para*-hydrogen (which can exist with $J = 0$) as nuclear spins slowly realign releases rotational energy, which vaporizes the liquid. Techniques are used to accelerate the conversion of *ortho*-hydrogen to *para*-hydrogen to avoid this problem. One such technique is to pass hydrogen over a metal surface: the molecules adsorb on the surface as atoms, which then recombine in the lower energy *para*-hydrogen form.

The vibrations of diatomic molecules

In this section, we adopt the same strategy of finding expressions for the energy levels, establishing the selection rules, and then discussing the form of the spectrum. We shall also see how the simultaneous excitation of rotation modifies the appearance of a vibrational spectrum.

13.9 Molecular vibrations

We base our discussion on Fig. 13.26, which shows a typical potential energy curve (as in Fig. 11.1) of a diatomic molecule. In regions close to R_e (at the minimum of the curve) the potential energy can be approximated by a parabola, so we can write

$$V = \tfrac{1}{2}kx^2 \qquad x = R - R_e \tag{13.44}$$

where k is the **force constant** of the bond. The steeper the walls of the potential (the stiffer the bond), the greater the force constant.

To see the connection between the shape of the molecular potential energy curve and the value of k, note that we can expand the potential energy around its minimum by using a Taylor series:

$$V(x) = V(0) + \left(\frac{dV}{dx}\right)_0 x + \tfrac{1}{2}\left(\frac{d^2V}{dx^2}\right)_0 x^2 + \cdots \tag{13.45}$$

The term $V(0)$ can be set arbitrarily to zero. The first derivative of V is 0 at the minimum. Therefore, the first surviving term is proportional to the square of the displacement. For small displacements we can ignore all the higher terms, and so write

$$V(x) \approx \tfrac{1}{2}\left(\frac{d^2V}{dx^2}\right)_0 x^2 \tag{13.46}$$

Therefore, the first approximation to a molecular potential energy curve is a parabolic potential, and we can identify the force constant as

$$k = \left(\frac{d^2V}{dx^2}\right)_0 \tag{13.47}$$

We see that if the potential energy curve is sharply curved close to its minimum, then k will be large. Conversely, if the potential energy curve is wide and shallow, then k will be small (Fig. 13.27).

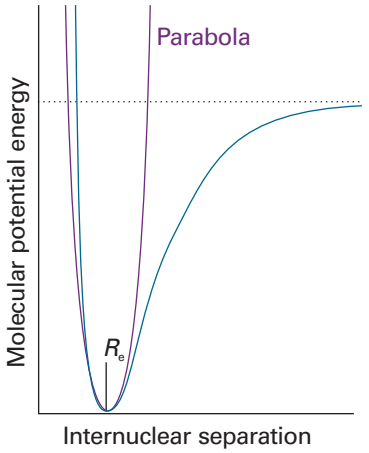

Fig. 13.26 A molecular potential energy curve can be approximated by a parabola near the bottom of the well. The parabolic potential leads to harmonic oscillations. At high excitation energies the parabolic approximation is poor (the true potential is less confining), and it is totally wrong near the dissociation limit.

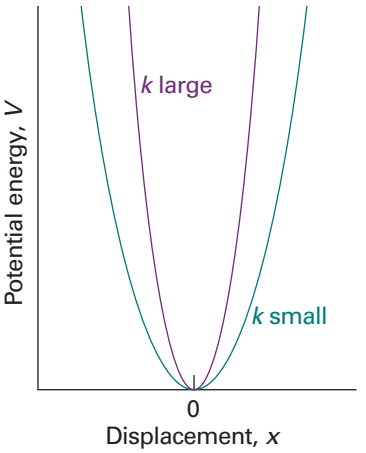

Fig. 13.27 The force constant is a measure of the curvature of the potential energy close to the equilibrium extension of the bond. A strongly confining well (one with steep sides, a stiff bond) corresponds to high values of k.

Comment 13.5

It is often useful to express a function $f(x)$ in the vicinity of $x = a$ as an infinite Taylor series of the form:

$$f(x) = f(a) + \left(\frac{df}{dx}\right)_a (x-a) + \frac{1}{2!}\left(\frac{d^2f}{dx^2}\right)_a (x-a)^2 + \cdots + \frac{1}{n!}\left(\frac{d^nf}{dx^n}\right)_a (x-a)^n + \cdots$$

where $n = 0, 1, 2, \ldots$.

The Schrödinger equation for the relative motion of two atoms of masses m_1 and m_2 with a parabolic potential energy is

$$-\frac{\hbar^2}{2m_{\text{eff}}}\frac{d^2\psi}{dx^2} + \tfrac{1}{2}kx^2\psi = E\psi \qquad (13.48)$$

where m_{eff} is the **effective mass**:

$$m_{\text{eff}} = \frac{m_1 m_2}{m_1 + m_2} \qquad [13.49]$$

These equations are derived in the same way as in *Further information 10.1*, but here the separation of variables procedure is used to separate the relative motion of the atoms from the motion of the molecule as a whole. In that context, the effective mass is called the 'reduced mass', and the name is widely used in this context too.

The Schrödinger equation in eqn 13.48 is the same as eqn 9.24 for a particle of mass m undergoing harmonic motion. Therefore, we can use the results of Section 9.4 to write down the permitted vibrational energy levels:

$$E_v = (v + \tfrac{1}{2})\hbar\omega \qquad \omega = \left(\frac{k}{m_{\text{eff}}}\right)^{1/2} \qquad v = 0, 1, 2, \ldots \qquad (13.50)$$

The **vibrational terms** of a molecule, the energies of its vibrational states expressed in wavenumbers, are denoted $G(v)$, with $E_v = hcG(v)$, so

$$G(v) = (v + \tfrac{1}{2})\tilde{\nu} \qquad \tilde{\nu} = \frac{1}{2\pi c}\left(\frac{k}{m_{\text{eff}}}\right)^{1/2} \qquad (13.51)$$

The vibrational wavefunctions are the same as those discussed in Section 9.5.

It is important to note that the vibrational terms depend on the effective mass of the molecule, not directly on its total mass. This dependence is physically reasonable, for if atom 1 were as heavy as a brick wall, then we would find $m_{\text{eff}} \approx m_2$, the mass of the

lighter atom. The vibration would then be that of a light atom relative to that of a stationary wall (this is approximately the case in HI, for example, where the I atom barely moves and $m_{\text{eff}} \approx m_{\text{H}}$). For a homonuclear diatomic molecule $m_1 = m_2$, and the effective mass is half the total mass: $m_{\text{eff}} = \frac{1}{2}m$.

Illustration 13.3 *Calculating a vibrational wavenumber*

An HCl molecule has a force constant of 516 N m^{-1}, a reasonably typical value for a single bond. The effective mass of $^{1}H^{35}Cl$ is 1.63×10^{-27} kg (note that this mass is very close to the mass of the hydrogen atom, 1.67×10^{-27} kg, so the Cl atom is acting like a brick wall). These values imply $\omega = 5.63 \times 10^{14}$ s^{-1}, $\nu = 89.5$ THz (1 THz $= 10^{12}$ Hz), $\tilde{\nu} = 2990$ cm^{-1}, $\lambda = 3.35$ μm. These characteristics correspond to electromagnetic radiation in the infrared region.

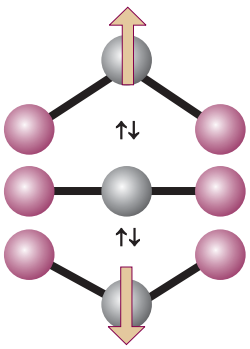

Fig. 13.28 The oscillation of a molecule, even if it is nonpolar, may result in an oscillating dipole that can interact with the electromagnetic field.

13.10 Selection rules

The gross selection rule for a change in vibrational state brought about by absorption or emission of radiation is that *the electric dipole moment of the molecule must change when the atoms are displaced relative to one another*. Such vibrations are said to be **infrared active**. The classical basis of this rule is that the molecule can shake the electromagnetic field into oscillation if its dipole changes as it vibrates, and vice versa (Fig. 13.28); its formal basis is given in *Further information 13.2*. Note that the molecule need not have a permanent dipole: the rule requires only a change in dipole moment, possibly from zero. Some vibrations do not affect the molecule's dipole moment (e.g. the stretching motion of a homonuclear diatomic molecule), so they neither absorb nor generate radiation: such vibrations are said to be **infrared inactive**. Homonuclear diatomic molecules are infrared inactive because their dipole moments remain zero however long the bond; heteronuclear diatomic molecules are infrared active.

Illustration 13.4 *Identifying infrared active molecules*

Of the molecules N_2, CO_2, OCS, H_2O, $CH_2{=}CH_2$, and C_6H_6, all except N_2 possess at least one vibrational mode that results in a change of dipole moment, so all except N_2 can show a vibrational absorption spectrum. Not all the modes of complex molecules are vibrationally active. For example, the symmetric stretch of CO_2, in which the O—C—O bonds stretch and contract symmetrically is inactive because it leaves the dipole moment unchanged (at zero).

Self-test 13.6 Which of the molecules H_2, NO, N_2O, and CH_4 have infrared active vibrations? [NO, N_2O, CH_4]

The specific selection rule, which is obtained from an analysis of the expression for the transition moment and the properties of integrals over harmonic oscillator wavefunctions (as shown in *Further information 13.2*), is

$$\Delta v = \pm 1 \tag{13.52}$$

Transitions for which $\Delta v = +1$ correspond to absorption and those with $\Delta v = -1$ correspond to emission.

It follows from the specific selection rules that the wavenumbers of allowed vibrational transitions, which are denoted $\Delta G_{v+\frac{1}{2}}$ for the transition $v+1 \leftarrow v$, are

$$\Delta G_{v+\frac{1}{2}} = G(v+1) - G(v) = \tilde{\nu} \tag{13.53}$$

As we have seen, $\tilde{\nu}$ lies in the infrared region of the electromagnetic spectrum, so vibrational transitions absorb and generate infrared radiation.

At room temperature $kT/hc \approx 200\ \text{cm}^{-1}$, and most vibrational wavenumbers are significantly greater than $200\ \text{cm}^{-1}$. It follows from the Boltzmann distribution that almost all the molecules will be in their vibrational ground states initially. Hence, the dominant spectral transition will be the **fundamental transition**, $1 \leftarrow 0$. As a result, the spectrum is expected to consist of a single absorption line. If the molecules are formed in a vibrationally excited state, such as when vibrationally excited HF molecules are formed in the reaction $H_2 + F_2 \rightarrow 2\,HF^*$, the transitions $5 \rightarrow 4$, $4 \rightarrow 3$, . . . may also appear (in emission). In the harmonic approximation, all these lines lie at the same frequency, and the spectrum is also a single line. However, as we shall now show, the breakdown of the harmonic approximation causes the transitions to lie at slightly different frequencies, so several lines are observed.

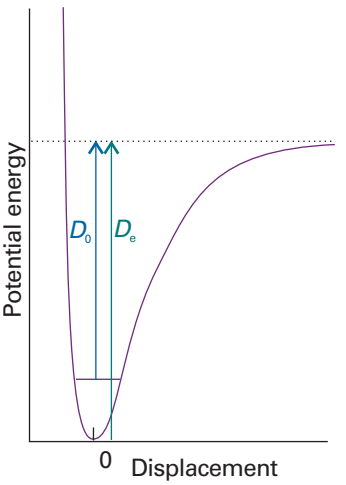

Fig. 13.29 The dissociation energy of a molecule, D_0, differs from the depth of the potential well, D_e, on account of the zero-point energy of the vibrations of the bond.

13.11 Anharmonicity

The vibrational terms in eqn 13.53 are only approximate because they are based on a parabolic approximation to the actual potential energy curve. A parabola cannot be correct at all extensions because it does not allow a bond to dissociate. At high vibrational excitations the swing of the atoms (more precisely, the spread of the vibrational wavefunction) allows the molecule to explore regions of the potential energy curve where the parabolic approximation is poor and additional terms in the Taylor expansion of V (eqn 13.45) must be retained. The motion then becomes **anharmonic**, in the sense that the restoring force is no longer proportional to the displacement. Because the actual curve is less confining than a parabola, we can anticipate that the energy levels become less widely spaced at high excitations.

(a) The convergence of energy levels

One approach to the calculation of the energy levels in the presence of anharmonicity is to use a function that resembles the true potential energy more closely. The **Morse potential energy** is

$$V = hcD_e\{1 - e^{-a(R-R_e)}\}^2 \qquad a = \left(\frac{m_{\text{eff}}\omega^2}{2hcD_e}\right)^{1/2} \tag{13.54}$$

where D_e is the depth of the potential minimum (Fig. 13.29). Near the well minimum the variation of V with displacement resembles a parabola (as can be checked by expanding the exponential as far as the first term) but, unlike a parabola, eqn 13.54 allows for dissociation at large displacements. The Schrödinger equation can be solved for the Morse potential and the permitted energy levels are

$$G(v) = (v+\tfrac{1}{2})\tilde{\nu} - (v+\tfrac{1}{2})^2 x_e\tilde{\nu} \qquad x_e = \frac{a^2\hbar}{2m_{\text{eff}}\omega} = \frac{\tilde{\nu}}{4D_e} \tag{13.55}$$

The parameter x_e is called the **anharmonicity constant**. The number of vibrational levels of a Morse oscillator is finite, and $v = 0, 1, 2, \ldots, v_{\text{max}}$, as shown in Fig. 13.30 (see also Problem 13.26). The second term in the expression for G subtracts from the first with increasing effect as v increases, and hence gives rise to the convergence of the levels at high quantum numbers.

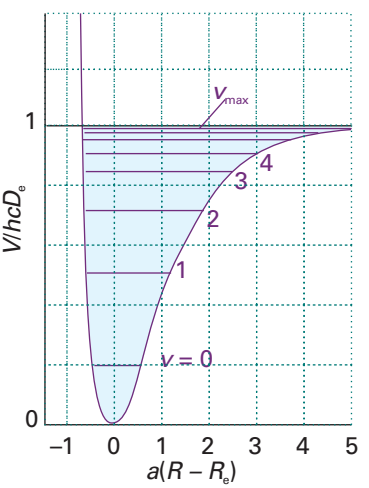

Fig. 13.30 The Morse potential energy curve reproduces the general shape of a molecular potential energy curve. The corresponding Schrödinger equation can be solved, and the values of the energies obtained. The number of bound levels is finite.

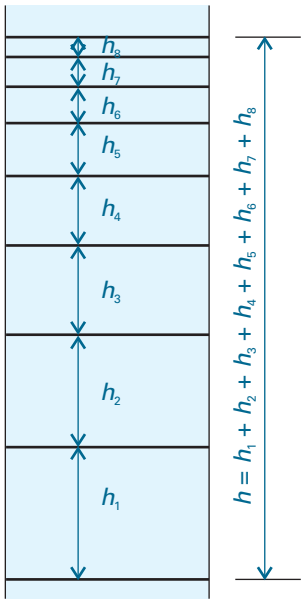

Fig. 13.31 The dissociation energy is the sum of the separations of the vibrational energy levels up to the dissociation limit just as the length of a ladder is the sum of the separations of its rungs.

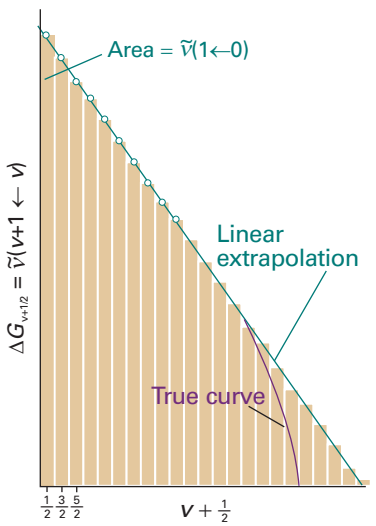

Fig. 13.32 The area under a plot of transition wavenumber against vibrational quantum number is equal to the dissociation energy of the molecule. The assumption that the differences approach zero linearly is the basis of the Birge–Sponer extrapolation.

Although the Morse oscillator is quite useful theoretically, in practice the more general expression

$$G(v) = (v+\tfrac{1}{2})\tilde{\nu} - (v+\tfrac{1}{2})^2 x_e\tilde{\nu} + (v+\tfrac{1}{2})^3 y_e\tilde{\nu} + \cdots \qquad (13.56)$$

where x_e, y_e, ... are empirical dimensionless constants characteristic of the molecule, is used to fit the experimental data and to find the dissociation energy of the molecule. When anharmonicities are present, the wavenumbers of transitions with $\Delta v = +1$ are

$$\Delta G_{v+\frac{1}{2}} = \tilde{\nu} - 2(v+1)x_e\tilde{\nu} + \cdots \qquad (13.57)$$

Equation 13.57 shows that, when $x_e > 0$, the transitions move to lower wavenumbers as v increases.

Anharmonicity also accounts for the appearance of additional weak absorption lines corresponding to the transitions $2 \leftarrow 0$, $3 \leftarrow 0$, ..., even though these first, second, ... **overtones** are forbidden by the selection rule $\Delta v = \pm 1$. The first overtone, for example, gives rise to an absorption at

$$G(v+2) - G(v) = 2\tilde{\nu} - 2(2v+3)x_e\tilde{\nu} + \cdots \qquad (13.58)$$

The reason for the appearance of overtones is that the selection rule is derived from the properties of harmonic oscillator wavefunctions, which are only approximately valid when anharmonicity is present. Therefore, the selection rule is also only an approximation. For an anharmonic oscillator, all values of Δv are allowed, but transitions with $\Delta v > 1$ are allowed only weakly if the anharmonicity is slight.

(b) The Birge–Sponer plot

When several vibrational transitions are detectable, a graphical technique called a **Birge–Sponer plot** may be used to determine the dissociation energy, D_0, of the bond. The basis of the Birge–Sponer plot is that the sum of successive intervals $\Delta G_{v+\frac{1}{2}}$ from the zero-point level to the dissociation limit is the dissociation energy:

$$D_0 = \Delta G_{1/2} + \Delta G_{3/2} + \cdots = \sum_v \Delta G_{v+\frac{1}{2}} \qquad (13.59)$$

just as the height of the ladder is the sum of the separations of its rungs (Fig. 13.31). The construction in Fig. 13.32 shows that the area under the plot of $\Delta G_{v+\frac{1}{2}}$ against $v+\frac{1}{2}$ is equal to the sum, and therefore to D_0. The successive terms decrease linearly when only the x_e anharmonicity constant is taken into account and the inaccessible part of the spectrum can be estimated by linear extrapolation. Most actual plots differ from the linear plot as shown in Fig. 13.32, so the value of D_0 obtained in this way is usually an overestimate of the true value.

Example 13.5 *Using a Birge–Sponer plot*

The observed vibrational intervals of H_2^+ lie at the following values for $1 \leftarrow 0$, $2 \leftarrow 1$, ... respectively (in cm^{-1}): 2191, 2064, 1941, 1821, 1705, 1591, 1479, 1368, 1257, 1145, 1033, 918, 800, 677, 548, 411. Determine the dissociation energy of the molecule.

Method Plot the separations against $v+\frac{1}{2}$, extrapolate linearly to the point cutting the horizontal axis, and then measure the area under the curve.

Answer The points are plotted in Fig. 13.33, and a linear extrapolation is shown as a dotted line. The area under the curve (use the formula for the area of a triangle or count the squares) is 214. Each square corresponds to 100 cm^{-1} (refer to the scale of the vertical axis); hence the dissociation energy is 21 400 cm^{-1} (corresponding to 256 kJ mol^{-1}).

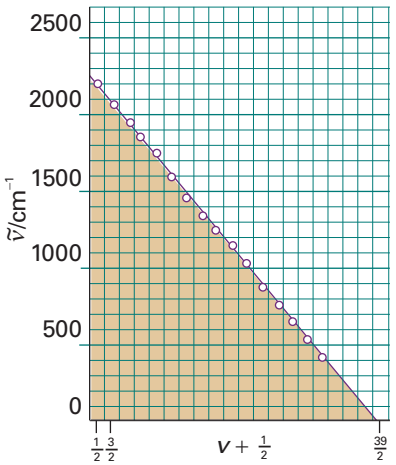

Fig. 13.33 The Birge–Sponer plot used in Example 13.5. The area is obtained simply by counting the squares beneath the line or using the formula for the area of a right triangle.

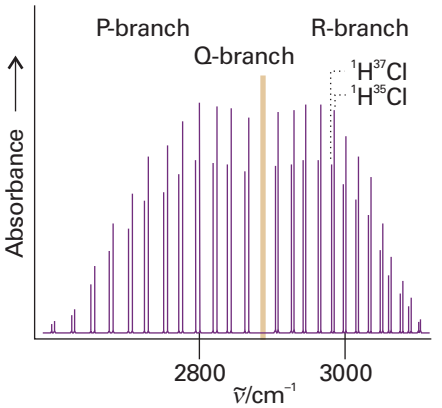

Fig. 13.34 A high-resolution vibration–rotation spectrum of HCl. The lines appear in pairs because $H^{35}Cl$ and $H^{37}Cl$ both contribute (their abundance ratio is 3:1). There is no Q branch, because $\Delta J = 0$ is forbidden for this molecule.

Self-test 13.7 The vibrational levels of HgH converge rapidly, and successive intervals are 1203.7 (which corresponds to the $1 \leftarrow 0$ transition), 965.6, 632.4, and 172 cm^{-1}. Estimate the dissociation energy. [35.6 kJ mol^{-1}]

13.12 Vibration–rotation spectra

Each line of the high resolution vibrational spectrum of a gas-phase heteronuclear diatomic molecule is found to consist of a large number of closely spaced components (Fig. 13.34). Hence, molecular spectra are often called **band spectra**. The separation between the components is less than 10 cm^{-1}, which suggests that the structure is due to rotational transitions accompanying the vibrational transition. A rotational change should be expected because classically we can think of the transition as leading to a sudden increase or decrease in the instantaneous bond length. Just as ice-skaters rotate more rapidly when they bring their arms in, and more slowly when they throw them out, so the molecular rotation is either accelerated or retarded by a vibrational transition.

(a) Spectral branches

A detailed analysis of the quantum mechanics of simultaneous vibrational and rotational changes shows that the rotational quantum number J changes by ± 1 during the vibrational transition of a diatomic molecule. If the molecule also possesses angular momentum about its axis, as in the case of the electronic orbital angular momentum of the paramagnetic molecule NO, then the selection rules also allow $\Delta J = 0$.

The appearance of the vibration–rotation spectrum of a diatomic molecule can be discussed in terms of the combined vibration–rotation terms, S:

$$S(v,J) = G(v) + F(J) \tag{13.60}$$

If we ignore anharmonicity and centrifugal distortion,

$$S(v,J) = (v + \tfrac{1}{2})\tilde{\nu} + BJ(J+1) \tag{13.61}$$

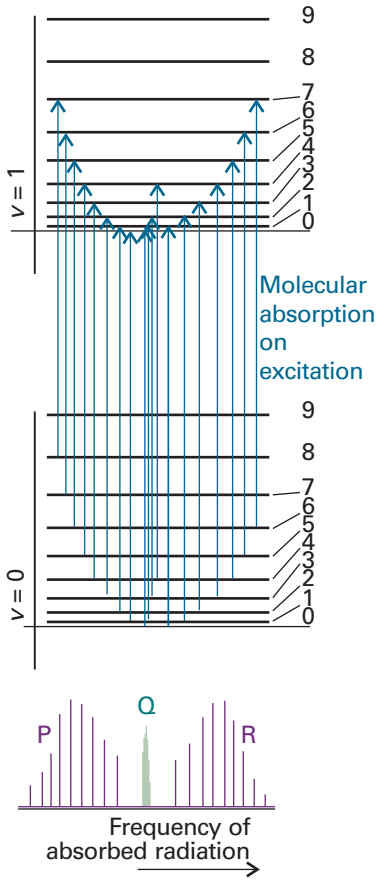

Fig. 13.35 The formation of P, Q, and R branches in a vibration–rotation spectrum. The intensities reflect the populations of the initial rotational levels.

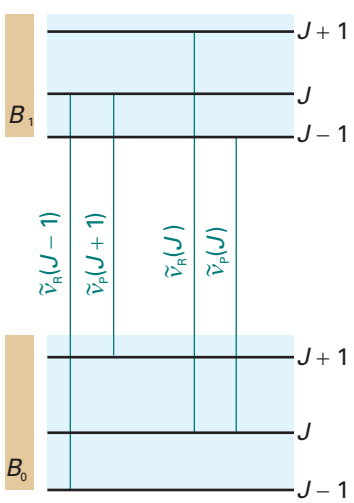

Fig. 13.36 The method of combination differences makes use of the fact that some transitions share a common level.

In a more detailed treatment, B is allowed to depend on the vibrational state because, as v increases, the molecule swells slightly and the moment of inertia changes. We shall continue with the simple expression initially.

When the vibrational transition $v+1 \leftarrow v$ occurs, J changes by ± 1 and in some cases by 0 (when $\Delta J = 0$ is allowed). The absorptions then fall into three groups called **branches** of the spectrum. The **P branch** consists of all transitions with $\Delta J = -1$:

$$\tilde{\nu}_P(J) = S(v+1, J-1) - S(v,J) = \tilde{\nu} - 2BJ \qquad (13.62a)$$

This branch consists of lines at $\tilde{\nu} - 2B$, $\tilde{\nu} - 4B$, . . . with an intensity distribution reflecting both the populations of the rotational levels and the magnitude of the $J-1 \leftarrow J$ transition moment (Fig. 13.35). The **Q branch** consists of all lines with $\Delta J = 0$, and its wavenumbers are all

$$\tilde{\nu}_Q(J) = S(v+1, J) - S(v,J) = \tilde{\nu} \qquad (13.62b)$$

for all values of J. This branch, when it is allowed (as in NO), appears at the vibrational transition wavenumber. In Fig. 13.35 there is a gap at the expected location of the Q branch because it is forbidden in HCl. The **R branch** consists of lines with $\Delta J = +1$:

$$\tilde{\nu}_R(J) = S(v+1, J+1) - S(v,J) = \tilde{\nu} + 2B(J+1) \qquad (13.62c)$$

This branch consists of lines displaced from $\tilde{\nu}$ to high wavenumber by $2B$, $4B$, ...

The separation between the lines in the P and R branches of a vibrational transition gives the value of B. Therefore, the bond length can be deduced without needing to take a pure rotational microwave spectrum. However, the latter is more precise.

(b) Combination differences

The rotational constant of the vibrationally excited state, B_1 (in general, B_v), is in fact slightly smaller than that of the ground vibrational state, B_0, because the anharmonicity of the vibration results in a slightly extended bond in the upper state. As a result, the Q branch (if it exists) consists of a series of closely spaced lines. The lines of the R branch converge slightly as J increases; and those of the P branch diverge:

$$\begin{aligned}\tilde{\nu}_P(J) &= \tilde{\nu} - (B_1 + B_0)J + (B_1 - B_0)J^2 \\ \tilde{\nu}_Q(J) &= \tilde{\nu} + (B_1 - B_0)J(J+1) \\ \tilde{\nu}_R(J) &= \tilde{\nu} + (B_1 + B_0)(J+1) + (B_1 - B_0)(J+1)^2\end{aligned} \qquad (13.63)$$

To determine the two rotational constants individually, we use the method of **combination differences**. This procedure is used widely in spectroscopy to extract information about a particular state. It involves setting up expressions for the difference in the wavenumbers of transitions to a common state; the resulting expression then depends solely on properties of the other state.

As can be seen from Fig. 13.36, the transitions $\tilde{\nu}_R(J-1)$ and $\tilde{\nu}_P(J+1)$ have a common upper state, and hence can be anticipated to depend on B_0. Indeed, it is easy to show from eqn 13.63 that

$$\tilde{\nu}_R(J-1) - \tilde{\nu}_P(J+1) = 4B_0(J + \tfrac{1}{2}) \qquad (13.64a)$$

Therefore, a plot of the combination difference against $J + \frac{1}{2}$ should be a straight line of slope $4B_0$, so the rotational constant of the molecule in the state $v = 0$ can be determined. (Any deviation from a straight line is a consequence of centrifugal distortion, so that effect can be investigated too.) Similarly, $\tilde{\nu}_R(J)$ and $\tilde{\nu}_P(J)$ have a common

lower state, and hence their combination difference gives information about the upper state:

$$\tilde{\nu}_R(J) - \tilde{\nu}_P(J) = 4B_1(J + \tfrac{1}{2}) \qquad (13.64b)$$

The two rotational constants of $^1H^{35}Cl$ found in this way are $B_0 = 10.440\ cm^{-1}$ and $B_1 = 10.136\ cm^{-1}$.

13.13 Vibrational Raman spectra of diatomic molecules

The gross selection rule for vibrational Raman transitions is that *the polarizability should change as the molecule vibrates*. As homonuclear and heteronuclear diatomic molecules swell and contract during a vibration, the control of the nuclei over the electrons varies, and hence the molecular polarizability changes. Both types of diatomic molecule are therefore vibrationally Raman active. The specific selection rule for vibrational Raman transitions in the harmonic approximation is $\Delta v = \pm 1$. The formal basis for the gross and specific selection rules is given in *Further information 13.2*.

The lines to high frequency of the incident radiation, the anti-Stokes lines, are those for which $\Delta v = -1$. The lines to low frequency, the Stokes lines, correspond to $\Delta v = +1$. The intensities of the anti-Stokes and Stokes lines are governed largely by the Boltzmann populations of the vibrational states involved in the transition. It follows that anti-Stokes lines are usually weak because very few molecules are in an excited vibrational state initially.

In gas-phase spectra, the Stokes and anti-Stokes lines have a branch structure arising from the simultaneous rotational transitions that accompany the vibrational excitation (Fig. 13.37). The selection rules are $\Delta J = 0, \pm 2$ (as in pure rotational Raman spectroscopy), and give rise to the **O branch** ($\Delta J = -2$), the **Q branch** ($\Delta J = 0$), and the **S branch** ($\Delta J = +2$):

$$\begin{aligned}\tilde{\nu}_O(J) &= \tilde{\nu}_i - \tilde{\nu} - 2B + 4BJ \\ \tilde{\nu}_Q(J) &= \tilde{\nu}_i - \tilde{\nu} \\ \tilde{\nu}_S(J) &= \tilde{\nu}_i - \tilde{\nu} - 6B - 4BJ\end{aligned} \qquad (13.65)$$

Note that, unlike in infrared spectroscopy, a Q branch is obtained for all linear molecules. The spectrum of CO, for instance, is shown in Fig. 13.38: the structure of the Q branch arises from the differences in rotational constants of the upper and lower vibrational states.

The information available from vibrational Raman spectra adds to that from infrared spectroscopy because homonuclear diatomics can also be studied. The spectra can be interpreted in terms of the force constants, dissociation energies, and bond lengths, and some of the information obtained is included in Table 13.2.

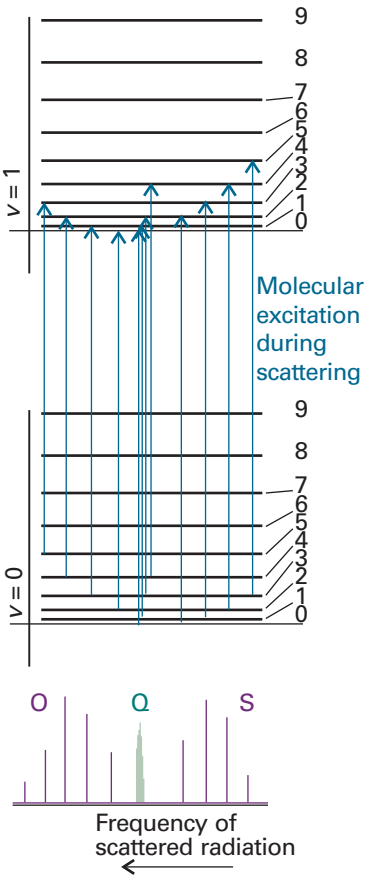

Fig. 13.37 The formation of O, Q, and S branches in a vibration–rotation Raman spectrum of a linear rotor. Note that the frequency scale runs in the opposite direction to that in Fig. 13.35, because the higher energy transitions (on the right) extract more energy from the incident beam and leave it at lower frequency.

Synoptic table 13.2* Properties of diatomic molecules

	$\tilde{\nu}$/cm^{-1}	R_e/pm	B/cm^{-1}	k/(N m^{-1})	D_e/(kJ mol^{-1})
$^1H_2$	4401	74	60.86	575	432
$^1H^{35}Cl$	2991	127	10.59	516	428
$^1H^{127}I$	2308	161	6.61	314	295
$^{35}Cl_2$	560	199	0.244	323	239

* More values are given in the *Data section*.

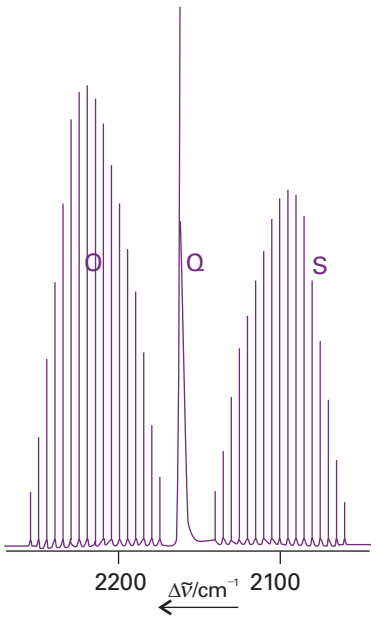

Fig. 13.38 The structure of a vibrational line in the vibrational Raman spectrum of carbon monoxide, showing the O, Q, and S branches.

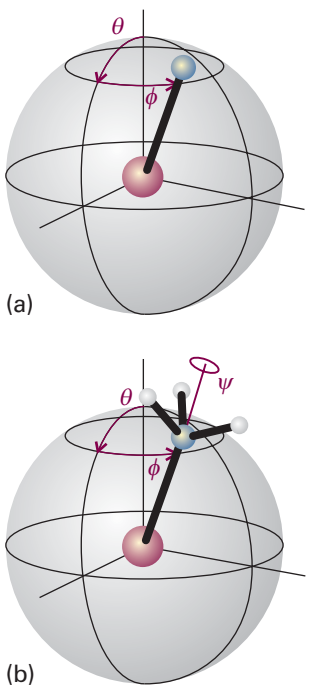

Fig. 13.39 (a) The orientation of a linear molecule requires the specification of two angles. (b) The orientation of a nonlinear molecule requires the specification of three angles.

The vibrations of polyatomic molecules

There is only one mode of vibration for a diatomic molecule, the bond stretch. In polyatomic molecules there are several modes of vibration because all the bond lengths and angles may change and the vibrational spectra are very complex. Nonetheless, we shall see that infrared and Raman spectroscopy can be used to obtain information about the structure of systems as large as animal and plant tissues (see *Impact I13.3*).

13.14 Normal modes

We begin by calculating the total number of vibrational modes of a polyatomic molecule. We then see that we can choose combinations of these atomic displacements that give the simplest description of the vibrations.

As shown in the *Justification* below, for a nonlinear molecule that consists of N atoms, there are $3N - 6$ independent modes of vibration. If the molecule is linear, there are $3N - 5$ independent vibrational modes.

Justification 13.5 *The number of vibrational modes*

The total number of coordinates needed to specify the locations of N atoms is $3N$. Each atom may change its location by varying one of its three coordinates (x, y, and z), so the total number of displacements available is $3N$. These displacements can be grouped together in a physically sensible way. For example, three coordinates are needed to specify the location of the centre of mass of the molecule, so three of the $3N$ displacements correspond to the translational motion of the molecule as a whole. The remaining $3N - 3$ are non-translational 'internal' modes of the molecule.

Two angles are needed to specify the orientation of a linear molecule in space: in effect, we need to give only the latitude and longitude of the direction in which the molecular axis is pointing (Fig. 13.39a). However, three angles are needed for a nonlinear molecule because we also need to specify the orientation of the molecule around the direction defined by the latitude and longitude (Fig. 13.39b). Therefore, two (linear) or three (nonlinear) of the $3N - 3$ internal displacements are rotational. This leaves $3N - 5$ (linear) or $3N - 6$ (nonlinear) displacements of the atoms relative to one another: these are the vibrational modes. It follows that the number of modes of vibration N_{vib} is $3N - 5$ for linear molecules and $3N - 6$ for nonlinear molecules.

Illustration 13.5 *Determining the number of vibrational modes*

Water, H_2O, is a nonlinear triatomic molecule, and has three modes of vibration (and three modes of rotation); CO_2 is a linear triatomic molecule, and has four modes of vibration (and only two modes of rotation). Even a middle-sized molecule such as naphthalene ($C_{10}H_8$) has 48 distinct modes of vibration.

The next step is to find the best description of the modes. One choice for the four modes of CO_2, for example, might be the ones in Fig. 13.40a. This illustration shows the stretching of one bond (the mode ν_L), the stretching of the other (ν_R), and the two perpendicular bending modes (ν_2). The description, while permissible, has a

disadvantage: when one CO bond vibration is excited, the motion of the C atom sets the other CO bond in motion, so energy flows backwards and forwards between ν_L and ν_R. Moreover, the position of the centre of mass of the molecule varies in the course of either vibration.

The description of the vibrational motion is much simpler if linear combinations of ν_L and ν_R are taken. For example, one combination is ν_1 in Fig. 13.40b: this mode is the **symmetric stretch**. In this mode, the C atom is buffeted simultaneously from each side and the motion continues indefinitely. Another mode is ν_3, the **antisymmetric stretch**, in which the two O atoms always move in the same direction and opposite to that of the C atom. Both modes are independent in the sense that, if one is excited, then it does not excite the other. They are two of the 'normal modes' of the molecule, its independent, collective vibrational displacements. The two other normal modes are the bending modes ν_2. In general, a **normal mode** is an independent, synchronous motion of atoms or groups of atoms that may be excited without leading to the excitation of any other normal mode and without involving translation or rotation of the molecule as a whole.

The four normal modes of CO_2, and the N_{vib} normal modes of polyatomics in general, are the key to the description of molecular vibrations. Each normal mode, q, behaves like an independent harmonic oscillator (if anharmonicities are neglected), so each has a series of terms

$$G_q(v) = (v + \tfrac{1}{2})\tilde{\nu}_q \quad \tilde{\nu}_q = \frac{1}{2\pi c}\left(\frac{k_q}{m_q}\right)^{1/2} \tag{13.66}$$

where $\tilde{\nu}_q$ is the wavenumber of mode q and depends on the force constant k_q for the mode and on the effective mass m_q of the mode. The effective mass of the mode is a measure of the mass that is swung about by the vibration and in general is a complicated function of the masses of the atoms. For example, in the symmetric stretch of CO_2, the C atom is stationary, and the effective mass depends on the masses of only the O atoms. In the antisymmetric stretch and in the bends, all three atoms move, so all contribute to the effective mass. The three normal modes of H_2O are shown in Fig. 13.41: note that the predominantly bending mode (ν_2) has a lower frequency than the others, which are predominantly stretching modes. It is generally the case that the frequencies of bending motions are lower than those of stretching modes. One point that must be appreciated is that only in special cases (such as the CO_2 molecule) are the normal modes purely stretches or purely bends. In general, a normal mode is a composite motion of simultaneous stretching and bending of bonds. Another point in this connection is that heavy atoms generally move less than light atoms in normal modes.

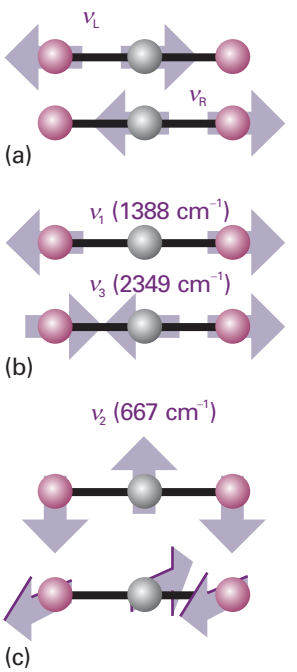

Fig. 13.40 Alternative descriptions of the vibrations of CO_2. (a) The stretching modes are not independent, and if one C—O group is excited the other begins to vibrate. They are not normal modes of vibration of the molecule. (b) The symmetric and antisymmetric stretches are independent, and one can be excited without affecting the other: they are normal modes. (c) The two perpendicular bending motions are also normal modes.

13.15 Infrared absorption spectra of polyatomic molecules

The gross selection rule for infrared activity is that *the motion corresponding to a normal mode should be accompanied by a change of dipole moment*. Deciding whether this is so can sometimes be done by inspection. For example, the symmetric stretch of CO_2 leaves the dipole moment unchanged (at zero, see Fig. 13.40), so this mode is infrared inactive. The antisymmetric stretch, however, changes the dipole moment because the molecule becomes unsymmetrical as it vibrates, so this mode is infrared active. Because the dipole moment change is parallel to the principal axis, the transitions arising from this mode are classified as **parallel bands** in the spectrum. Both bending modes are infrared active: they are accompanied by a changing dipole perpendicular to the principal axis, so transitions involving them lead to a **perpendicular band** in the spectrum. The latter bands eliminate the linearity of the molecule, and as a result a Q branch is observed; a parallel band does not have a Q branch.

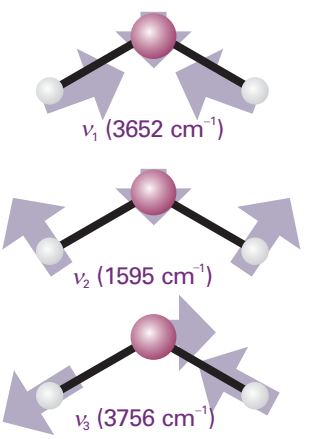

Fig. 13.41 The three normal modes of H_2O. The mode ν_2 is predominantly bending, and occurs at lower wavenumber than the other two.

Comment 13.6
The web site for this text contains links to sites where you can perform quantum mechanical calculations of frequencies and atomic displacements of normal modes of simple molecules.

Comment 13.7
The web site for this text contains links to databases of infrared spectra.

Synoptic table 13.3* Typical vibrational wavenumbers

Vibration type	$\tilde{\nu}$/cm^{-1}
C—H stretch	2850–2960
C—H bend	1340–1465
C—C stretch, bend	700–1250
C=C stretch	1620–1680

* More values are given in the *Data section*.

The active modes are subject to the specific selection rule $\Delta v_q = \pm 1$ in the harmonic approximation, so the wavenumber of the fundamental transition (the 'first harmonic') of each active mode is $\tilde{\nu}_q$. From the analysis of the spectrum, a picture may be constructed of the stiffness of various parts of the molecule, that is, we can establish its **force field**, the set of force constants corresponding to all the displacements of the atoms. The force field may also be estimated by using the semi-empirical, *ab initio*, and DFT computational techniques described in Section 11.7. Superimposed on the simple force field scheme are the complications arising from anharmonicities and the effects of molecular rotation. Very often the sample is a liquid or a solid, and the molecules are unable to rotate freely. In a liquid, for example, a molecule may be able to rotate through only a few degrees before it is struck by another, so it changes its rotational state frequently. This random changing of orientation is called **tumbling**.

The lifetimes of rotational states in liquids are very short, so in most cases the rotational energies are ill-defined. Collisions occur at a rate of about 10^{13} s^{-1} and, even allowing for only a 10 per cent success rate in knocking the molecule into another rotational state, a lifetime broadening (eqn 13.19) of more than 1 cm^{-1} can easily result. The rotational structure of the vibrational spectrum is blurred by this effect, so the infrared spectra of molecules in condensed phases usually consist of broad lines spanning the entire range of the resolved gas-phase spectrum, and showing no branch structure.

One very important application of infrared spectroscopy to condensed phase samples, and for which the blurring of the rotational structure by random collisions is a welcome simplification, is to chemical analysis. The vibrational spectra of different groups in a molecule give rise to absorptions at characteristic frequencies because a normal mode of even a very large molecule is often dominated by the motion of a small group of atoms. The intensities of the vibrational bands that can be identified with the motions of small groups are also transferable between molecules. Consequently, the molecules in a sample can often be identified by examining its infrared spectrum and referring to a table of characteristic frequencies and intensities (Table 13.3).

IMPACT ON ENVIRONMENTAL SCIENCE

I13.2 Global warming[1]

Solar energy strikes the top of the Earth's atmosphere at a rate of 343 W m^{-2}. About 30 per cent of this energy is reflected back into space by the Earth or the atmosphere. The Earth–atmosphere system absorbs the remaining energy and re-emits it into space as black-body radiation, with most of the intensity being carried by infrared radiation in the range 200–2500 cm^{-1} (4–50 μm). The Earth's average temperature is maintained by an energy balance between solar radiation absorbed by the Earth and black-body radiation emitted by the Earth.

The trapping of infrared radiation by certain gases in the atmosphere is known as the *greenhouse effect*, so called because it warms the Earth as if the planet were enclosed in a huge greenhouse. The result is that the natural greenhouse effect raises the average surface temperature well above the freezing point of water and creates an environment in which life is possible. The major constituents to the Earth's atmosphere, O_2 and N_2, do not contribute to the greenhouse effect because homonuclear diatomic molecules cannot absorb infrared radiation. However, the minor atmospheric gases, water vapour and CO_2, do absorb infrared radiation and hence are responsible for the

[1] This section is based on a similar contribution initially prepared by Loretta Jones and appearing in *Chemical principles*, Peter Atkins and Loretta Jones, W.H. Freeman and Co., New York (2005).

greenhouse effect (Fig. 13.42). Water vapour absorbs strongly in the ranges 1300–1900 cm^{-1} (5.3–7.7 μm) and 3550–3900 cm^{-1} (2.6–2.8 μm), whereas CO_2 shows strong absorption in the ranges 500–725 cm^{-1} (14–20 μm) and 2250–2400 cm^{-1} (4.2–4.4 μm).

Increases in the levels of greenhouse gases, which also include methane, dinitrogen oxide, ozone, and certain chlorofluorocarbons, as a result of human activity have the potential to enhance the natural greenhouse effect, leading to significant warming of the planet. This problem is referred to as *global warming*, which we now explore in some detail.

The concentration of water vapour in the atmosphere has remained steady over time, but concentrations of some other greenhouse gases are rising. From about the year 1000 until about 1750, the CO_2 concentration remained fairly stable, but, since then, it has increased by 28 per cent. The concentration of methane, CH_4, has more than doubled during this time and is now at its highest level for 160 000 years (160 ka; a is the SI unit denoting 1 year). Studies of air pockets in ice cores taken from Antarctica show that increases in the concentration of both atmospheric CO_2 and CH_4 over the past 160 ka correlate well with increases in the global surface temperature.

Human activities are primarily responsible for the rising concentrations of atmospheric CO_2 and CH_4. Most of the atmospheric CO_2 comes from the burning of hydrocarbon fuels, which began on a large scale with the Industrial Revolution in the middle of the nineteenth century. The additional methane comes mainly from the petroleum industry and from agriculture.

The temperature of the surface of the Earth has increased by about 0.5 K since the late nineteenth century (Fig. 13.43). If we continue to rely on hydrocarbon fuels and current trends in population growth and energy are not reversed, then by the middle of the twenty-first century, the concentration of CO_2 in the atmosphere will be about twice its value prior to the Industrial Revolution. The Intergovernmental Panel on Climate Change (IPCC) estimated in 1995 that, by the year 2100, the Earth will undergo an increase in temperature of 3 K. Furthermore, the rate of temperature change is likely to be greater than at any time in the last 10 ka. To place a temperature rise of 3 K in perspective, it is useful to consider that the average temperature of the Earth during the last ice age was only 6 K colder than at present. Just as cooling the planet (for example, during an ice age) can lead to detrimental effects on ecosystems, so too can a dramatic warming of the globe. One example of a significant change in the

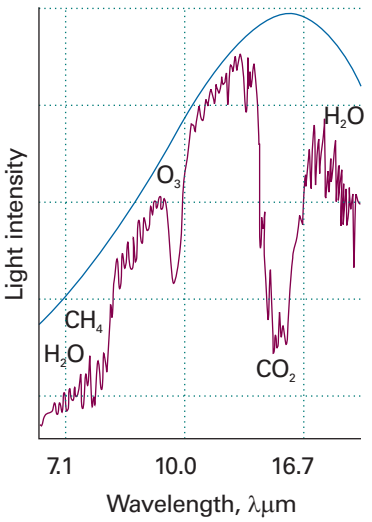

Fig. 13.42 The intensity of infrared radiation that would be lost from Earth in the absence of greenhouse gases is shown by the blue line. The purple line is the intensity of the radiation actually emitted. The maximum wavelength of radiation absorbed by each greenhouse gas is indicated.

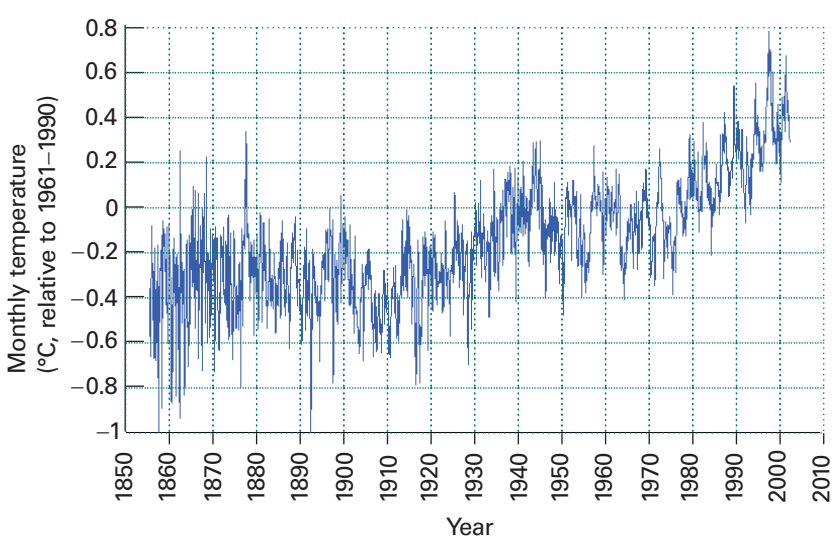

Fig. 13.43 The average change in surface temperature of the Earth from 1855 to 2002.

environment caused by a temperature increase of 3 K is a rise in sea level by about 0.5 m, which is sufficient to alter weather patterns and submerge currently coastal ecosystems.

Computer projections for the next 200 years predict further increases in atmospheric CO_2 levels and suggest that, to maintain CO_2 at its current concentration, we would have to reduce hydrocarbon fuel consumption immediately by about 50 per cent. Clearly, in order to reverse global warming trends, we need to develop alternatives to fossil fuels, such as hydrogen (which can be used in fuel cells, *Impact I25.3*) and solar energy technologies.

13.16 Vibrational Raman spectra of polyatomic molecules

The normal modes of vibration of molecules are Raman active if they are accompanied by a changing polarizability. It is sometimes quite difficult to judge by inspection when this is so. The symmetric stretch of CO_2, for example, alternately swells and contracts the molecule: this motion changes the polarizability of the molecule, so the mode is Raman active. The other modes of CO_2 leave the polarizability unchanged, so they are Raman inactive.

A more exact treatment of infrared and Raman activity of normal modes leads to the **exclusion rule**:

> If the molecule has a centre of symmetry, then no modes can be both infrared and Raman active.

(A mode may be inactive in both.) Because it is often possible to judge intuitively if a mode changes the molecular dipole moment, we can use this rule to identify modes that are not Raman active. The rule applies to CO_2 but to neither H_2O nor CH_4 because they have no centre of symmetry. In general, it is necessary to use group theory to predict whether a mode is infrared or Raman active (Section 13.17).

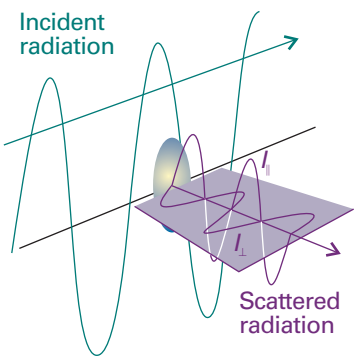

Fig. 13.44 The definition of the planes used for the specification of the depolarization ratio, ρ, in Raman scattering.

(a) Depolarization

The assignment of Raman lines to particular vibrational modes is aided by noting the state of polarization of the scattered light. The **depolarization ratio**, ρ, of a line is the ratio of the intensities, I, of the scattered light with polarizations perpendicular and parallel to the plane of polarization of the incident radiation:

$$\rho = \frac{I_\perp}{I_\parallel} \qquad [13.67]$$

To measure ρ, the intensity of a Raman line is measured with a polarizing filter (a 'half-wave plate') first parallel and then perpendicular to the polarization of the incident beam. If the emergent light is not polarized, then both intensities are the same and ρ is close to 1; if the light retains its initial polarization, then $I_\perp = 0$, so $\rho = 0$ (Fig. 13.44). A line is classified as **depolarized** if it has ρ close to or greater than 0.75 and as **polarized** if $\rho < 0.75$. Only totally symmetrical vibrations give rise to polarized lines in which the incident polarization is largely preserved. Vibrations that are not totally symmetrical give rise to depolarized lines because the incident radiation can give rise to radiation in the perpendicular direction too.

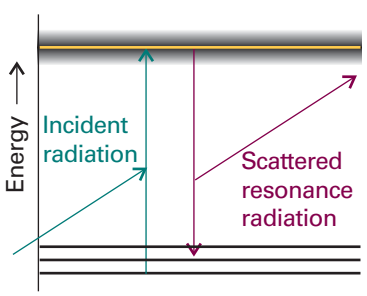

Fig. 13.45 In the *resonance Raman effect*, the incident radiation has a frequency corresponding to an actual electronic excitation of the molecule. A photon is emitted when the excited state returns to a state close to the ground state.

(b) Resonance Raman spectra

A modification of the basic Raman effect involves using incident radiation that nearly coincides with the frequency of an electronic transition of the sample (Fig. 13.45). The

technique is then called **resonance Raman spectroscopy**. It is characterized by a much greater intensity in the scattered radiation. Furthermore, because it is often the case that only a few vibrational modes contribute to the more intense scattering, the spectrum is greatly simplified.

Resonance Raman spectroscopy is used to study biological molecules that absorb strongly in the ultraviolet and visible regions of the spectrum. Examples include the pigments β-carotene and chlorophyll, which capture solar energy during plant photosynthesis (see *Impact I23.2*). The resonance Raman spectra of Fig. 13.46 show vibrational transitions from only the few pigment molecules that are bound to very large proteins dissolved in an aqueous buffer solution. This selectivity arises from the fact that water (the solvent), amino acid residues, and the peptide group do not have electronic transitions at the laser wavelengths used in the experiment, so their *conventional* Raman spectra are weak compared to the enhanced spectra of the pigments. Comparison of the spectra in Figs. 13.46a and 13.46b also shows that, with proper choice of excitation wavelength, it is possible to examine individual classes of pigments bound to the same protein: excitation at 488 nm, where β-carotene absorbs strongly, shows vibrational bands from β-carotene only, whereas excitation at 442 nm, where chlorophyll *a* and β-carotene absorb, reveals features from both types of pigments.

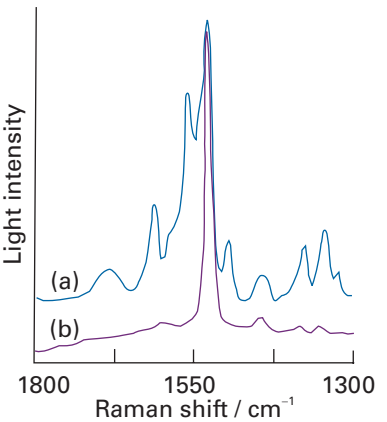

Fig. 13.46 The resonance Raman spectra of a protein complex that is responsible for some of the initial electron transfer events in plant photosynthesis. (a) Laser excitation of the sample at 407 nm shows Raman bands due to both chlorophyll *a* and β-carotene bound to the protein because both pigments absorb light at this wavelength. (b) Laser excitation at 488 nm shows Raman bands from β-carotene only because chlorophyll *a* does not absorb light very strongly at this wavelength. (Adapted from D.F. Ghanotakis *et al.*, *Biochim. Biophys. Acta* **974**, 44 (1989).)

(c) Coherent anti-Stokes Raman spectroscopy

The intensity of Raman transitions may be enhanced by **coherent anti-Stokes Raman spectroscopy** (CARS, Fig. 13.47). The technique relies on the fact that, if two laser beams of frequencies ν_1 and ν_2 pass through a sample, then they may mix together and give rise to coherent radiation of several different frequencies, one of which is

$$\nu' = 2\nu_1 - \nu_2 \tag{13.68}$$

Suppose that ν_2 is varied until it matches any Stokes line from the sample, such as the one with frequency $\nu_1 - \Delta\nu$; then the coherent emission will have frequency

$$\nu' = 2\nu_1 - (\nu_1 - \Delta\nu) = \nu_1 + \Delta\nu \tag{13.69}$$

which is the frequency of the corresponding anti-Stokes line. This coherent radiation forms a narrow beam of high intensity.

An advantage of CARS is that it can be used to study Raman transitions in the presence of competing incoherent background radiation, and so can be used to observe the Raman spectra of species in flames. One example is the vibration–rotation CARS spectrum of N_2 gas in a methane–air flame shown in Fig 13.48.

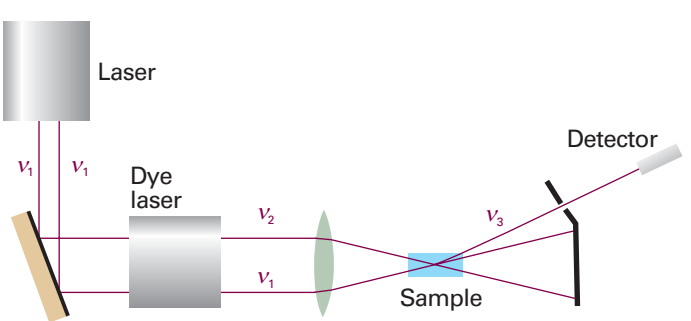

Fig. 13.47 The experimental arrangement for the CARS experiment.

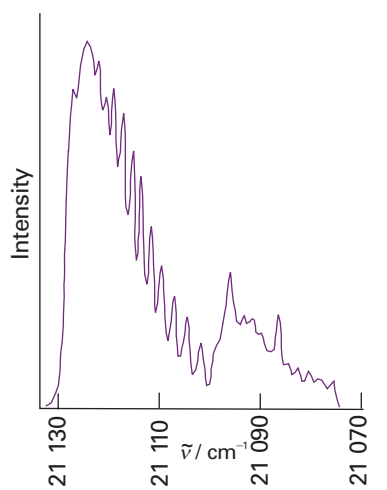

Fig. 13.48 CARS spectrum of a methane–air flame at 2104 K. The peaks correspond to the Q branch of the vibration–rotation spectrum of N_2 gas. (Adapted from J.F. Verdieck *et al.*, *J. Chem. Educ.* **59**, 495 (1982).)

IMPACT ON BIOCHEMISTRY

I13.3 Vibrational microscopy

Optical microscopes can now be combined with infrared and Raman spectrometers and the vibrational spectra of specimens as small as single biological cells obtained. The techniques of *vibrational microscopy* provide details of cellular events that cannot be observed with traditional light or electron microscopy.

The principles behind the operation of infrared and Raman microscopes are simple: radiation illuminates a small area of the sample, and the transmitted, reflected, or scattered light is first collected by a microscope and then analysed by a spectrometer. The sample is then moved by very small increments along a plane perpendicular to the direction of illumination and the process is repeated until vibrational spectra for all sections the sample are obtained. The size of a sample that can be studied by vibrational microscopy depends on a number of factors, such as the area of illumination and the excitance and wavelength of the incident radiation. Up to a point, the smaller the area that is illuminated, the smaller the area from which a spectrum can be obtained. High excitance is required to increase the rate of arrival of photons at the detector from small illuminated areas. For this reason, lasers and synchrotron radiation (see *Further information 13.1*) are the preferred radiation sources.

In a conventional light microscope, an image is constructed from a pattern of diffracted light waves that emanate from the illuminated object. As a result, some information about the specimen is lost by destructive interference of scattered light waves. Ultimately, this *diffraction limit* prevents the study of samples that are much smaller than the wavelength of light used as a probe. In practice, two objects will appear as distinct images under a microscope if the distance between their centres is greater than the *Airy radius*, $r_{\text{Airy}} = 0.61\lambda/a$, where λ is the wavelength of the incident beam of radiation and a is the numerical aperture of the *objective lens*, the lens that collects light scattered by the object. The numerical aperture of the objective lens is defined as $a = n_r \sin\alpha$, where n_r is the refractive index of the lens material (the greater the refractive index, the greater the bending of a ray of light by the lens) and the angle α is the half-angle of the widest cone of scattered light that can collected by the lens (so the lens collects light beams sweeping a cone with angle 2α). Use of the best equipment makes it possible to probe areas as small as 9 μm^2 by vibrational microscopy.

Figure 13.49 shows the infrared spectra of a single mouse cell, living and dying. Both spectra have features at 1545 cm^{-1} and 1650 cm^{-1} that are due to the peptide carbonyl groups of proteins and a feature at 1240 cm^{-1} that is due to the phosphodiester (PO_2^-) groups of lipids. The dying cell shows an additional absorption at 1730 cm^{-1}, which is due to the ester carbonyl group from an unidentified compound. From a plot of the intensities of individual absorption features as a function of position in the cell, it has been possible to map the distribution of proteins and lipids during cell division and cell death.

Vibrational microscopy has also been used in biomedical and pharmaceutical laboratories. Examples include the determination of the size and distribution of a drug in a tablet, the observation of conformational changes in proteins of cancerous cells upon administration of anti-tumour drugs, and the measurement of differences between diseased and normal tissue, such as diseased arteries and the white matter from brains of multiple sclerosis patients.

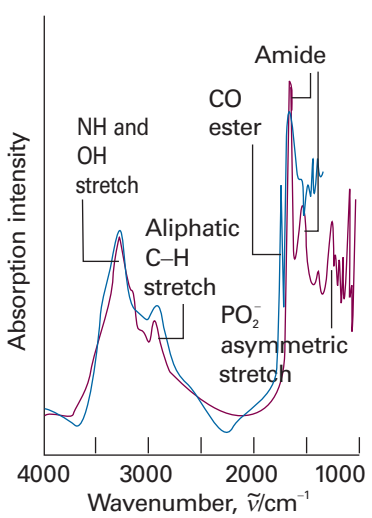

Fig. 13.49 Infrared absorption spectra of a single mouse cell: (purple) living cell, (blue) dying cell. Adapted from N. Jamin *et al.*, *Proc. Natl. Acad. Sci. USA* **95**, 4837 (1998).

13.17 Symmetry aspects of molecular vibrations

One of the most powerful ways of dealing with normal modes, especially of complex molecules, is to classify them according to their symmetries. Each normal mode must

belong to one of the symmetry species of the molecular point group, as discussed in Chapter 12.

Example 13.6 *Identifying the symmetry species of a normal mode*

Establish the symmetry species of the normal mode vibrations of CH_4, which belongs to the group T_d.

Method The first step in the procedure is to identify the symmetry species of the irreducible representations spanned by all the $3N$ displacements of the atoms, using the characters of the molecular point group. Find these characters by counting 1 if the displacement is unchanged under a symmetry operation, −1 if it changes sign, and 0 if it is changed into some other displacement. Next, subtract the symmetry species of the translations. Translational displacements span the same symmetry species as x, y, and z, so they can be obtained from the right-most column of the character table. Finally, subtract the symmetry species of the rotations, which are also given in the character table (and denoted there by R_x, R_y, or R_z).

Answer There are $3 \times 5 = 15$ degrees of freedom, of which $(3 \times 5) - 6 = 9$ are vibrations. Refer to Fig. 13.50. Under E, no displacement coordinates are changed, so the character is 15. Under C_3, no displacements are left unchanged, so the character is 0. Under the C_2 indicated, the z-displacement of the central atom is left unchanged, whereas its x- and y-components both change sign. Therefore $\chi(C_2) = 1 - 1 - 1 + 0 + 0 + \cdots = -1$. Under the S_4 indicated, the z-displacement of the central atom is reversed, so $\chi(S_4) = -1$. Under σ_d, the x- and z-displacements of C, H_3, and H_4 are left unchanged and the y-displacements are reversed; hence $\chi(\sigma_d) = 3 + 3 - 3 = 3$. The characters are therefore 15, 0, −1, −1, 3. By decomposing the direct product (Section 12.5a), we find that this representation spans $A_1 + E + T_1 + 3T_2$. The translations span T_2; the rotations span T_1. Hence, the nine vibrations span $A_1 + E + 2T_2$.

The modes themselves are shown in Fig. 13.51. We shall see that symmetry analysis gives a quick way of deciding which modes are active.

Self-test 13.8 Establish the symmetry species of the normal modes of H_2O. $[2A_1 + B_2]$

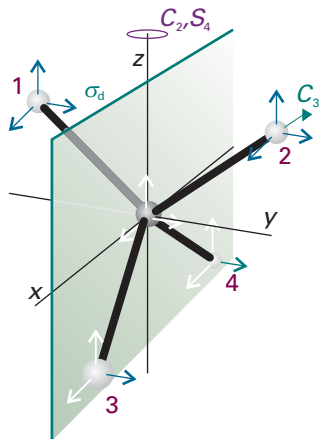

Fig. 13.50 The atomic displacements of CH_4 and the symmetry elements used to calculate the characters.

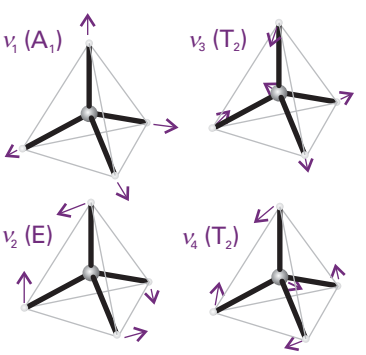

Fig. 13.51 Typical normal modes of vibration of a tetrahedral molecule. There are in fact two modes of symmetry species E and three modes of each T_2 symmetry species.

(a) Infrared activity of normal modes

It is best to use group theory to judge the activities of more complex modes of vibration. This is easily done by checking the character table of the molecular point group for the symmetry species of the irreducible representations spanned by x, y, and z, for their species are also the symmetry species of the components of the electric dipole moment. Then apply the following rule:

> If the symmetry species of a normal mode is the same as any of the symmetry species of x, y, or z, then the mode is infrared active.

Justification 13.6 *Using group theory to identify infrared active normal modes*

The rule hinges on the form of the transition dipole moment between the ground-state vibrational wavefunction, ψ_0, and that of the first excited state, ψ_1. The x-component is

$$\mu_{x,10} = -e\int \psi_1^* x \psi_0 \, d\tau \tag{13.70}$$

with similar expressions for the two other components of the transition moment. The ground-state vibrational wavefunction is a Gaussian function of the form e^{-x^2}, so it is symmetrical in x. The wavefunction for the first excited state gives a non-vanishing integral only if it is proportional to x, for then the integrand is proportional to x^2 rather than to xy or xz. Consequently, the excited state wavefunction must have the same symmetry as the displacement x.

Example 13.7 *Identifying infrared active modes*

Which modes of CH_4 are infrared active?

Method Refer to the T_d character table to establish the symmetry species of x, y, and z for this molecule, and then use the rule given above.

Answer The functions x, y, and z span T_2. We found in Example13.6 that the symmetry species of the normal modes are $A_1 + E + 2T_2$. Therefore, only the T_2 modes are infrared active. The distortions accompanying these modes lead to a changing dipole moment. The A_1 mode, which is inactive, is the symmetrical 'breathing' mode of the molecule.

Self-test 13.9 Which of the normal modes of H_2O are infrared active? [All three]

(b) Raman activity of normal modes

Group theory provides an explicit recipe for judging the Raman activity of a normal mode. In this case, the symmetry species of the quadratic forms (x^2, xy, etc.) listed in the character table are noted (they transform in the same way as the polarizability), and then we use the following rule:

If the symmetry species of a normal mode is the same as the symmetry species of a quadratic form, then the mode is Raman active.

Illustration 13.6 *Identifying Raman active modes*

To decide which of the vibrations of CH_4 are Raman active, refer to the T_d character table. It was established in Example 13.6 that the symmetry species of the normal modes are $A_1 + E + 2T_2$. Because the quadratic forms span $A_1 + E + T_2$, all the normal modes are Raman active. By combining this information with that in Example 13.6, we see how the infrared and Raman spectra of CH_4 are assigned. The assignment of spectral features to the T_2 modes is straightforward because these are the only modes that are both infrared and Raman active. This leaves the A_1 and E modes to be assigned in the Raman spectrum. Measurement of the depolarization ratio distinguishes between these modes because the A_1 mode, being totally symmetric, is polarized and the E mode is depolarized.

Self-test 13.10 Which of the vibrational modes of H_2O are Raman active? [All three]

Checklist of key ideas

- ☐ 1. Emission spectroscopy is based on the detection of a transition from a state of high energy to a state of lower energy; absorption spectroscopy is based on the detection of the net absorption of nearly monochromatic incident radiation as the radiation is swept over a range of frequencies.
- ☐ 2. In Raman spectroscopy molecular energy levels are explored by examining the frequencies present in scattered radiation. Stokes and anti-Stokes radiation are scattered radiation at a lower and higher frequency, respectively, than the incident radiation. Rayleigh radiation is the component of radiation scattered into the forward direction without change of frequency.
- ☐ 3. The Beer–Lambert law is $I(\tilde{\nu}) = I_0(\tilde{\nu})10^{-\varepsilon(\tilde{\nu})[J]l}$, where $I(\tilde{\nu})$ is the transmitted intensity, $I_0(\tilde{\nu})$ is the incident intensity, and $\varepsilon(\tilde{\nu})$ is the molar absorption coefficient.
- ☐ 4. The transmittance, $T = I/I_0$, and the absorbance, A, of a sample at a given wavenumber are related by $A = -\log T$.
- ☐ 5. The integrated absorption coefficient, $\mathcal{A}$, is the sum of the absorption coefficients over the entire band, $\mathcal{A} = \int_{\text{band}} \varepsilon(\tilde{\nu})\mathrm{d}\tilde{\nu}$.
- ☐ 6. Stimulated absorption is the radiation-driven transition from a low energy state to one of higher energy. Stimulated emission is the radiation-driven transition from a high energy state to one of lower energy. Spontaneous emission is radiative emission independent of the intensity of the radiation (of any frequency) that is already present.
- ☐ 7. The natural linewidth of a spectral line is due to spontaneous emission. Spectral lines are affected by Doppler broadening, lifetime broadening, and collisional deactivation of excited states.
- ☐ 8. A rigid rotor is a body that does not distort under the stress of rotation. A spherical rotor is a rigid rotor with three equal moments of inertia. A symmetric rotor is a rigid rotor with two equal moments of inertia. A linear rotor is a rigid rotor with one moment of inertia equal to zero. An asymmetric rotor is a rigid rotor with three different moments of inertia.
- ☐ 9. The rotational terms of a spherical rotor are $F(J) = BJ(J+1)$ with $B = \hbar/4\pi cI$, $J = 0, 1, 2, \ldots$, and are $(2J+1)^2$-fold degenerate.
- ☐ 10. The principal axis (figure axis) is the unique axis of a symmetric top. In an oblate top, $I_\parallel > I_\perp$. In a prolate top, $I_\parallel < I_\perp$.
- ☐ 11. The rotational terms of a symmetric rotor are $F(J,K) = BJ(J+1) + (A-B)K^2$, $J = 0, 1, 2, \ldots, K = 0, \pm1, \ldots, \pm J$.
- ☐ 12. The rotational terms of a linear rotor are $F(J) = BJ(J+1)$, $J = 0, 1, 2, \ldots$ and are $(2J+1)$-fold degenerate.
- ☐ 13. The centrifugal distortion constant, D_J, is the empirical constant in the expression $F(J) = BJ(J+1) - D_J J^2(J+1)^2$ that takes into account centrifugal distortion, $D_J \approx 4B^3/\tilde{\nu}^2$.
- ☐ 14. The gross rotational selection rule for microwave spectra is: for a molecule to give a pure rotational spectrum, it must be polar. The specific rotational selection rule is: $\Delta J = \pm1$, $\Delta M_J = 0, \pm1$, $\Delta K = 0$. The rotational wavenumbers in the absence and presence of centrifugal distortion are given by eqns 13.37 and 13.38, respectively.
- ☐ 15. The gross selection rule for rotational Raman spectra is: the molecule must be anisotropically polarizable. The specific selection rules are: (i) linear rotors, $\Delta J = 0, \pm2$; (ii) symmetric rotors, $\Delta J = 0, \pm1, \pm2$; $\Delta K = 0$.
- ☐ 16. The appearance of rotational spectra is affected by nuclear statistics, the selective occupation of rotational states that stems from the Pauli principle.
- ☐ 17. The vibrational energy levels of a diatomic molecule modelled as a harmonic oscillator are $E_v = (v + \frac{1}{2})\hbar\omega$, $\omega = (k/m_{\text{eff}})^{1/2}$; the vibrational terms are $G(v) = (v + \frac{1}{2})\tilde{\nu}$, $\tilde{\nu} = (1/2\pi c)(k/m_{\text{eff}})^{1/2}$.
- ☐ 18. The gross selection rule for infrared spectra is: the electric dipole moment of the molecule must change when the atoms are displaced relative to one another. The specific selection rule is: $\Delta v = \pm1$.
- ☐ 19. Morse potential energy, eqn 13.54, describes anharmonic motion, oscillatory motion in which the restoring force is not proportional to the displacement; the vibrational terms of a Morse oscillator are given by eqn 13.55.
- ☐ 20. A Birge–Sponer plot is a graphical procedure for determining the dissociation energy of a bond.
- ☐ 21. The P branch consists of vibration–rotation infrared transitions with $\Delta J = -1$; the Q branch has transitions with $\Delta J = 0$; the R branch has transitions with $\Delta J = +1$.
- ☐ 22. The gross selection rule for vibrational Raman spectra is: the polarizability must change as the molecule vibrates. The specific selection rule is: $\Delta v = \pm1$.
- ☐ 23. A normal mode is an independent, synchronous motion of atoms or groups of atoms that may be excited without leading to the excitation of any other normal mode. The number of normal modes is $3N - 6$ (for nonlinear molecules) or $3N - 5$ (linear molecules).
- ☐ 24. A symmetric stretch is a symmetrically stretching vibrational mode. An antisymmetric stretch is a stretching mode, one half of which is the mirror image of the other half.
- ☐ 25. The exclusion rule states that, if the molecule has a centre of symmetry, then no modes can be both infrared and Raman active.
- ☐ 26. The depolarization ratio, ρ, the ratio of the intensities, I, of the scattered light with polarizations perpendicular and parallel to the plane of polarization of the incident radiation, $\rho = I_\perp/I_\parallel$. A depolarized line is a line with ρ close to or greater than 0.75. A polarized line is a line with $\rho < 0.75$.
- ☐ 27. Resonance Raman spectroscopy is a Raman technique in which the frequency of the incident radiation nearly coincides with the frequency of an electronic transition of the sample. Coherent anti-Stokes Raman spectroscopy (CARS) is a

Raman technique that relies on the use of two incident beams of radiation.

☐ 28. A normal mode is infrared active if its symmetry species is the same as any of the symmetry species of x, y, or z, then the mode is infrared active. A normal mode is Raman active if its symmetry species is the same as the symmetry species of a quadratic form.

Further reading

Articles and texts

L. Glasser, Fourier transforms for chemists. Part I. Introduction to the Fourier transform. *J. Chem. Educ.* **64**, A228 (1987). Part II. Fourier transforms in chemistry and spectroscopy. *J. Chem. Educ.* **64**, A260 (1987).

H.-U. Gremlich and B. Yan, *Infrared and Raman spectroscopy of biological materials*. Marcel Dekker, New York (2001).

G. Herzberg, *Molecular spectra and molecular structure I. Spectra of diatomic molecules.* Krieger, Malabar (1989).

G. Herzberg, *Molecular spectra and molecular structure II. Infrared and Raman spectra of polyatomic molecules*. Van Nostrand–Reinhold, New York (1945).

J.C. Lindon, G.E. Tranter, and J.L. Holmes (ed.), *Encyclopedia of spectroscopy and spectrometry*. Academic Press, San Diego (2000).

D.P. Strommen, Specific values of the depolarization ratio in Raman spectroscopy: Their origins and significance. *J. Chem. Educ.* **69**, 803 (1992).

E.B. Wilson, J.C. Decius, and P.C. Cross, *Molecular vibrations*. Dover, New York (1980).

J.M. Brown and A. Carrington, *Rotational spectroscopy of diatomic molecules*. Cambridge University Press (2003).

Sources of data and information

M.E. Jacox, *Vibrational and electronic energy levels of polyatomic transient molecules.* Journal of Physical and Chemical Reference Data, Monograph No. 3 (1994).

K.P. Huber and G. Herzberg, *Molecular spectra and molecular structure IV. Constants of diatomic molecules.* Van Nostrand-Reinhold, New York (1979).

B. Schrader, *Raman/IR atlas of organic compounds.* VCH, New York (1989).

G. Socrates, *Infrared and Raman characteristic group frequencies: tables and charts*. Wiley, New York (2000).

Further information

Further information 13.1 *Spectrometers*

Here we provide additional detail on the principles of operation of spectrometers, describing radiation sources, dispersing elements, detectors, and Fourier transform techniques.

Sources of radiation

Sources of radiation are either *monochromatic*, those spanning a very narrow range of frequencies around a central value, or *polychromatic*, those spanning a wide range of frequencies. Monochromatic sources that can be tuned over a range of frequencies include the *klystron* and the *Gunn diode*, which operate in the microwave range, and lasers, which are discussed in Chapter 14.

Polychromatic sources that take advantage of black-body radiation from hot materials. For far infrared radiation with $35\ \text{cm}^{-1} < \tilde{\nu} < 200\ \text{cm}^{-1}$, a typical source is a mercury arc inside a quartz envelope, most of the radiation being generated by the hot quartz. Either a *Nernst filament* or a *globar* is used as a source of mid-infrared radiation with $200\ \text{cm}^{-1} < \tilde{\nu} < 4000\ \text{cm}^{-1}$. The Nernst filament consists of a ceramic filament of lanthanoid oxides that is heated to temperatures ranging from 1200 to 2000 K. The globar consists of a rod of silicon carbide, which is heated electrically to about 1500 K.

A *quartz–tungsten–halogen lamp* consists of a tungsten filament that, when heated to about 3000 K, emits light in the range $320\ \text{nm} < \lambda < 2500\ \text{nm}$. Near the surface of the lamp's quartz envelope, iodine atoms and tungsten atoms ejected from the filament combine to make a variety of tungsten–iodine compounds that decompose at the hot filament, replenishing it with tungsten atoms.

A *gas discharge lamp* is a common source of ultraviolet and visible radiation. In a *xenon discharge lamp*, an electrical discharge excites xenon atoms to excited states, which then emit ultraviolet radiation. At pressures exceeding 1 kPa, the output consists of sharp lines on a broad, intense background due to emission from a mixture of ions formed by the electrical discharge. These high-pressure xenon lamps have emission profiles similar to that of a black body heated to 6000 K. In a *deuterium lamp*, excited D_2 molecules dissociate into electronically excited D atoms, which emit intense radiation between 200–400 nm.

For certain applications, synchrotron radiation is generated in a *synchrotron storage ring*, which consists of an electron beam travelling in a circular path with circumferences of up to several hunderd metres. As electrons travelling in a circle are constantly accelerated by the forces that constrain them to their path, they generate radiation (Fig. 13.52). Synchrotron radiation spans a wide range of frequencies,

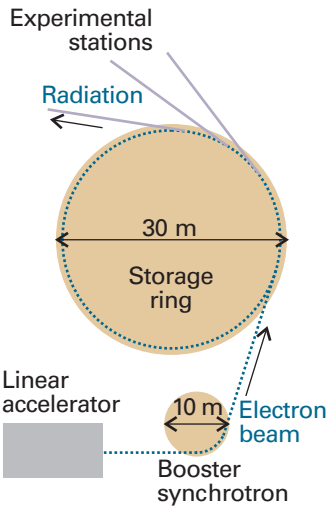

Fig. 13.52 A synchrotron storage ring. The electrons injected into the ring from the linear accelerator and booster synchrotron are accelerated to high speed in the main ring. An electron in a curved path is subject to constant acceleration, and an accelerated charge radiates electromagnetic energy.

including the infrared and X-rays. Except in the microwave region, synchrotron radiation is much more intense than can be obtained by most conventional sources.

The dispersing element

The dispersing element in most absorption spectrometers operating in the ultraviolet to near-infrared region of the spectrum is a **diffraction grating**, which consists of a glass or ceramic plate into which fine grooves have been cut and covered with a reflective aluminium coating. The grating causes interference between waves reflected from its surface, and constructive interference occurs when

$$n\lambda = d(\sin\theta - \sin\phi) \qquad (13.71)$$

where $n = 1, 2, \ldots$ is the *diffraction order*, λ is the wavelength of the diffracted radiation, d is the distance between grooves, θ is the angle of incidence of the beam, and ϕ is the angle of emergence of the beam (Fig. 13.53). For given values of n and θ, larger differences in ϕ are

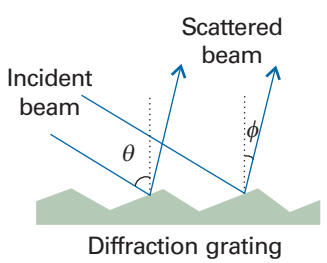

Fig. 13.53 One common dispersing element is a diffraction grating, which separates wavelengths spatially as a result of the scattering of light by fine grooves cut into a coated piece of glass. When a polychromatic light beam strikes the surface at an angle θ, several light beams of different wavelengths emerge at different angles ϕ (eqn 13.71).

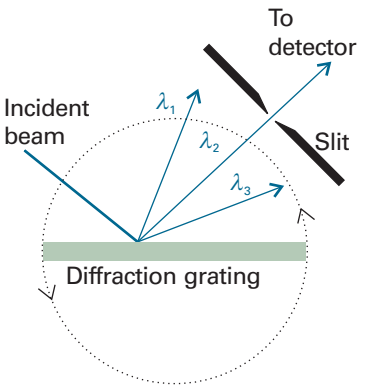

Fig. 13.54 A polychromatic beam is dispersed by a diffraction grating into three component wavelengths λ_1, λ_2, and λ_3. In the configuration shown, only radiation with λ_2 passes through a narrow slit and reaches the detector. Rotating the diffraction grating as shown by the double arrows allows λ_1 or λ_3 to reach the detector.

observed for different wavelengths when d is similar to the wavelength of radiation being analysed. Wide angular separation results in wide spatial separation between wavelengths some distance away from the grating, where a detector is placed.

In a **monochromator**, a narrow exit slit allows only a narrow range of wavelengths to reach the detector (Fig. 13.54). Turning the grating around an axis perpendicular to the incident and diffracted beams allows different wavelengths to be analysed; in this way, the absorption spectrum is built up one narrow wavelength range at a time. Typically, the grating is swept through an angle that investigates only the first order of diffraction ($n = 1$). In a **polychromator**, there is no slit and a broad range of wavelengths can be analysed simultaneously by *array detectors*, such as those discussed below.

Fourier transform techniques

In a Fourier transform instrument, the diffraction grating is replaced by a Michelson interferometer, which works by splitting the beam from the sample into two and introducing a varying path difference, p, into one of them (Fig. 13.55). When the two components

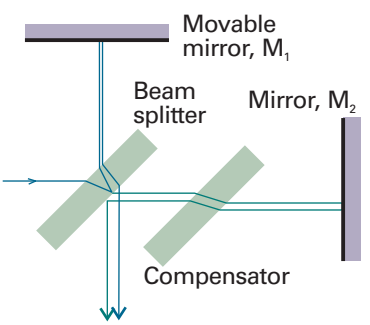

Fig. 13.55 A Michelson interferometer. The beam-splitting element divides the incident beam into two beams with a path difference that depends on the location of the mirror M_1. The compensator ensures that both beams pass through the same thickness of material.

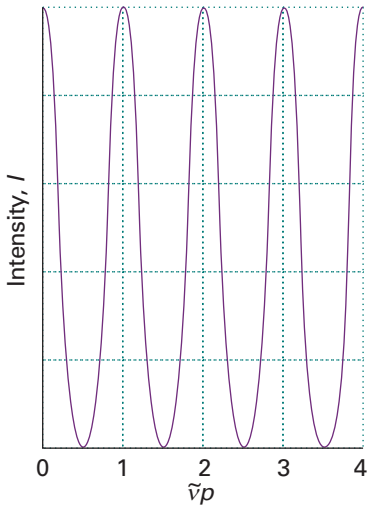

Fig. 13.56 An interferogram produced as the path length p is changed in the interferometer shown in Fig. 13.55. Only a single frequency component is present in the signal, so the graph is a plot of the function $I(p) = I_0(1 + \cos 2\pi\tilde{\nu}p)$, where I_0 is the intensity of the radiation.

Exploration Referring to Fig. 13.55, the mirror M_1 moves in finite distance increments, so the path difference p is also incremented in finite steps. Explore the effect of increasing the step size on the shape of the interferogram for a monochromatic beam of wavenumber $\tilde{\nu}$ and intensity I_0. That is, draw plots of $I(p)/I_0$ against $\tilde{\nu}p$, each with a different number of data points spanning the same total distance path taken by the movable mirror M_1.

recombine, there is a phase difference between them, and they interfere either constructively or destructively depending on the difference in path lengths. The detected signal oscillates as the two components alternately come into and out of phase as the path difference is changed (Fig. 13.56). If the radiation has wavenumber $\tilde{\nu}$, the intensity of the detected signal due to radiation in the range of wavenumbers $\tilde{\nu}$ to $\tilde{\nu} + d\tilde{\nu}$, which we denote $I(p,\tilde{\nu})d\tilde{\nu}$, varies with p as

$$I(p,\tilde{\nu})d\tilde{\nu} = I(\tilde{\nu})(1 + \cos 2\pi\tilde{\nu}p)d\tilde{\nu} \qquad (13.72)$$

Hence, the interferometer converts the presence of a particular wavenumber component in the signal into a variation in intensity of the radiation reaching the detector. An actual signal consists of radiation spanning a large number of wavenumbers, and the total intensity at the detector, which we write $I(p)$, is the sum of contributions from all the wavenumbers present in the signal (Fig. 13.57):

$$I(p) = \int_0^\infty I(p,\tilde{\nu})d\tilde{\nu} = \int_0^\infty I(\tilde{\nu})(1 + \cos 2\pi\tilde{\nu}p)d\tilde{\nu} \qquad (13.73)$$

The problem is to find $I(\tilde{\nu})$, the variation of intensity with wavenumber, which is the spectrum we require, from the record of values of $I(p)$. This step is a standard technique of mathematics, and is the 'Fourier transformation' step from which this form of spectroscopy takes its name. Specifically:

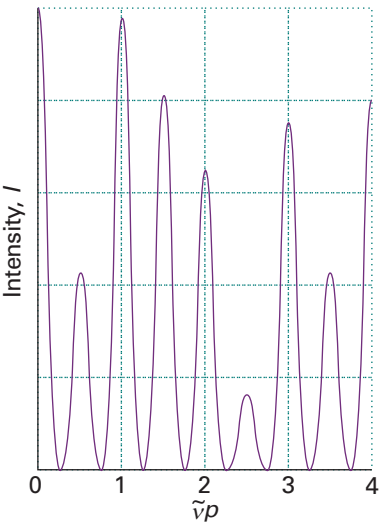

Fig. 13.57 An interferogram obtained when several (in this case, three) frequencies are present in the radiation.

Exploration For a signal consisting of only a few monochromatic beams, the integral in eqn 13.73 can be replaced by a sum over the finite number of wavenumbers. Use this information to draw your own version of Fig. 13.57. Then, go on to explore the effect of varying the wavenumbers and intensities of the three components of the radiation on the shape of the interferogram.

$$I(\tilde{\nu}) = 4\int_0^\infty \{I(p) - \tfrac{1}{2}I(0)\} \cos 2\pi\tilde{\nu}p \, dp \qquad (13.74)$$

where $I(0)$ is given by eqn 13.73 with $p = 0$. This integration is carried out numerically in a computer connected to the spectrometer, and the output, $I(\tilde{\nu})$, is the transmission spectrum of the sample (Fig. 13.58).

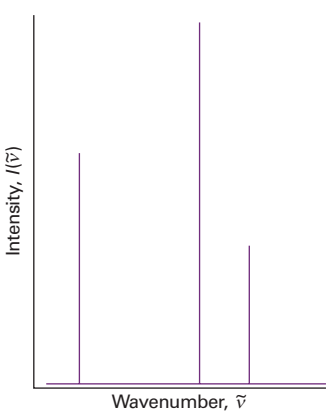

Fig. 13.58 The three frequency components and their intensities that account for the appearance of the interferogram in Fig. 13.57. This spectrum is the Fourier transform of the interferogram, and is a depiction of the contributing frequencies.

Exploration Calculate the Fourier transforms of the functions you generated in the previous *Exploration*.

A major advantage of the Fourier transform procedure is that all the radiation emitted by the source is monitored continuously. This is in contrast to a spectrometer in which a monochromator discards most of the generated radiation. As a result, Fourier transform spectrometers have a higher sensitivity than conventional spectrometers.

Detectors

A **detector** is a device that converts radiation into an electric current or voltage for appropriate signal processing and display. Detectors may consist of a single radiation sensing element or of several small elements arranged in one or two-dimensional arrays.

A microwave detector is typically a *crystal diode* consisting of a tungsten tip in contact with a semiconductor. The most common detectors found in commercial infrared spectrometers are sensitive in the mid-infrared region. In a *photovoltaic device* the potential difference changes upon exposure to infrared radiation. In a *pyroelectric device* the capacitance is sensitive to temperature and hence the presence of infrared radiation.

A common detector for work in the ultraviolet and visible ranges is the *photomultiplier tube* (PMT), in which the photoelectric effect (Section 8.2a) is used to generate an electrical signal proportional to the intensity of light that strikes the detector. In a PMT, photons first strike the *photocathode*, usually a metallic surface to which a large negative potential is applied. Each electron ejected from the photocathode is accelerated by a potential difference to another metallic surface, called the *dynode*, from which more electrons are ejected. After travelling through a chain of dynodes, with each dynode at a more positive potential than the preceding dynode in the chain, all the ejected electrons are collected at a final metallic surface called the *anode*. Depending on how the detector is constructed, a PMT can produce up to 10^8 electrons per photon that strikes the photocathode. This sensitivity is important for the detection of light from weak sources, but can pose problems as well. At room temperature, a small number of electrons on the surfaces of the photocathode and dynodes have sufficient energy to be ejected even in the dark. When amplified through the dynode chain, these electrons give rise to a *dark current*, which interferes with measurements on the sample of interest. To minimize the dark current, it is common to lower the temperature of the PMT detector.

A common, but less sensitive, alternative to the PMT is the *photodiode*, a solid-state device that conducts electricity when struck by photons because light-induced electron transfer reactions in the detector material create mobile charge carriers (negatively charged electrons and positively charged 'holes'). In an *avalanche photodiode*, the photo-generated electrons are accelerated through a very large electrical potential difference. The high-energy electrons then collide with other atoms in the solid and ionize them, thus creating an avalanche of secondary charge carriers and increasing the sensitivity of the device toward photons.

The *charge-coupled device* (CCD) is a two-dimensional array of several million small photodiode detectors. With a CCD, a wide range of wavelengths that emerge from a polychromator are detected simultaneously, thus eliminating the need to measure light intensity one narrow wavelength range at a time. CCD detectors are the imaging devices in digital cameras, but are also used widely in spectroscopy to measure absorption, emission, and Raman scattering. In Raman microscopy, a CCD detector can be used in a variation of the technique known as *Raman imaging*: a special optical filter allows only one Stokes line to reach the two-dimensional detector, which then contains a map of the distribution of the intensity of that line in the illuminated area.

Resolution

A number of factors determine a spectrometer's resolution, the smallest observable separation between two closely spaced spectral bands. We have already seen that the ability of a diffraction grating to disperse light depends on the distance between the grating's grooves and on the wavelength of the incident radiation. Furthermore, the distance between the grating and the slit placed in front of a detector must be long enough and the slit's width must be narrow enough so full advantage can be taken of the grating's dispersing ability (Fig. 13.54). It follows that a bad choice of grating, slit width, and detector placement may result in the failure to distinguish between closely spaced lines or to measure the actual linewidth of any one band in the spectrum.

The resolution of Fourier transform spectrometers is determined by the maximum path length difference, p_{max}, of the interferometer:

$$\Delta\tilde{\nu} = \frac{1}{2p_{max}} \tag{13.75}$$

To achieve a resolution of 0.1 cm^{-1} requires a maximum path length difference of 5 cm.

Assuming that all instrumental factors have been optimized, the highest resolution is obtained when the sample is gaseous and at such low pressure that collisions between the molecules are infrequent (see Section 13.3b). In liquids and solids, the actual linewidths can be so broad that the sample itself can limit the resolution.

Further information 13.2 *Selection rules for rotational and vibrational spectroscopy*

Here we derive the gross and specific selection rules for microwave, infrared, and rotational and vibrational Raman spectroscopy. The starting point for our discussion is the total wavefunction for a molecule, which can be written as

$$\psi_{total} = \psi_{c.m.}\psi$$

where $\psi_{c.m.}$ describes the motion of the centre of mass and ψ describes the internal motion of the molecule. If we neglect the effect of electron spin, the Born–Oppenheimer approximation allows us to write ψ as the product of an electronic part, $|\varepsilon\rangle$, a vibrational part, $|v\rangle$, and a rotational part, which for a diatomic molecule can be represented by the spherical harmonics $Y_{J,M_J}(\theta,\phi)$ (Section 9.7). To simplify the form of the integrals that will soon follow, we are using the Dirac bracket notation introduced in *Further information 9.1*. The transition dipole moment for a spectroscopic transition can now be written as:

$$\boldsymbol{\mu}_{fi} = \langle \varepsilon_f v_f Y_{J,f,M_J,f} | \hat{\boldsymbol{\mu}} | \varepsilon_i v_i Y_{J,i,M_J,i} \rangle \tag{13.76}$$

and our task is to explore conditions for which this integral vanishes or has a non-zero value.

Microwave spectra

During a pure rotational transition the molecule does not change electronic or vibrational states, so that $\langle \varepsilon_f v_f| = \langle \varepsilon_i v_i| = \langle \varepsilon v|$ and we identify $\boldsymbol{\mu}_{\varepsilon v} = \langle \varepsilon v|\hat{\boldsymbol{\mu}}|\varepsilon v\rangle$ with the *permanent* electric dipole moment of the molecule in the state εv. Equation 13.76 becomes

$$\boldsymbol{\mu}_{fi} = \langle Y_{J,f,M_{J,f}}|\hat{\boldsymbol{\mu}}_{\varepsilon v}|Y_{J,i,M_{J,i}}\rangle$$

The electric dipole moment has components $\mu_{\varepsilon v,x}$, $\mu_{\varepsilon v,y}$, and $\mu_{\varepsilon v,z}$, which, in spherical polar coordinates, are written in terms of μ_0, the magnitude of the vector, and the angles θ and ϕ as

$$\mu_{\varepsilon v,x} = \mu_0 \sin\theta\cos\phi \qquad \mu_{\varepsilon v,y} = \mu_0 \sin\theta\sin\phi \qquad \mu_{\varepsilon v,z} = \mu_0\cos\theta$$

Here, we have taken the z-axis to be coincident with the figure axis. The transition dipole moment has three components, given by:

$$\mu_{fi,x} = \mu_0\langle Y_{J,f,M_{J,f}}|\sin\theta\cos\phi|Y_{J,i,M_{J,i}}\rangle$$
$$\mu_{fi,y} = \mu_0\langle Y_{J,f,M_{J,f}}|\sin\theta\sin\phi|Y_{J,i,M_{J,i}}\rangle$$
$$\mu_{fi,z} = \mu_0\langle Y_{J,f,M_{J,f}}|\cos\theta|Y_{J,i,M_{J,i}}\rangle$$

We see immediately that the molecule must have a permanent dipole moment in order to have a microwave spectrum. This is the gross selection rule for microwave spectroscopy.

For the specific selection rules we need to examine the conditions for which the integrals do not vanish, and we must consider each component. For the z-component, we simplify the integral by using $\cos\theta \propto Y_{1,0}$ (Table 9.3). It follows that

$$\mu_{fi,z} \propto \langle Y_{J,f,M_{J,f}}|Y_{1,0}|Y_{J,i,M_{J,i}}\rangle$$

According to the properties of the spherical harmonics (*Comment* 13.8), this integral vanishes unless $J_f - J_i = \pm 1$ and $M_{J,f} - M_{J,i} = 0$. These are two of the selection rules stated in eqn 13.35.

Comment 13.8

An important 'triple integral' involving the spherical harmonics is

$$\int_0^{\pi}\int_0^{2\pi} Y_{l'',m_l''}(\theta,\phi)^* Y_{l',m_l'}(\theta,\phi) Y_{l,m_l}(\theta,\phi)\sin\theta\,d\theta\,d\phi = 0$$

unless $m_l'' = m_l' + m_l$ and lines of length l'', l', and l can form a triangle.

For the x- and y-components, we use $\cos\phi = \frac{1}{2}(e^{i\phi} + e^{-i\phi})$ and $\sin\phi = -\frac{1}{2}i(e^{i\phi} - e^{-i\phi})$ to write $\sin\theta\cos\phi \propto Y_{1,1} + Y_{1,-1}$ and $\sin\theta\sin\phi \propto Y_{1,1} - Y_{1,-1}$. It follows that

$$\mu_{fi,x} \propto \langle Y_{J,f,M_{J,f}}|(Y_{1,1} + Y_{1,-1})|Y_{J,i,M_{J,i}}\rangle$$
$$\mu_{fi,y} \propto \langle Y_{J,f,M_{J,f}}|(Y_{1,1} - Y_{1,-1})|Y_{J,i,M_{J,i}}\rangle$$

According to the properties of the spherical harmonics, these integrals vanish unless $J_f - J_i = \pm 1$ and $M_{J,f} - M_{J,i} = \pm 1$. This completes the selection rules of eqn 13.35.

Rotational Raman spectra

We understand the origin of the gross and specific selection rules for rotational Raman spectroscopy by using a diatomic molecule as an example. The incident electric field of a wave of electromagnetic radiation of frequency ω_i induces a molecular dipole moment that is given by

$$\mu_{ind} = \alpha\mathcal{E}(t) = \alpha\mathcal{E}\cos\omega_i t$$

If the molecule is rotating at a circular frequency ω_R, to an external observer its polarizability is also time dependent (if it is anisotropic), and we can write

$$\alpha = \alpha_0 + \Delta\alpha\cos 2\omega_R t$$

where $\Delta\alpha = \alpha_\parallel - \alpha_\perp$ and α ranges from $\alpha_0 + \Delta\alpha$ to $\alpha_0 - \Delta\alpha$ as the molecule rotates. The 2 appears because the polarizability returns to its initial value twice each revolution (Fig. 13.59). Substituting this expression into the expression for the induced dipole moment gives

$$\begin{aligned}\mu_{ind} &= (\alpha_0 + \Delta\alpha\cos 2\omega_R t)\times(\mathcal{E}\cos\omega_i t)\\ &= \alpha_0\mathcal{E}\cos\omega_i t + \mathcal{E}\Delta\alpha\cos 2\omega_R t\cos\omega_i t\\ &= \alpha_0\mathcal{E}\cos\omega_i t + \tfrac{1}{2}\mathcal{E}\Delta\alpha\{\cos(\omega_i + 2\omega_R)t + \cos(\omega_i - 2\omega_R)t\}\end{aligned}$$

This calculation shows that the induced dipole has a component oscillating at the incident frequency (which generates Rayleigh radiation), and that it also has two components at $\omega_i \pm 2\omega_R$, which give rise to the shifted Raman lines. These lines appear only if $\Delta\alpha \neq 0$; hence the polarizability must be anisotropic for there to be Raman lines. This is the gross selection rule for rotational Raman spectroscopy. We also see that the distortion induced in the molecule by the incident electric field returns to its initial value after a rotation of 180° (that is, twice a revolution). This is the origin of the specific selection rule $\Delta J = \pm 2$.

We now use a quantum mechanical formalism to understand the selection rules. First, we write the x-, y-, and z-components of the induced dipole moment as

$$\mu_{ind,x} = \mu_x\sin\theta\cos\phi \qquad \mu_{ind,y} = \mu_y\sin\theta\sin\phi \qquad \mu_{ind,z} = \mu_z\cos\theta$$

where μ_x, μ_y, and μ_z are the components of the electric dipole moment of the molecule and the z-axis is coincident with the molecular figure axis. The incident electric field also has components along the x-, y-, and z-axes:

$$\mathcal{E}_x = \mathcal{E}\sin\theta\cos\phi \qquad \mathcal{E}_y = \mathcal{E}\sin\theta\sin\phi \qquad \mathcal{E}_z = \mathcal{E}\cos\theta$$

Using eqn 13.40 and the preceding equations, it follows that

$$\begin{aligned}\mu_{ind} &= \alpha_\perp\mathcal{E}_x\sin\theta\cos\phi + \alpha_\perp\mathcal{E}_y\sin\theta\sin\phi + \alpha_\parallel\mathcal{E}\cos\theta\\ &= \alpha_\perp\mathcal{E}\sin^2\theta + \alpha_\parallel\mathcal{E}\cos^2\theta\end{aligned}$$

By using the spherical harmonic $Y_{2,0}(\theta,\phi) = (5/16\pi)^{1/2}(3\cos^2\theta - 1)$ and the relation $\sin^2\theta = 1 - \cos^2\theta$, it follows that:

$$\mu_{ind} = \left\{\tfrac{1}{3}\alpha_\parallel + \tfrac{2}{3}\alpha_\perp + \tfrac{4}{3}\left(\frac{\pi}{5}\right)^{1/2}\Delta\alpha Y_{2,0}(\theta,\phi)\right\}\mathcal{E}$$

For a transition between two rotational states, we calculate the integral $\langle Y_{J,f,M_{J,f}}|\mu_{ind}|Y_{J,i,M_{J,i}}\rangle$, which has two components:

$$(\tfrac{1}{3}\alpha_\parallel + \tfrac{2}{3}\alpha_\perp)\langle Y_{J_f,M_{J,f}}|(Y_{J_i,M_{J,i}}\rangle \quad \text{and} \quad \mathcal{E}\Delta\alpha\langle Y_{J_f,M_{J,f}}|Y_{2,0}Y_{J_i,M_{J,i}}\rangle$$

According to the properties of the spherical harmonics (Table 9.3), the first integral vanishes unless $J_f - J_i = 0$ and the second integral vanishes unless $J_f - J_i = \pm 2$ and $\Delta\alpha \neq 0$. These are the gross and specific selection rules for linear rotors.

Infrared spectra

The gross selection rule for infrared spectroscopy is based on an analysis of the transition dipole moment $\langle v_f|\hat{\boldsymbol{\mu}}|v_i\rangle$, which arises from eqn 13.76 when the molecule does not change electronic or rotational

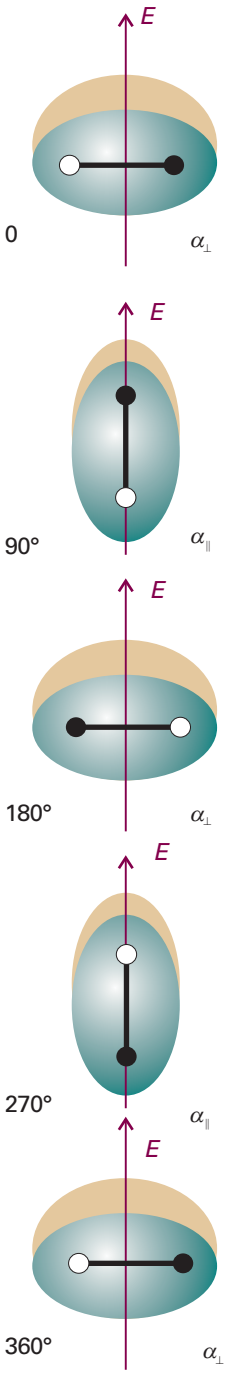

Fig. 13.59 The distortion induced in a molecule by an applied electric field returns to its initial value after a rotation of only 180° (that is, twice a revolution). This is the origin of the $\Delta J = \pm 2$ selection rule in rotational Raman spectroscopy.

states. For simplicity, we shall consider a one-dimensional oscillator (like a diatomic molecule). The electric dipole moment operator depends on the location of all the electrons and all the nuclei in the molecule, so it varies as the internuclear separation changes

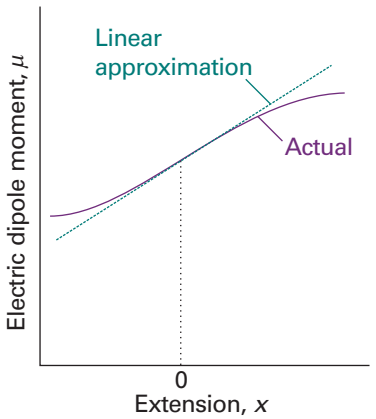

Fig. 13.60 The electric dipole moment of a heteronuclear diatomic molecule varies as shown by the purple curve. For small displacements the change in dipole moment is proportional to the displacement.

(Fig. 13.60). If we think of the dipole moment as arising from two partial charges $\pm\delta q$ separated by a distance $R = R_e + x$, we can write its variation with displacement from the equilibrium separation, x, as

$$\mu = R\delta q = R_e\delta q + x\delta q = \mu_0 + x\delta q$$

where μ_0 is the electric dipole moment operator when the nuclei have their equilibrium separation. It then follows that, with $f \neq i$,

$$\langle v_f|\hat{\mu}|v_i\rangle = \mu_0\langle v_f|v_i\rangle + \delta q\langle v_f|x|v_i\rangle$$

The term proportional to μ_0 is zero because the states with different values of v are orthogonal. It follows that the transition dipole moment is

$$\langle v_f|\hat{\mu}|v_i\rangle = \langle v_f|x|v_i\rangle\delta q$$

Because

$$\delta q = \frac{d\mu}{dx}$$

we can write the transition dipole moment more generally as

$$\langle v_f|\hat{\mu}|v_i\rangle = \langle v_f|x|v_i\rangle\left(\frac{d\mu}{dx}\right)$$

and we see that the right-hand side is zero unless the dipole moment varies with displacement. This is the gross selection rule for infrared spectroscopy.

The specific selection rule is determined by considering the value of $\langle v_f|x|v_i\rangle$. We need to write out the wavefunctions in terms of the Hermite polynomials given in Section 9.5 and then to use their properties (Example 9.4 should be reviewed, for it gives further details of the calculation). We note that $x = \alpha y$ with $\alpha = (\hbar^2/m_{\text{eff}}k)^{1/4}$ (eqn 9.28; note that in this context α is not the polarizability). Then we write

$$\langle v_f|x|v_i\rangle = N_{v_f}N_{v_i}\int_{-\infty}^{\infty} H_{v_f}xH_{v_i}e^{-y^2}dx = \alpha^2 N_{v_f}N_{v_i}\int_{-\infty}^{\infty} H_{v_f}yH_{v_i}e^{-y^2}dy$$

To evaluate the integral we use the recursion relation

$$yH_v = vH_{v-1} + \tfrac{1}{2}H_{v+1}$$

which turns the matrix element into

$$\langle v_f|x|v_i\rangle = \alpha^2 N_{v_f} N_{v_i}\left\{v_i\int_{-\infty}^{\infty} H_{v_f}H_{v_i-1}e^{-y^2}dy + \tfrac{1}{2}\int_{-\infty}^{\infty} H_{v_f}H_{v_i+1}e^{-y^2}dy\right\}$$

The first integral is zero unless $v_f = v_i - 1$ and that the second is zero unless $v_f = v_i + 1$. It follows that the transition dipole moment is zero unless $\Delta v = \pm 1$.

Comment 13.9

An important integral involving Hermite polynomials is

$$\int_{-\infty}^{\infty} H_{v'}H_v e^{-y^2}dy = \begin{cases} 0 & \text{if } v' \neq v \\ \pi^{1/2}2^v v! & \text{if } v' = v \end{cases}$$

Vibrational Raman spectra

The gross selection rule for vibrational Raman spectroscopy is based on an analysis of the transition dipole moment $\langle \varepsilon v_f|\hat{\boldsymbol{\mu}}|\varepsilon v_i\rangle$, which is written from eqn 13.76 by using the Born–Oppenheimer approximation and neglecting the effect of rotation and electron spin. For simplicity, we consider a one-dimensional harmonic oscillator (like a diatomic molecule).

First, we use eqn 13.40 to write the transition dipole moment as

$$\mu_{fi} = \langle \varepsilon v_f|\hat{\mu}|\varepsilon v_i\rangle = \langle \varepsilon v_f|\alpha|\varepsilon v_i\rangle \mathcal{E} = \langle v_f|\alpha(x)|v_i\rangle \mathcal{E}$$

where $\alpha(x) = \langle \varepsilon|\alpha|\varepsilon\rangle$ is the polarizability of the molecule, which we expect to be a function of small displacements x from the equilibrium bond length of the molecule (Section 13.13). Next, we expand $\alpha(x)$ as a Taylor series, so the transition dipole moment becomes

$$\mu_{fi} = \left\langle v_f \middle| \alpha(0) + \left(\frac{d\alpha}{dx}\right)_0 x + \cdots \middle| v_i \right\rangle \mathcal{E}$$

$$= \langle v_f|v_i\rangle \alpha(0)\mathcal{E} + \left(\frac{d\alpha}{dx}\right)_0 \langle v_f|x|v_i\rangle \mathcal{E} + \cdots$$

The term containing $\langle v_f|v_i\rangle$ vanishes for $f \neq i$ because the harmonic oscillator wavefunctions are orthogonal. Therefore, the vibration is Raman active if $(d\alpha/dx)_0 \neq 0$ and $\langle v_f|x|v_i\rangle \neq 0$. Therefore, the polarizability of the molecule must change during the vibration; this is the gross selection rule of Raman spectroscopy. Also, we already know that $\langle v_f|x|v_i\rangle \neq 0$ if $v_f - v_i = \pm 1$; this is the specific selection rule of Raman spectroscopy.

Discussion questions

13.1 Describe the physical origins of linewidths in the absorption and emission spectra of gases, liquids, and solids.

13.2 Discuss the physical origins of the gross selection rules for microwave and infrared spectroscopy.

13.3 Discuss the physical origins of the gross selection rules for rotational and vibrational Raman spectroscopy.

13.4 Consider a diatomic molecule that is highly susceptible to centrifugal distortion in its ground vibrational state. Do you expect excitation to high rotational energy levels to change the equilibrium bond length of this molecule? Justify your answer.

13.5 Suppose that you wish to characterize the normal modes of benzene in the gas phase. Why is it important to obtain both infrared absorption and Raman spectra of your sample?

Exercises

13.1a Calculate the ratio of the Einstein coefficients of spontaneous and stimulated emission, A and B, for transitions with the following characteristics: (a) 70.8 pm X-rays, (b) 500 nm visible light, (c) 3000 cm^{-1} infrared radiation.

13.1b Calculate the ratio of the Einstein coefficients of spontaneous and stimulated emission, A and B, for transitions with the following characteristics: (a) 500 MHz radiofrequency radiation, (e) 3.0 cm microwave radiation.

13.2a What is the Doppler-shifted wavelength of a red (660 nm) traffic light approached at 80 km h^{-1}?

13.2b At what speed of approach would a red (660 nm) traffic light appear green (520 nm)?

13.3a Estimate the lifetime of a state that gives rise to a line of width (a) 0.10 cm^{-1}, (b) 1.0 cm^{-1}.

13.3b Estimate the lifetime of a state that gives rise to a line of width (a) 100 MHZ, (b) 2.14 cm^{-1}.

13.4a A molecule in a liquid undergoes about 1.0×10^{13} collisions in each second. Suppose that (a) every collision is effective in deactivating the molecule vibrationally and (b) that one collision in 100 is effective. Calculate the width (in cm^{-1}) of vibrational transitions in the molecule.

13.4b A molecule in a gas undergoes about 1.0×10^9 collisions in each second. Suppose that (a) every collision is effective in deactivating the molecule rotationally and (b) that one collision in 10 is effective. Calculate the width (in hertz) of rotational transitions in the molecule.

13.5a Calculate the frequency of the $J = 4 \leftarrow 3$ transition in the pure rotational spectrum of $^{14}N^{16}O$. The equilibrium bond length is 115 pm.

13.5b Calculate the frequency of the $J = 3 \leftarrow 2$ transition in the pure rotational spectrum of $^{12}C^{16}O$. The equilibrium bond length is 112.81 pm.

13.6a If the wavenumber of the $J = 3 \leftarrow 2$ rotational transition of $^{1}H^{35}Cl$ considered as a rigid rotator is 63.56 cm^{-1}, what is (a) the moment of inertia of the molecule, (b) the bond length?

13.6b If the wavenumber of the $J = 1 \leftarrow 0$ rotational transition of $^{1}H^{81}Br$ considered as a rigid rotator is 16.93 cm^{-1}, what is (a) the moment of inertia of the molecule, (b) the bond length?

13.7a Given that the spacing of lines in the microwave spectrum of $^{27}Al^{1}H$ is constant at 12.604 cm^{-1}, calculate the moment of inertia and bond length of the molecule ($m(^{27}Al) = 26.9815$ u).

13.7b Given that the spacing of lines in the microwave spectrum of $^{35}Cl^{19}F$ is constant at 1.033 cm^{-1}, calculate the moment of inertia and bond length of the molecule ($m(^{35}Cl) = 34.9688$ u, $m(^{19}F) = 18.9984$ u).

13.8a The rotational constant of $^{127}I^{35}Cl$ is 0.1142 cm^{-1}. Calculate the ICl bond length ($m(^{35}Cl) = 34.9688$ u, $m(^{127}I) = 126.9045$ u).

13.8b The rotational constant of $^{12}C^{16}O_2$ is 0.39021 cm^{-1}. Calculate the bond length of the molecule ($m(^{12}C) = 12$ u exactly, $m(^{16}O) = 15.9949$ u).

13.9a Determine the HC and CN bond lengths in HCN from the rotational constants $B(^{1}H^{12}C^{14}N) = 44.316$ GHz and $B(^{2}H^{12}C^{14}N) = 36.208$ GHz.

13.9b Determine the CO and CS bond lengths in OCS from the rotational constants $B(^{16}O^{12}C^{32}S) = 6081.5$ MHz, $B(^{16}O^{12}C^{34}S) = 5932.8$ MHz.

13.10a The wavenumber of the incident radiation in a Raman spectrometer is 20 487 cm^{-1}. What is the wavenumber of the scattered Stokes radiation for the $J = 2 \leftarrow 0$ transition of $^{14}N_2$?

13.10b The wavenumber of the incident radiation in a Raman spectrometer is 20 623 cm^{-1}. What is the wavenumber of the scattered Stokes radiation for the $J = 4 \leftarrow 2$ transition of $^{16}O_2$?

13.11a The rotational Raman spectrum of $^{35}Cl_2$ ($m(^{35}Cl) = 34.9688$ u) shows a series of Stokes lines separated by 0.9752 cm^{-1} and a similar series of anti-Stokes lines. Calculate the bond length of the molecule.

13.11b The rotational Raman spectrum of $^{19}F_2$ ($m(^{19}F) = 18.9984$ u) shows a series of Stokes lines separated by 3.5312 cm^{-1} and a similar series of anti-Stokes lines. Calculate the bond length of the molecule.

13.12a Which of the following molecules may show a pure rotational microwave absorption spectrum: (a) H_2, (b) HCl, (c) CH_4, (d) CH_3Cl, (e) CH_2Cl_2?

13.12b Which of the following molecules may show a pure rotational microwave absorption spectrum: (a) H_2O, (b) H_2O_2, (c) NH_3, (d) N_2O?

13.13a Which of the following molecules may show a pure rotational Raman spectrum: (a) H_2, (b) HCl, (c) CH_4, (d) CH_3Cl?

13.13b Which of the following molecules may show a pure rotational Raman spectrum: (a) CH_2Cl_2, (b) CH_3CH_3, (c) SF_6, (d) N_2O?

13.14a An object of mass 1.0 kg suspended from the end of a rubber band has a vibrational frequency of 2.0 Hz. Calculate the force constant of the rubber band.

13.14b An object of mass 2.0 g suspended from the end of a spring has a vibrational frequency of 3.0 Hz. Calculate the force constant of the spring.

13.15a Calculate the percentage difference in the fundamental vibration wavenumber of $^{23}Na^{35}Cl$ and $^{23}Na^{37}Cl$ on the assumption that their force constants are the same.

13.15b Calculate the percentage difference in the fundamental vibration wavenumber of $^{1}H^{35}Cl$ and $^{2}H^{37}Cl$ on the assumption that their force constants are the same.

13.16a The wavenumber of the fundamental vibrational transition of $^{35}Cl_2$ is 564.9 cm^{-1}. Calculate the force constant of the bond ($m(^{35}Cl) = 34.9688$ u).

13.16b The wavenumber of the fundamental vibrational transition of $^{79}Br^{81}Br$ is 323.2 cm^{-1}. Calculate the force constant of the bond ($m(^{79}Br) = 78.9183$ u, $m(^{81}Br) = 80.9163$ u).

13.17a Calculate the relative numbers of Cl_2 molecules ($\tilde{\nu} = 559.7$ cm^{-1}) in the ground and first excited vibrational states at (a) 298 K, (b) 500 K.

13.17b Calculate the relative numbers of Br_2 molecules ($\tilde{\nu} = 321$ cm^{-1}) in the second and first excited vibrational states at (a) 298 K, (b) 800 K.

13.18a The hydrogen halides have the following fundamental vibrational wavenumbers: 4141.3 cm^{-1} (HF); 2988.9 cm^{-1} ($H^{35}Cl$); 2649.7 cm^{-1} ($H^{81}Br$); 2309.5 cm^{-1} ($H^{127}I$). Calculate the force constants of the hydrogen–halogen bonds.

13.18b From the data in Exercise 13.18a, predict the fundamental vibrational wavenumbers of the deuterium halides.

13.19a For $^{16}O_2$, ΔG values for the transitions $v = 1 \leftarrow 0$, $2 \leftarrow 0$, and $3 \leftarrow 0$ are, respectively, 1556.22, 3088.28, and 4596.21 cm^{-1}. Calculate $\tilde{\nu}$ and x_e. Assume y_e to be zero.

13.19b For $^{14}N_2$, ΔG values for the transitions $v = 1 \leftarrow 0$, $2 \leftarrow 0$, and $3 \leftarrow 0$ are, respectively, 2345.15, 4661.40, and 6983.73 cm^{-1}. Calculate $\tilde{\nu}$ and x_e. Assume y_e to be zero.

13.20a The first five vibrational energy levels of HCl are at 1481.86, 4367.50, 7149.04, 9826.48, and 12 399.8 cm^{-1}. Calculate the dissociation energy of the molecule in reciprocal centimetres and electronvolts.

13.20b The first five vibrational energy levels of HI are at 1144.83, 3374.90, 5525.51, 7596.66, and 9588.35 cm^{-1}. Calculate the dissociation energy of the molecule in reciprocal centimetres and electronvolts.

13.21a Infrared absorption by $^{1}H^{81}Br$ gives rise to an R branch from $v = 0$. What is the wavenumber of the line originating from the rotational state with $J = 2$? Use the information in Table 13.2.

13.21b Infrared absorption by $^{1}H^{127}I$ gives rise to an R branch from $v = 0$. What is the wavenumber of the line originating from the rotational state with $J = 2$? Use the information in Table 13.2.

13.22a Which of the following molecules may show infrared absorption spectra: (a) H_2, (b) HCl, (c) CO_2, (d) H_2O?

13.22b Which of the following molecules may show infrared absorption spectra: (a) CH_3CH_3, (b) CH_4, (c) CH_3Cl, (d) N_2?

13.23a How many normal modes of vibration are there for the following molecules: (a) H_2O, (b) H_2O_2, (c) C_2H_4?

13.23b How many normal modes of vibration are there for the following molecules: (a) C_6H_6, (b) $C_6H_6CH_3$, (c) HC≡C—C≡CH.

13.24a Which of the three vibrations of an AB_2 molecule are infrared or Raman active when it is (a) angular, (b) linear?

13.24b Which of the vibrations of an AB_3 molecule are infrared or Raman active when it is (a) trigonal planar, (b) trigonal pyramidal?

13.25a Consider the vibrational mode that corresponds to the uniform expansion of the benzene ring. Is it (a) Raman, (b) infrared active?

13.25b Consider the vibrational mode that corresponds to the boat-like bending of a benzene ring. Is it (a) Raman, (b) infrared active?

13.26a The molecule CH_2Cl_2 belongs to the point group C_{2v}. The displacements of the atoms span $5A_1 + 2A_2 + 4B_1 + 4B_2$. What are the symmetries of the normal modes of vibration?

13.26b A carbon disulfide molecule belongs to the point group $D_{\infty h}$. The nine displacements of the three atoms span $A_{1g} + A_{1u} + A_{2g} + 2E_{1u} + E_{1g}$. What are the symmetries of the normal modes of vibration?

Problems*

Numerical problems

13.1 Use mathematical software to evaluate the Planck distribution at any temperature and wavelength or frequency, and evaluate integrals for the energy density of the radiation between any two wavelengths. Calculate the total energy density in the visible region (700 nm to 400 nm) for a black body at (a) 1500 K, a typical operating temperature for globars, (b) 2500 K, a typical operating temperature for tungsten filament lamps, (c) 5800 K, the surface temperature of the Sun. What are the classical values at these temperatures?

13.2 Calculate the Doppler width (as a fraction of the transition wavelength) for any kind of transition in (a) HCl, (b) ICl at 25°C. What would be the widths of the rotational and vibrational transitions in these molecules (in MHz and cm^{-1}, respectively), given $B(ICl) = 0.1142\ cm^{-1}$ and $\tilde{\nu}(ICl) = 384\ cm^{-1}$ and additional information in Table 13.2.

13.3 The collision frequency z of a molecule of mass m in a gas at a pressure p is $z = 4\sigma(kT/\pi m)^{1/2}p/kT$, where σ is the collision cross-section. Find an expression for the collision-limited lifetime of an excited state assuming that every collision is effective. Estimate the width of rotational transition in HCl ($\sigma = 0.30\ nm^2$) at 25°C and 1.0 atm. To what value must the pressure of the gas be reduced in order to ensure that collision broadening is less important than Doppler broadening?

13.4 The rotational constant of NH_3 is equivalent to 298 GHz. Compute the separation of the pure rotational spectrum lines in GHz, cm^{-1}, and mm, and show that the value of B is consistent with an N—H bond length of 101.4 pm and a bond angle of 106.78°.

13.5 The rotational constant for CO is $1.9314\ cm^{-1}$ and $1.6116\ cm^{-1}$ in the ground and first excited vibrational states, respectively. By how much does the internuclear distance change as a result of this transition?

13.6 Pure rotational Raman spectra of gaseous C_6H_6 and C_6D_6 yield the following rotational constants: $B(C_6H_6) = 0.189\ 60\ cm^{-1}$, $B(C_6D_6) = 0.156\ 81\ cm^{-1}$. The moments of inertia of the molecules about any axis perpendicular to the C_6 axis were calculated from these data as $I(C_6H_6) = 1.4759 \times 10^{-45}\ kg\ m^2$, $I(C_6D_6) = 1.7845 \times 10^{-45}\ kg\ m^2$. Calculate the CC, CH, and CD bond lengths.

13.7 Rotational absorption lines from $^1H^{35}Cl$ gas were found at the following wavenumbers (R.L. Hausler and R.A. Oetjen, *J. Chem. Phys.* **21**, 1340 (1953)): 83.32, 104.13, 124.73, 145.37, 165.89, 186.23, 206.60, 226.86 cm^{-1}. Calculate the moment of inertia and the bond length of the molecule. Predict the positions of the corresponding lines in $^2H^{35}Cl$.

13.8 Is the bond length in HCl the same as that in DCl? The wavenumbers of the $J = 1 \leftarrow 0$ rotational transitions for $H^{35}Cl$ and $^2H^{35}Cl$ are 20.8784 and 10.7840 cm^{-1}, respectively. Accurate atomic masses are 1.007825 u and 2.0140 u for ^1H and ^2H, respectively. The mass of ^{35}Cl is 34.96885 u. Based on this information alone, can you conclude that the bond lengths are the same or different in the two molecules?

13.9 Thermodynamic considerations suggest that the copper monohalides CuX should exist mainly as polymers in the gas phase, and indeed it proved difficult to obtain the monomers in sufficient abundance to detect spectroscopically. This problem was overcome by flowing the halogen gas over copper heated to 1100 K (E.L. Manson, F.C. de Lucia, and W. Gordy, *J. Chem. Phys.* **63**, 2724 (1975)). For CuBr the J = 13–14, 14–15, and 15–16 transitions occurred at 84 421.34, 90 449.25, and 96 476.72 MHz, respectively. Calculate the rotational constant and bond length of CuBr.

13.10 The microwave spectrum of $^{16}O^{12}CS$ (C.H. Townes, A.N. Holden, and F.R. Merritt, *Phys. Rev.* **74**, 1113 (1948)) gave absorption lines (in GHz) as follows:

J	1	2	3	4
^{32}S	24.325 92	36.488 82	48.651 64	60.814 08
^{34}S	23.732 33		47.462 40	

Use the expressions for moments of inertia in Table 13.1 and assume that the bond lengths are unchanged by substitution; calculate the CO and CS bond lengths in OCS.

13.11‡ In a study of the rotational spectrum of the linear FeCO radical, K. Tanaka, M. Shirasaka, and T. Tanaka (*J. Chem. Phys.* **106**, 6820 (1997)) report the following $J + 1 \leftarrow J$ transitions:

J	24	25	26	27	28	29
$\tilde{\nu}/m^{-1}$	214 777.7	223 379.0	231 981.2	240 584.4	249 188.5	257 793.5

Evaluate the rotational constant of the molecule. Also, estimate the value of J for the most highly populated rotational energy level at 298 K and at 100 K.

13.12 The vibrational energy levels of NaI lie at the wavenumbers 142.81, 427.31, 710.31, and 991.81 cm^{-1}. Show that they fit the expression $(v + \frac{1}{2})\tilde{\nu} - (v + \frac{1}{2})^2 x\tilde{\nu}$, and deduce the force constant, zero-point energy, and dissociation energy of the molecule.

13.13 Predict the shape of the nitronium ion, NO_2^+, from its Lewis structure and the VSEPR model. It has one Raman active vibrational mode at 1400 cm^{-1}, two strong IR active modes at 2360 and 540 cm^{-1}, and one weak IR mode at 3735 cm^{-1}. Are these data consistent with the predicted shape of the molecule? Assign the vibrational wavenumbers to the modes from which they arise.

13.14 At low resolution, the strongest absorption band in the infrared absorption spectrum of $^{12}C^{16}O$ is centred at 2150 cm^{-1}. Upon closer examination at higher resolution, this band is observed to be split into two sets of closely spaced peaks, one on each side of the centre of the spectrum at 2143.26 cm^{-1}. The separation between the peaks immediately to the right and left of the centre is 7.655 cm^{-1}. Make the harmonic oscillator and rigid rotor approximations and calculate from these data: (a) the vibrational wavenumber of a CO molecule, (b) its molar zero-point vibrational energy, (c) the force constant of the CO bond, (d) the rotational constant B, and (e) the bond length of CO.

13.15 The HCl molecule is quite well described by the Morse potential with $D_e = 5.33$ eV, $\tilde{\nu} = 2989.7\ cm^{-1}$, and $x\tilde{\nu} = 52.05\ cm^{-1}$. Assuming that the potential is unchanged on deuteration, predict the dissociation energies (D_0) of (a) HCl, (b) DCl.

13.16 The Morse potential (eqn 13.54) is very useful as a simple representation of the actual molecular potential energy. When RbH was studied, it was found that $\tilde{\nu} = 936.8\ cm^{-1}$ and $x\tilde{\nu} = 14.15\ cm^{-1}$. Plot the potential energy curve from 50 pm to 800 pm around $R_e = 236.7$ pm. Then go on to explore how the rotation of a molecule may weaken its bond by allowing for the kinetic energy of rotation of a molecule and plotting $V^* = V + hcBJ(J + 1)$ with $B = \hbar/4\pi c\mu R^2$. Plot these curves on the same diagram for J = 40, 80, and 100, and observe how the dissociation energy is affected by the

* Problems denoted with the symbol ‡ were supplied by Charles Trapp, Carmen Giunta, and Marshall Cady.

rotation. (Taking $B = 3.020\ \text{cm}^{-1}$ at the equilibrium bond length will greatly simplify the calculation.)

13.17‡ F. Luo, G.C. McBane, G. Kim, C.F. Giese, and W.R. Gentry (*J. Chem. Phys.* **98**, 3564 (1993)) reported experimental observation of the He_2 complex, a species that had escaped detection for a long time. The fact that the observation required temperatures in the neighbourhood of 1 mK is consistent with computational studies that suggest that hcD_e for He_2 is about 1.51×10^{-23} J, hcD_0 about 2×10^{-26} J, and R_e about 297 pm. (a) Estimate the fundamental vibrational wavenumber, force constant, moment of inertia, and rotational constant based on the harmonic oscillator and rigid-rotor approximations. (b) Such a weakly bound complex is hardly likely to be rigid. Estimate the vibrational wavenumber and anharmonicity constant based on the Morse potential.

13.18 As mentioned in Section 13.15, the semi-empirical, *ab initio*, and DFT methods discussed in Chapter 11 can be used to estimate the force field of a molecule. The molecule's vibrational spectrum can be simulated, and it is then possible to determine the correspondence between a vibrational frequency and the atomic displacements that give rise to a normal mode. (a) Using molecular modelling software[3] and the computational method of your choice (semi-empirical, *ab initio*, or DFT methods), calculate the fundamental vibrational wavenumbers and visualize the vibrational normal modes of SO_2 in the gas phase. (b) The experimental values of the fundamental vibrational wavenumbers of SO_2 in the gas phase are 525 cm^{-1}, 1151 cm^{-1}, and 1336 cm^{-1}. Compare the calculated and experimental values. Even if agreement is poor, is it possible to establish a correlation between an experimental value of the vibrational wavenumber with a specific vibrational normal mode?

13.19 Consider the molecule CH_3Cl. (a) To what point group does the molecule belong? (b) How many normal modes of vibration does the molecule have? (c) What are the symmetries of the normal modes of vibration for this molecule? (d) Which of the vibrational modes of this molecule are infrared active? (e) Which of the vibrational modes of this molecule are Raman active?

13.20 Suppose that three conformations are proposed for the nonlinear molecule H_2O_2 (**2**, **3**, and **4**). The infrared absorption spectrum of gaseous H_2O_2 has bands at 870, 1370, 2869, and 3417 cm^{-1}. The Raman spectrum of the same sample has bands at 877, 1408, 1435, and 3407 cm^{-1}. All bands correspond to fundamental vibrational wavenumbers and you may assume that: (i) the 870 and 877 cm^{-1} bands arise from the same normal mode, and (ii) the 3417 and 3407 cm^{-1} bands arise from the same normal mode. (a) If H_2O_2 were linear, how many normal modes of vibration would it have? (b) Give the symmetry point group of each of the three proposed conformations of nonlinear H_2O_2. (c) Determine which of the proposed conformations is inconsistent with the spectroscopic data. Explain your reasoning.

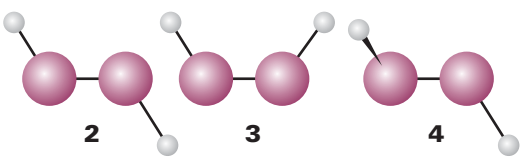

Theoretical problems

13.21 Show that the moment of inertia of a diatomic molecule composed of atoms of masses m_A and m_B and bond length R is equal to $m_{\text{eff}}R^2$, where $m_{\text{eff}} = m_A m_B/(m_A + m_B)$.

13.22 Derive eqn 13.34 for the centrifugal distortion constant D_J of a diatomic molecule of effective mass m_{eff}. Treat the bond as an elastic spring with force constant k and equilibrium length r_e that is subjected to a centrifugal distortion to a new length r_c. Begin the derivation by letting the particles experience a restoring force of magnitude $k(r_c - r_e)$ that is countered perfectly by a centrifugal force $m_{\text{eff}}\omega^2 r_c$, where ω is the angular velocity of the rotating molecule. Then introduce quantum mechanical effects by writing the angular momentum as $\{J(J+1)\}^{1/2}\hbar$. Finally, write an expression for the energy of the rotating molecule, compare it with eqn 13.33, and write an expression for D_J. For help with the classical aspects of this derivation, see *Appendix 3*.

13.23 In the group theoretical language developed in Chapter 12, a spherical rotor is a molecule that belongs to a cubic or icosahedral point group, a symmetric rotor is a molecule with at least a threefold axis of symmetry, and an asymmetric rotor is a molecule without a threefold (or higher) axis. Linear molecules are linear rotors. Classify each of the following molecules as a spherical, symmetric, linear, or asymmetric rotor and justify your answers with group theoretical arguments: (a) CH_4, (b) CH_3CN, (c) CO_2, (d) CH_3OH, (e) benzene, (f) pyridine.

13.24 Derive an expression for the value of J corresponding to the most highly populated rotational energy level of a diatomic rotor at a temperature T remembering that the degeneracy of each level is $2J + 1$. Evaluate the expression for ICl (for which $B = 0.1142\ \text{cm}^{-1}$) at 25°C. Repeat the problem for the most highly populated level of a spherical rotor, taking note of the fact that each level is $(2J + 1)^2$-fold degenerate. Evaluate the expression for CH_4 (for which $B = 5.24\ \text{cm}^{-1}$) at 25°C.

13.25 The moments of inertia of the linear mercury(II) halides are very large, so the O and S branches of their vibrational Raman spectra show little rotational structure. Nevertheless, the peaks of both branches can be identified and have been used to measure the rotational constants of the molecules (R.J.H. Clark and D.M. Rippon, *J. Chem. Soc. Faraday Soc. II*, **69**, 1496 (1973)). Show, from a knowledge of the value of J corresponding to the intensity maximum, that the separation of the peaks of the O and S branches is given by the Placzek–Teller relation $\delta\tilde{\nu} = (32BkT/hc)^{1/2}$. The following widths were obtained at the temperatures stated:

	$HgCl_2$	$HgBr_2$	HgI_2
θ/°C	282	292	292
$\delta\tilde{\nu}/\text{cm}^{-1}$	23.8	15.2	11.4

Calculate the bond lengths in the three molecules.

13.26 Confirm that a Morse oscillator has a finite number of bound states, the states with $V < hcD_e$. Determine the value of v_{max} for the highest bound state.

Applications: to biology, environmental science, and astrophysics

13.27 The protein haemerythrin is responsible for binding and carrying O_2 in some invertebrates. Each protein molecule has two Fe^{2+} ions that are in very close proximity and work together to bind one molecule of O_2. The Fe_2O_2 group of oxygenated haemerythrin is coloured and has an electronic absorption band at 500 nm. The resonance Raman spectrum of oxygenated haemerythrin obtained with laser excitation at 500 nm has a band at 844 cm^{-1} that has been attributed to the O—O stretching mode of bound $^{16}O_2$. (a) Why is resonance Raman spectroscopy and not infrared spectroscopy the method of choice for the study of the binding of O_2 to haemerythrin? (b) Proof that the 844 cm^{-1} band arises from a bound O_2 species may be obtained by conducting experiments on samples of haemerythrin that have been mixed with $^{18}O_2$, instead of $^{16}O_2$. Predict the fundamental vibrational wavenumber of the ^{18}O—^{18}O stretching mode in a sample of haemerythrin that has been treated with $^{18}O_2$. (c) The fundamental vibrational wavenumbers for the

[3] The web site contains links to molecular modelling freeware and to other sites where you may perform molecular orbital calculations directly from your web browser.

O—O stretching modes of O_2, O_2^- (superoxide anion), and O_2^{2-} (peroxide anion) are 1555, 1107, and 878 cm^{-1}, respectively. Explain this trend in terms of the electronic structures of O_2, O_2^-, and O_2^{2-}. *Hint:* Review Section 11.4. What are the bond orders of O_2, O_2^-, and O_2^{2-}? (d) Based on the data given above, which of the following species best describes the Fe_2O_2 group of haemerythrin: $Fe_2^{2+}O_2$, $Fe^{2+}Fe^{3+}O_2^-$, or $Fe_2^{3+}O_2^{2-}$? Explain your reasoning. (e) The resonance Raman spectrum of haemerythrin mixed with $^{16}O^{18}O$ has two bands that can be attributed to the O—O stretching mode of bound oxygen. Discuss how this observation may be used to exclude one or more of the four proposed schemes (**5**–**8**) for binding of O_2 to the Fe_2 site of haemerythrin.

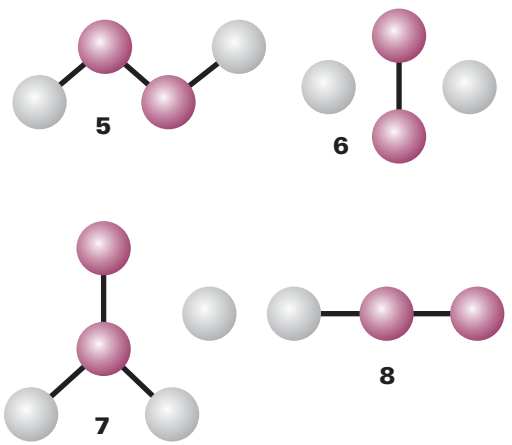

13.28‡ A mixture of carbon dioxide (2.1 per cent) and helium, at 1.00 bar and 298 K in a gas cell of length 10 cm has an infrared absorption band centred at 2349 cm^{-1} with absorbances, $A(\tilde{\nu})$, described by:

$$A(\tilde{\nu}) = \frac{a_1}{1 + a_2(\tilde{\nu} - a_3)^2} + \frac{a_4}{1 + a_5(\tilde{\nu} - a_6)^2}$$

where the coefficients are $a_1 = 0.932$, $a_2 = 0.005050$ cm^2, $a_3 = 2333$ cm^{-1}, $a_4 = 1.504$, $a_5 = 0.01521$ cm^2, $a_6 = 2362$ cm^{-1}. (a) Draw graphs of $A(\tilde{\nu})$ and $\varepsilon(\tilde{\nu})$. What is the origin of both the band and the band width? What are the allowed and forbidden transitions of this band? (b) Calculate the transition wavenumbers and absorbances of the band with a simple harmonic oscillator-rigid rotor model and compare the result with the experimental spectra. The CO bond length is 116.2 pm. (c) Within what height, h, is basically all the infrared emission from the Earth in this band absorbed by atmospheric carbon dioxide? The mole fraction of CO_2 in the atmosphere is 3.3×10^{-4} and $T/K = 288 - 0.0065(h/m)$ below 10 km. Draw a surface plot of the atmospheric transmittance of the band as a function of both height and wavenumber.

13.29 In Problem 10.27, we saw that Doppler shifts of atomic spectral lines are used to estimate the speed of recession or approach of a star. From the discussion in Section 13.3a, it is easy to see that Doppler broadening of an atomic spectral line depends on the temperature of the star that emits the radiation. A spectral line of $^{48}Ti^{8+}$ (of mass 47.95 u) in a distant star was found to be shifted from 654.2 nm to 706.5 nm and to be broadened to 61.8 pm. What is the speed of recession and the surface temperature of the star?

13.30 A. Dalgarno, in Chemistry in the interstellar medium, *Frontiers of Astrophysics*, E.H. Avrett (ed.), Harvard University Press, Cambridge (1976), notes that although both CH and CN spectra show up strongly in the interstellar medium in the constellation Ophiuchus, the CN spectrum has become the standard for the determination of the temperature of the cosmic microwave background radiation. Demonstrate through a calculation why CH would not be as useful for this purpose as CN. The rotational constant B_0 for CH is 14.190 cm^{-1}.

13.31‡ There is a gaseous interstellar cloud in the constellation Ophiuchus that is illuminated from behind by the star ζ-Ophiuci. Analysis of the electronic–vibrational–rotational absorption lines obtained by H.S. Uhler and R.A. Patterson (*Astrophys. J.* **42**, 434 (1915)) shows the presence of CN molecules in the interstellar medium. A strong absorption line in the ultraviolet region at $\lambda = 387.5$ nm was observed corresponding to the transition $J = 0$–1. Unexpectedly, a second strong absorption line with 25 per cent of the intensity of the first was found at a slightly longer wavelength ($\Delta\lambda = 0.061$ nm) corresponding to the transition $J = 1$–1 (here allowed). Calculate the temperature of the CN molecules. Gerhard Herzberg, who was later to receive the Nobel Prize for his contributions to spectroscopy, calculated the temperature as 2.3 K. Although puzzled by this result, he did not realize its full significance. If he had, his prize might have been for the discovery of the cosmic microwave background radiation.

13.32‡ The H_3^+ ion has recently been found in the interstellar medium and in the atmospheres of Jupiter, Saturn, and Uranus. The rotational energy levels of H_3^+, an oblate symmetric rotor, are given by eqn 13.29, with C replacing A, when centrifugal distortion and other complications are ignored. Experimental values for vibrational–rotational constants are $\tilde{\nu}(E') = 2521.6$ cm^{-1}, $B = 43.55$ cm^{-1}, and $C = 20.71$ cm^{-1}. (a) Show that, for a nonlinear planar molecule (such as H_3^+), $I_C = 2I_B$. The rather large discrepancy with the experimental values is due to factors ignored in eqn 13.29. (b) Calculate an approximate value of the H—H bond length in H_3^+. (c) The value of R_e obtained from the best quantum mechanical calculations by J.B. Anderson (*J. Chem. Phys.* **96**, 3702 (1991)) is 87.32 pm. Use this result to calculate the values of the rotational constants B and C. (d) Assuming that the geometry and force constants are the same in D_3^+ and H_3^+, calculate the spectroscopic constants of D_3^+. The molecular ion D_3^+ was first produced by J.T. Shy, J.W. Farley, W.E. Lamb Jr, and W.H. Wing (*Phys. Rev. Lett* **45**, 535 (1980)) who observed the $\nu_2(E')$ band in the infrared.

13.33 The space immediately surrounding stars, also called the *circumstellar space*, is significantly warmer because stars are very intense black-body emitters with temperatures of several thousand kelvin. Discuss how such factors as cloud temperature, particle density, and particle velocity may affect the rotational spectrum of CO in an interstellar cloud. What new features in the spectrum of CO can be observed in gas ejected from and still near a star with temperatures of about 1000 K, relative to gas in a cloud with temperature of about 10 K? Explain how these features may be used to distinguish between circumstellar and interstellar material on the basis of the rotational spectrum of CO.